SOL-GEL PROCESSING SCIENCE USING A SOL-GEL OPTICS RESEARCH FACILITY (SGORF)

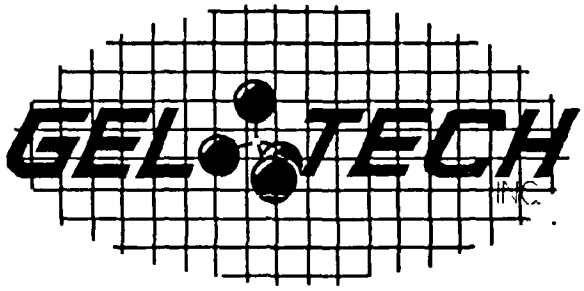

FINAL REPORT PREPARED FOR
AIR FORCE OFFICE OF SCIENTIFIC RESEARCH
BOLLING AFB DC 20332

CONTRACT # F49620-86-C-0120

UNCLASSIFIED
SECURITY CLASSIFICATION OF THIS PAGE

REPORT DOCUMENTATION PAGE

1a. REPORT SECURITY CLASSIFICATION: Unclassified	1b. RESTRICTIVE MARKINGS
2a. SECURITY CLASSIFICATION AUTHORITY	3. DISTRIBUTION / AVAILABILITY OF REPORT: Approved for public release Distribution unlimited
2b. DECLASSIFICATION / DOWNGRADING SCHEDULE	
4. PERFORMING ORGANIZATION REPORT NUMBER(S)	5. MONITORING ORGANIZATION REPORT NUMBER(S): AFOSR-TR- 89-1248
6a. NAME OF PERFORMING ORGANIZATION: Geltech, Inc. / 6b. OFFICE SYMBOL (If applicable)	7a. NAME OF MONITORING ORGANIZATION: AFSOR/NC
6c. ADDRESS (City, State, and ZIP Code): One Progress Blvd. #18 Alachua, FL 32615	7b. ADDRESS (City, State, and ZIP Code): Building 410 Bolling Air Force Base Washington, DC 20332-6448
8a. NAME OF FUNDING / SPONSORING ORGANIZATION: A.F.S.O.R. / 8b. OFFICE SYMBOL (If applicable): NC	9. PROCUREMENT INSTRUMENT IDENTIFICATION NUMBER: F49620-86-C-0120
8c. ADDRESS (City, State, and ZIP Code): Building 410 Bolling Air Force Base Washington, DC 20332-6448	10. SOURCE OF FUNDING NUMBERS: PROGRAM ELEMENT NO. 61102-F / PROJECT NO. D8I2 / TASK NO. A1 / WORK UNIT ACCESSION NO.

11. TITLE (Include Security Classification): Optics Sol-Gel Science S.G.O.R.F.
Sol-Gel Processing Science Using a Sol-Gel Optics Research Facility (U)

12. PERSONAL AUTHOR(S): Nogues, Jean-Luc Robert

13a. TYPE OF REPORT	13b. TIME COVERED	14. DATE OF REPORT (Year, Month, Day)	15. PAGE COUNT
Final Report	FROM 86-9-1 TO 88-9-30	89-9-10	100

16. SUPPLEMENTARY NOTATION

17. COSATI CODES			18. SUBJECT TERMS (Continue on reverse if necessary and identify by block number)
FIELD	GROUP	SUB-GROUP	
			Sol-Gel, optics, silica, porous silica, mixing, casting, aging, drying, stabilization, densification, radiation.

19. ABSTRACT (Continue on reverse if necessary and identify by block number)

Next Page

20. DISTRIBUTION / AVAILABILITY OF ABSTRACT: [X] UNCLASSIFIED/UNLIMITED [X] SAME AS RPT [ ] DTIC USERS	21. ABSTRACT SECURITY CLASSIFICATION: Unclassified
22a. NAME OF RESPONSIBLE INDIVIDUAL: Donald R. Ulrich	22b. TELEPHONE (Include Area Code): (202) 767-4960 / 22c. OFFICE SYMBOL: NC

DD FORM 1473, 84 MAR 83 APR edition may be used until exhausted
All other editions are obsolete

SECURITY CLASSIFICATION OF THIS PAGE
UNCLASSIFIED

19. Abstract

Fundamental studies of sol-gel processing science have led to two major accomplishments: 1) Development of a generic sol-gel process for producing fully dense silica monoliths, and 2) Identification of the need for a broad range of characterization methods to apply to processing steps. In order to achieve the production of reliable and reproducible sol-gel monoliths, a series of seven tasks are pursued.

Task 1: SOL-GEL PROCESSING: The characterization methods applied during processing allowed the optimization of the process and led to a reproducibility yield of about hundred percent after aging and drying. Even if some complementary understandings are necessary for the densification step, the progress accomplished during the period of this contract allowed many times a reproducibility rate of hundred percent after stabilization and good results for complete densification.

Task 2: NEAR NET SHAPE OPTICS: To achieve this objective it has been necessary to develop a scientific understanding of the shrinkage of the gels. The results of this study show the shrinkage can be monitored during the process and the reproducibility of the shrinkage is very good after each processing step.

Task 3: EFFECTS OF ULTRASTRUCTURE: During this contract a laboratory to do the analysis required for this project has been installed at the University of Florida (AMRC).

Task 4: OPTICAL PROPERTIES AND HOMOGENEITY: A major accomplishment has been done in the definition of a relationship between several properties of the sol-gel and the densification processing. Potential applications for porous Gelsil™ have been investigated. The results acquired during this task allowed the definition of various porous and dense Gelsil™ materials with an extensive characterization and a comparison with products available today.

Task 5: RADIATION AND SEVERE ENVIRONMENT SENSITIVITY: The first study was done on porous silica. This investigation showed no damage in the optical transmission property after irradiation of the samples with a gamma source and for a total dose of 100 Megarad.

Task 6: EFFECTS OF MULTICOMPONENT: Special attention was devoted to the Silica-Titania system which yields glasses with potential zero thermal expansion coefficients. Preliminary studies have established that various volume fractions of second phase additives can be added to silica and multicomponent gels thereby producing cast ceramic matrix composites.

Task 7: EFFECT OF SAMPLE DIMENSIONS: This contract allowed the collection of a first set of data on many properties and reproducibility rates for small size monolithic samples.

Two new types of silicas have been developed using the organometallic sol-gel processing:

- 1) Fully dense gel silica has excellent optical transmission throughout the uv,vis,nir,ir spectra range. Physical properties and structural characteristics of gel silica are generally equivalent or superior to the best grades of optical silica available today.
- 2) Optically transparent porous gel silicas which can be doped with a broad range of compounds with excellent transmission out to 290-300 nm to make new type of optical materials.

GELTECH, Inc. - One Progress Blvd. #18, Alachua, Florida 32615 - USA Ph: (904) 462 2358 - FAX: (904) 462 2993

EXECUTIVE SUMMARY

The major challenge facing sol-gel processing of advanced materials, and in fact the entire field of chemically derived ceramics, is to relate processing variables to final properties. In order to develop fundamental processing-properties relationships it is essential to characterize the material after each step of the process: mixing, aging, drying, stabilization and densification.

Fundamental studies of sol-gel processing science pursued at GELTECH and at the University of Florida's Advanced Materials Research Center (AMRC) have led to two major accomplishments: 1) Development of a generic sol-gel process for producing fully dense silica monoliths (termed GELSIL™), and 2) Identification of the need for a broad range of characterization methods to apply to processing steps.

In order to achieve the production of reliable and reproducible sol-gel monoliths, a series of seven tasks have been identified. These tasks and a summary of results to date are given below:

Task 1: SOL-GEL PROCESSING SCIENCE FOR CONTINUOUS OPTICS PROCESSING

- The major objectives of this task are to understand the process variables that influence the five steps of sol-gel processing and to use this scientific understanding to optimize and control a continuous batch process for making sol-gel derived optical components.

- The characterization methods applied during processing allowed the optimization of the process, and led to a reproducibility yield of about 100% after aging and drying. Even if some complementary understandings are necessary for the densification step, the progress accomplished during the period of this contract allowed many times a reproducibility rate of 100% after stabilization and good results for complete densification. Characteristics of porous and dense gel silica are presented at the end of this executive summary.

- To permit the reproducibility study, a Sol-Gel Optics Research Facility has been designed and installed.

Task 2: FABRICATION SCIENCE FOR NET SHAPE PRECISION OPTICS

- The primary objective of this task is to apply the science of sol-gel processing, developed in Task 1, to the production of net shape precision optics.

- To achieve this objective it has been necessary to develop a scientific understanding of the shrinkage of the gels in order to accurately predict three dimensional changes. The results of this study show: 1) the shrinkage can be monitored during the process, and 2) the reproducibility of the shrinkage is very good after each processing step and will allow the fabrication of as cast optical components with the minimum grinding and polishing requirement.

Task 3: EFFECTS OF ULTRASTRUCTURE ON THERMAL AND MECHANICAL PROPERTIES OF SOL-GEL OPTICS

- The objective of this task is to investigate the physics of both thermal and mechanical behavior of sol-gel derived silica as a function of the processing variables.

- During the duration of this contract a laboratory to do the analysis required for this project has been installed at the University of Florida (AMRC). These analysis will produce the statistical data which will be the basis for lifetime predictions in severe environments such as for critical military applications.

Task 4: EFFECTS OF ULTRASTRUCTURE ON THE OPTICAL PROPERTIES AND OPTICAL HOMOGENEITY OF GELSIL™

- One of the most important objectives of this task is the understanding of the property variations, such as optical transmission, during the densification process.

- A major accomplishment has been done in the definition of a relationship between several properties of the sol-gel and the densification processing.

- Potential applications for porous Gelsil™ have been investigated.

- The results acquired during this task allowed the definition of porous and dense Gelsil™ materials with an extensive characterization and a comparison with products available today.

A-1

Task 5: RADIATION AND SEVERE ENVIRONMENT SENSITIVITY OF GELSIL™, MULTICOMPONENT AND GEL-DERIVED COMPOSITES

- The objective of this task is to evaluate the radiation sensitivity of various gel silica, multicomponent and composite materials.
- A first study was done on pure silica porous Gelsil™. This investigation showed no damage in the optical transmission property after irradiation of the samples with a ^{60}Co gamma source and for a total dose of 100 Megarad.

Task 6: EFFECTS OF MULTICOMPONENT SPECIES AND MULTIPHASE ON PROCESSING-PROPERTIES RELATIONSHIPS

- The objective of this task is to extend the pure silica understanding developed in tasks 1-5 to various multicomponent oxide glasses and multiphase systems.
- Special attention was devoted to the SiO_2-TiO_2 system which yields glasses with potential zero thermal expansion coefficients.
- Preliminary studies have established that various volume fractions of second phase additives can be added to silica and multicomponent gels thereby producing cast ceramic matrix composites. Addition of SiO_2 powder to decrease the shrinkage of the silica gel during the processing has been investigated with mixed results, therefore the project was terminated to allow faster progress in other tasks.

Task 7: EFFECT OF SAMPLE DIMENSIONS ON RELIABILITY

- The principal objective of Task 7 is to evaluate the effects of batch size and sample dimensions on the properties of the final product.
- This contract allowed the collection of a first set of data on many properties and reproducibility rates for small size monolithic samples.

Two new types of optical silicas have been developed using the organometallic sol-gel processing.

- 1) Fully dense gel silica (Type V) has excellent optical transmission throughout the ultra-violet, visible, near infrared and infrared spectra range. Physical properties and structural characteristics of Type V gel silica are generally equivalent or superior to the best grades of optical silica available today.

- Total cation impurity (ppm)	1 - 2
- OH impurity (ppm)	≤ 5
- Cl impurity (ppm)	0 - >1000
- 50% UV transmission (nm)	165 - 168
- Bubbles and inclusions (#/cub. in)	0
- Strain (nm/cm)	5
- Refractive index (n[d])	1.458 - 1.463
- Dispersion (v[d])	67.8 - 66.4
- Index of homogeneity (10-6)	≤ 10
- Density (g/cc)	2.20

- 2) Optically transparent porous gel silicas are termed Type VIA, B and C depending upon the total pore volume, density, surface area and microhardness. Type VIA gel silica can be doped with a broad range of optical polymers or compounds with excellent transmission out to 290-300 nm to make new type of optical materials.

- Total cation impurity (ppm)	1 - 2
- OH impurity (ppm)	> 2000
- Cl impurity (ppm)	0
- 50% UV transmission (nm)	250 - 300
- Bubbles and inclusions (#/cub. in)	0
- Refractive index (n[d])	1.28 - 1.45
- Density (g/cc)	1.3 - 2.1

LIST OF PROFESSIONAL PERSONNEL ASSOCIATED WITH THE RESEARCH EFFORT

Larry L. Hench - Principal Investigator

James G. Hermann - President & CEO (Former)

Anthony J. LaPaglia - President & CEO (Present)

Dennis A. LeSage - General Manager

Jean-Luc R. Noguès - Manager R&D

Canan Balaban - Senior Research Engineer

Rong-Shenq Sheu - Research Scientist

William V. Moreshead - Research Scientist

Fred Chapman - Maintenance Technician

Subcontract to Advanced Materials Research Center at University of Florida

Jon K. West - University of Florida (AMRC) Subcontract Manager

Steve Wallace

Rounan Li

Randy Nikles

Guy LaTorre

Martin J.R. Wilson

Wander L. Vasconcelos

R.T. DeHoff

B.F. Zhu

F. Wang

LIST OF PUBLICATIONS AND PRESENTATIONS INCLUDED IN THIS FINAL REPORT

1. **Dielectric Relaxation Analysis of Water Adsorption in Sol Gel Derived Silica Gel Monoliths** - S. Wallace, L.L. Hench - In Better Ceramics Through Chemistry III, Ed. C.J. Brinker, D.E. Clark, D.R. Ulrich, Materials Research Society, Vol. 121 (1988)

2. **Physical Properties of Dried Na_2O-SiO_2 Monoliths** - Rounan Li, L.L. Hench - In Better Ceramics Through Chemistry III, Ed. C.J. Brinker, D.E. Clark, D.R. Ulrich, Materials Research Society, Vol. 121 (1988)

3. **Correlations Between Processing Parameters, Ultrastructure, and Strength of Gel-Silica** - J.K. West, R. Nikles, G. LaTorre - In Better Ceramics Through Chemistry III, Ed. C.J. Brinker, D.E. Clark, D.R. Ulrich, Materials Research Society, Vol. 121 (1988)

4. **Sol-Gel Processing of Large Silica Optics** - L.L. Hench, M.J.R. Wilson, C. Balaban, J.L. Noguès - In Proceedings of the Fourth International Conference on Ultrastructure Processing of Ceramics, Glasses and Composites, Ed. D.R. Uhlmann, D.R. Ulrich (1989)

5. **A Topological Model of the Sintering of Sol-Gel silica** - W.L. Vasconcelos, R.T. DeHoff, L.L. Hench - In Proceedings of the Fourth International Conference on Ultrastructure Processing of Ceramics, Glasses and Composites, Ed. D.R. Uhlmann, D.R. Ulrich (1989)

6. **Processing, Properties and Applications of Sol-Gel Silica Optics** - J.L. Noguès, A.J. LaPaglia - In Proceedings of the SPIE's 33rd Annual International Technical Symposium on Optical & Optoelectronic Applied Science and Engineering (1989)

7. **Porous Gel Silica, A Matrix for Optically Active Components** - J.L. Noguès, W.V. Moreshead - In Proceedings of the Fifth International Workshop on Glasses and Ceramics from Gels, Ed. M.A. Aegerter (1989)

8. **Silica Optics Manufacture Via Sol-Gel Technology** - J.L. Noguès, C. Balaban, W.V. Moreshead, R.S. Sheu - In Proceedings of the First Florida-Brazil Seminar on Materials (Advanced Ceramics), Ed. W. Pirró e Longo, S. Neves Monteiro, J.D. Filho (1989), pp. 51-60

9. **Dilatometric Measurements for Low Thermal Expansion Gels** - B.F. Zhu, F. Wang, J.K. West - To be published

LIST OF PUBLICATIONS AND PRESENTATIONS INCLUDED IN THE ANNUAL TECHNICAL REPORT OF MARCH 31, 1988

1. **Optical Properties of Gel Silica Glasses** - S-H. Wang, C. Campbell, L.L. Hench - Presented and Published in the Proceedings of the Third International Ultrastructure Symposium on Processing of Ceramics, Glasses and Composites, J. Wiley & Sons (D. Mackenzie and D.R. Ulrich, eds.) - See appendix D

2. **Preparation and Characterization of Monolithic Si-Ce-O Gels** - A. Sivade, G. Orcel, L.L. Hench, J. Bouaziz, R. Sempéré, D. Bourret - Presented at the 40th Pacific Coast Regional Meeting of the American Ceramic Society, San Diego, CA - See appendix F

3. **Gel Silica Optics** - L.L. Hench, S-H. Wang, J.L. Noguès - Presented and Published in the Proceedings of the 1988 SPIE Conference, Los Angeles, CA. - See appendix E

4. **Physical and Structural Evolution of Sol-Gel Derived TiO_2-SiO_2 Glasses** - Y-C. Cheng, L.L. Hench - Presented and Published in the Proceedings of the 1988 Spring Meeting of the Materials Research Society, Reno, NV - See appendix G

5. **Fast, Radiation Hard Scintillating Detector, a Potential Application for Sol-Gel Glass** - J.L. Noguès, S. Majewski, J.K. Walker, M. Bowen, R. Wojcik, W.V. Moreshead - Submitted for publication in American Ceramic Society Bulletin - See appendix C

6. **Processing and Properties of Porous Gel Silica** - J.L. Noguès, W.V. Moreshead - To be submitted for publication in Journal of Non-Cristalline Solids - See appendix B

7. **Radiation Resistance of Porous Gel Silica** - J.L. Noguès, S. Majewski, M. Bowen, W.V. Moreshead - To be submitted for publication in Materials Research Society Letters - In preparation

CONTENTS

DIELECTRIC RELAXATION ANALYSIS OF WATER ADSORPTION IN SOL GEL DERIVED SILICA GEL MONOLITHS

S. WALLACE AND L.L. HENCH
University of Florida, Advanced Materials Research Center, One Progress Blvd. #14, Alachua, FL 32615

ABSTRACT

The polarization mechanism of the low frequency dielectric relaxation (R1) observed in water adsorbed in porous silica gel is investigated using monolithic samples. It is attributed to electrode polarization involving proton hopping conduction. The influence of the thickness of the adsorbed water layer on the relaxation mechanism is discussed.

INTRODUCTION

The dielectric properties of water adsorbed in the pores of sol-gel derived silica gel monoliths is of practical as well as scientific interest. For example, porous silica gel could potentially meet the requirements of a low loss, low dielectric constant substrate material for integrated circuits, but the effects of adsorbed water could be a major limitation. Cracking caused by the removal of water from the pores of gel monoliths during drying is in itself an area of major concern. This problem can be solved by keeping the rate of water removal below a critical drying rate [1]. In an earlier paper [2] we examined the possibility of using Dielectric Relaxation Spectroscopy (DRS) as a means of monitoring the rate of water removal during drying. We found a Debye type dielectric relaxation associated with the adsorbed water. We also concluded that the dielectric constant E' measured at 10 MHz, which is a linear function of water content, was the most suitable parameter to monitor during drying, as long as the problem of interfacing the measuring electrode with the gel could be solved.

Pure, dry, dehydrated silica gel is a porous form of amorphous silica which exhibits no dielectric relaxation between 1 Hz and 1 THz. Liquid water has one dipolar relaxation at 23.4 GHz. However, the dielectric relaxation spectra, between 1 Hz and 1 THz, of pure water adsorbed in the pores of particulate silica gel can exhibit up to three relaxations (R1, R2, and R3), depending on the water content and texture of the gel.

Relaxation I (R1)

A low frequency relaxation (R1) is observed at frequencies below 10 MHz [3-10] and is generally attributed to Maxwell-Wagner type interfacial polarization, i.e. conducting inclusions in an insulating matrix. This polarization is related to the "bulk water" adsorbed [4] in the granules of the particulate gels used in previous investigations, and is caused by the conduction of protons dissociated from surface silanols [7]. The absolute magnitude and frequency of R1 for a specific gel sample depends upon a complex interdependence of gel structure and adsorption variables. These variables include: gel particle size, average pore size $\bar{r}$, pore volume V, surface area S, silanol concentration [SiOH], impurity ion concentration and adsorbed water structure. A relaxation can be characterized by the frequency, $F\varepsilon$, of the maximum of its dielectric loss factor spectra $E''(f)$, where f = frequency. The characteristic frequency $F\varepsilon$ of R1, called $F\varepsilon 1$, shows a logarithmic type dependence on water content, W = gm H_2O/gm gel, and an Arhennius type dependence on temperature T [3,12], e.g.

$$F\varepsilon 1 = C\, W^{n} e^{-Q/kT} \qquad (1)$$

where n varies between 3 and 6, depending on the sample [3,4,8,10] and Q is the activation energy. The magnitude of the dielectric loss factor at Fε1, called $|\varepsilon 1|$, which is roughly constant for all values of W, also varies from sample to sample, e.g. $|\varepsilon 1| = 8$ at 25°C [6], $|\varepsilon 1| = 3$ at 25°C [3]. The influence of [SiOH] on R1 is unclear.

Relaxation 2 (R2)

For a gel containing no adsorbed water, e.g. W = 0 g/g, only R2, due to dipolar orientation of the surface silanols, Si-OH, around the Si-O bond axis [11], is seen. $|\varepsilon 2|$ is proportional to [SiOH], which depends on thermal history of the sample. The absolute value of Fε2 varies from 1 to 10 GHz [4,5,7-12], depending on [SiOH]. When water molecules are adsorbed into pores, they hydrogen bond to the silanols. This causes $|\varepsilon 2|$ to increase as W increases. At T < 0°C, Fε2 decreases as W increases. As T increases to 0°C, for all values of W, Fε2 increases to a constant value equal to that for W = 0 g/g, i.e. 10 GHz in this case [12]. For W > 0 g/g, R2 is attributed both to the relative lifetimes of hydrogen bonds formed by clusters of water molecules H-bonded to the surface SiOH groups [7,8], and to the rate of transfer of protons between adjacent H-bonded water molecules adsorbed on surface SiOH groups [5,9].

Relaxation 3 (R3)

Zhilenkov et al. [12] have observed a third relaxation at Fε3 = 14 GHz at 0°C, which appears for W > 0.2 g/g for their sample. Fε3 and $|\varepsilon 3|$ increase as W and T increase. R3 appears after the formation of a second phase in the adsorbed water. The second phase forms upon completion of the "bound" water layer at a critical water content Wc = 0.2 g/g. This phase exhibits no melting transition [6]. Two phases of adsorbed water have also been observed using proton NMR spectroscopy [6].

When the temperature is lowered far enough for the second phase to freeze, Fε3 disappears, whereas Fε2 does not disappear but keeps decreasing as T decreases. Thus R2 must be related only to the bound phase, while R3 must involve the second "free" water phase.

OBJECTIVE

The dielectric relaxation of water adsorbed in monolithic silica gels described in [2] was similar to R1 in its frequency dependence on W, but the value of Fε1 which we observed was much lower and $|\varepsilon 1|$ was much larger than the values seen for particulate gels with the same W. The Debye type shape of R1 could be attributed to either dipolar or interfacial polarization [13], but it is generally attributed to the interfacial polarization. In this paper the unique geometry, compared to particles, of monolithic silica gel samples is used to investigate the mechanism of relaxation due to water adsorption using a digital a.c impedance bridge.

METHOD

The admittance spectra Y(f), from which the dielectric relaxation spectra can be calculated, of sol-gel derived cylindrical silica gel samples were measured between 5 HZ and 13 MHz using a Hewlett Packard HP4192A a.c

impedance analyzer. All gels were made from acid catalyzed tetramethoxysilane sols, and have a pore radius of about 14 Å. Their texture and structure depends on thermal history. Details of the experimental method and theory are presented elsewhere [2]. The impedance analyzer allows the amplitude of the a.c signal to be varied and a d.c bias to be applied. Silver paint was used as the measuring electrode material. The values of the texture of the sample characterized in Ref. [2] are: S = 752 M^2/g, V = 0.553 cc/g and R = 14.7 Å as measured by isothermal gas adsorption, with a bulk density of 1.04 g/cc (Note: previous textural values in Ref [2] are incorrect).

RESULTS

The dielectric relaxation spectra of water adsorbed in monolithic silica gel samples consists of an R1 relaxation superimposed on another relaxation occurring at lower frequencies (called RS). In an equilibrated gel, R1 is stable and reproducible. If water is allowed to evaporate from the surface of a saturated gel the low frequency relaxation RS decreases in magnitude. This implies that RS is due to conduction on the external surface of the gel. The Fε frequency of RS, called FεS, is far too low to be measured, but the intensity of the relaxation is large enough for the tail of the relaxation to obscure the loss factor spectra of R1 and make accurate measurement of Fε1 difficult. The dielectric loss tangent spectra, Tan δ(f), can be used to separate these two relaxations. The tail of RS is just visible on the low frequency side of the loss tangent peak of R1 for samples measured using Ag paint electrodes (Fig. 1, curve A). The frequency of the maximum of the loss tangent spectra, Fδ1, can be accurately measured and is directly proportional to Fε1 [2]. Thus the loss tangent spectra and Fδ1 can be used to characterize R1, and also be related to previous investigations.

FδI of R1 of a cylindrical gel is an exponential function of the sample thickness D, i.e. the electrode separation. Fig. 2 shows this as a log-log plot for a saturated gel with W = 0.154 g/g, e.g.

$$F\delta I = 471\ D^{-1.929} \qquad (2)$$

The same exponential relationship is seen with other samples, but the exponent varies between -0.6 and -2.0.

The material used as measurement electrodes influences the intensity, |δ1|, and frequency, Fδ1, of the Tan δ(f) spectra of R1. The overall shape of the relaxation is the same for both silver and carbon paint and vapor deposited Pt electrodes (Fig. 1).

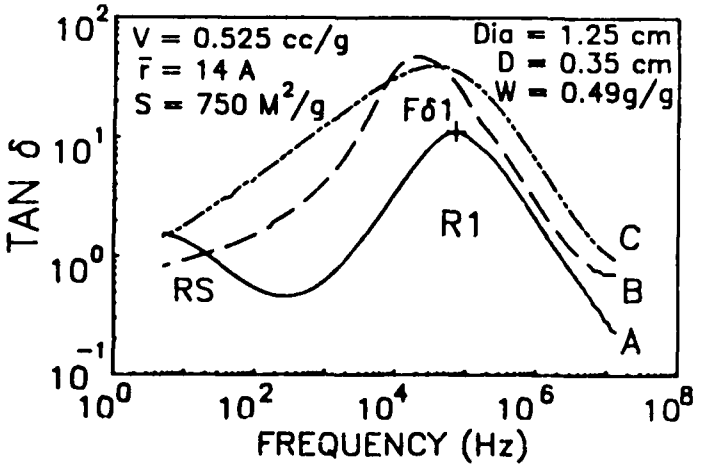

Fig. 1. Dependence of the Dielectric Loss Tangent spectra on the material used as measuring electrodes. Curve A: silver paint, showing the R1 peak and the fail of the RS peak. B: carbon paint showing just the R1 peak. C: vapor deposited platinum showing just the R1 peak.

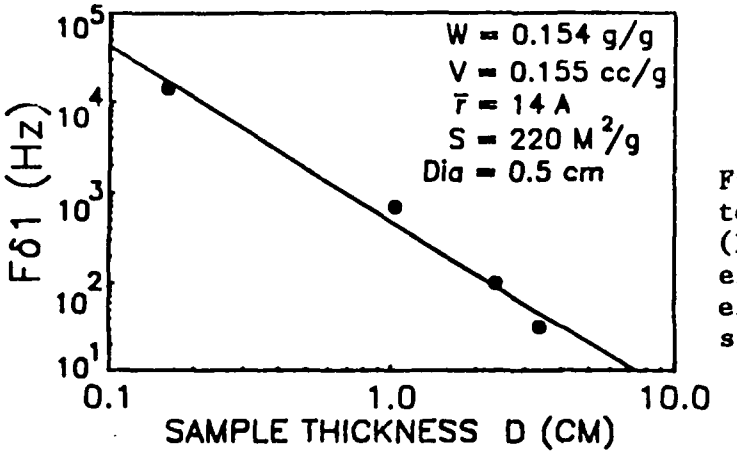

Fig. 2. Variation of the characteristic Loss Tangent frequency (Fδ1) of Relaxation 1 with electrode thickness D, i.e. with electrode separation, using silver paint electrodes.

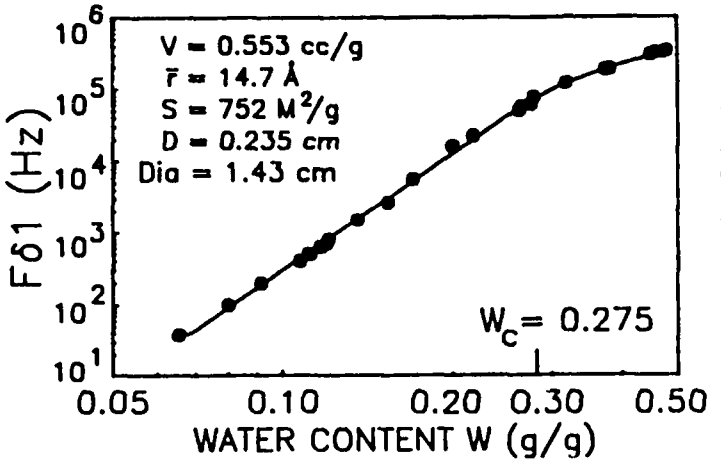

Fig. 3. Exponential dependence of the characteristic Loss Tangent frequency (Fδ1) of Relaxation 1 on the water content W. T = 25°C.

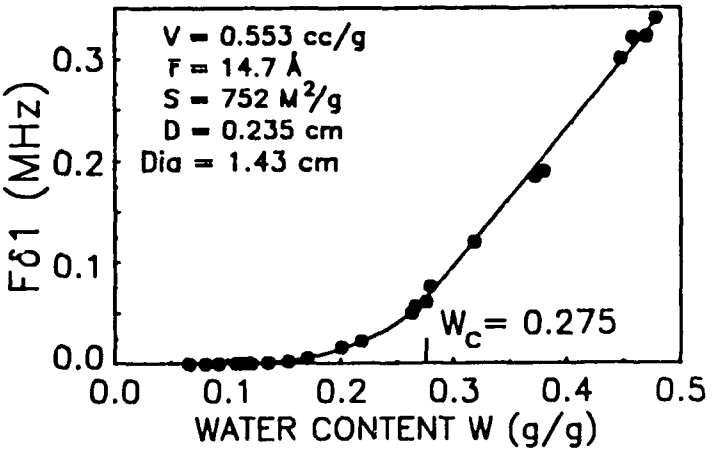

Fig. 4. Linear dependence of the characteristic Loss Tangent frequency (Fδ1) of Relaxation 1 on the water content W. T = 25°C.

Figure 1 of Ref. [2] shows the dependence of Fδ1 on W for a silica gel sample. This data is replotted in Figs. 3 and 4 as log-log and linear plots respectively, showing a transition from an exponential to a linear dependence on W at W = 0.275 g/g. The equations best fitting these curves are:

$$F\delta 1 = 6.88 \times 10^{7} W^{5.353} \quad \text{for} \quad 0.06 < W < 0.275 \text{ g/g} \qquad (3)$$

$$F\delta 1 = 1.34 \times 10^{7} W - 305{,}000 \quad \text{for} \quad 0.275 < W < 0.50 \text{ g/g} \qquad (4)$$

The loss tangent spectra of R1 is independent of the magnitude of the a.c voltage signal from 0.01 V to 1.0 V, whereas RS is strongly affected. Applying a d.c offset voltage to the a.c signal also effects RS, whereas R1 is unaffected.

DISCUSSION

The properties of R1 due to water adsorption in silica gel monoliths are explained by an interfacial polarization mechanism due to charge build up at the electrodes, i.e. electrode polarization. The charge carriers are protons which conduct via a hopping mechanism.

The evidence for the electrode polarization mechanism includes: (a) the frequency $F\delta 1$ of R1 observed in monolithic silica gel samples varies with sample thickness (Fig. 2) and electrode material (Fig. 1). RS shows a similar behavior. (b) The loss factor magnitude, $|\delta 1|$, is 1000 times larger, and $F\varepsilon 1$ (and $F\delta 1$) is much lower, in monolithic gels than in particulate gels for the same W. (c) An intrinsic dipolar polarization is modelled by a parallel RC circuit, and an extrinsic electrode polarization is modelled by a series RC circuit. Relaxation I is modelled by a series RC circuit.

In pure water, conductivity is due to the hopping of protons created by an autodissociation mechanism. Proton hopping occurs via the tunnelling of protons between the electron clouds of hydronium ions and correctly oriented adjacent water molecules. The hopping of protons dissociated from acidic surface silanols is also believed to be the conduction mechanism of water adsorbed in silica gel [14-16]. The specific hopping mechanism depends on the statistical thickness of the adsorbed water layer, i.e. W/S (gm H_2O/1000 M^2/g gel) [14]. When only the bound non-freezing water layer is adsorbed, i.e. $W < Wc$, the conductivity G of water adsorbed in silica gel is proportional to W raised to the power n, where n varies between 3 and 7, depending on the sample [15,16]. For $W > Wc$, G is directly proportional to W [15].

The Nuclear Correlation Relaxation Time, τ_n, of protons in water adsorbed in silica gel is calculated from the proton NMR spectra [17]. τ_n is associated with the movement of protons in the two phases, the bound and free water, present in the adsorbed system. The bound water is the phase showing no melting or freezing transition and is the water adsorbed up to $W = Wc$. The free water phase is the water adsorbed on top of the bound layer for $W > Wc$, and exhibits a suppressed melting point [7]. τ_n exhibits the same type of dependence on W as does G, i.e. exponential for $W < Wc$, and linear for $W > Wc$ [17].

The charge carriers for R1 could be protons or impurity ions such as sodium. We conclude that the charge carriers are protons since: (a) $F\delta 1$ of R1 of the silica gel monoliths shows the same type of dependence on W as reported for G and τ_n (Fig. 3 and 4). The transition from exponential to linear dependence on W occurs at the same statistical thickness of adsorbed water, i.e. W/S, of about 0.36 g/1000 M^2/g for $F\delta 1$, G and τ_n. (b) ICP analysis of a saturated gel detected no impurity ion concentrations greater than 1 ppm. (c) The diffusion of a 0.1 M NaCl solution into a gel does not affect R1, but increases the magnitude of RS.

Proton conduction could occur via a bound hopping or an ionic diffusion mechanism. Neither increasing the amplitude of the a.c signal, applying a d.c bias or diffusing a 0.1 M NaCl solution into the gel affects R1, whereas RS is strongly affected. This means that R1 has a different conduction mechanism, e.g. proton hopping, than RS, e.g. ionic diffusion.

CONCLUSIONS

Relaxation I is due to electrode polarization resulting from proton conduction in the adsorbed water layer via a hopping mechanism. Therefore the interfacial polarization attributed to R1 in particulate gels is correct for monolithic gels as well. The similarity of the dependence of $F\delta 1$, G and

τ_n on W and the change from an exponential to linear dependence at the same statistical thickness (W/S ≈ 0.36 g H_2O/1000 M^2/g gel) suggest that the proton hopping mechanism depends on the structure of the adsorbed water, which also depends on the statistical thickness. In contrast, the surface conduction relaxation, RS, is due to the diffusion of impurity ions.

ACKNOWLEDGEMENTS

The authors gratefully acknowledge the U.S. AFOSR Contract No. F49620-85-C-0079 for support of this work.

REFERENCES

1. J. Zarzychi, in Ultrastructure Processing of Ceramics, Glasses and Composites, edited by L.L. Hench and D.R. Ulrich (J. Wiley, New York, 1984), p 27.

2. S. Wallace and L.L. Hench, in Proceedings of the International Conference on Ultrastructure Processing of Ceramics, Glasses and Composites, edited by J.D.Mackenzie and D. Ulrich (J. Wiley, NY, 1988).

3. K. Kamiyoshi and T. Odake, Sci. Rep. Res. Inst. Tohuka Univ. 5, 271 (1953); J. Chem. Phys. 21, 1295 (1953).

4. S.Kondo and M.Muroya, Bull. Chem. Soc. Japan 42, 1165 (1969); 42, 2724 (1969).

5. V.P Dushchenko and I.A. Romanovskii, Russ. J. Phys. Chem. 44,826 (1970).

6. P.G. Hall, R.T. Williams and R.C.T. Slade, J.Chem. Soc. Far. Trans. 1, 81, 847 (1985).

7. J.M. Wacrenier, J. Fontaine, A. Chapertone and A. Lebrun, Rev. Gen. Elec. 76, 719 (1967).

8. J. Fontaine and B. Vandorpe, Bull. Soc. Chim. France 3,872 (1970); C. R. Acad. Sc. Serie B 266, 1227 (1968).

9. L Gengembre, J. Fontaine and B. Vandorpe, C. R. Acad. Sc. Paris, Serie C, 277, 477 (1973).

10. J.M. Thorp and N.K. Nair, Trans. Far. Soc. 61, 962, 975, (1965); 65, 1741 (1969).

11. L. Gengembre, A Chaperton, B. Vandorpe, C. R. Acad. Sc. Paris, Serie C, 284, 541 (1977); J. Chimie Phys. 76, 959 (1979).

12. I.V. Zhilenkov and E.G. Nekrasova, Russ. J. Phys. Chem. 47, 93 (1973); 49, 406 (1975); 54, 1503 (1980); 46, 913 (1972).

13. E.McCafferty, J. Phys. Chem. 82, 2044 (1978).

14. J.H. Anderson and G.A. Parks, J. Phys. Chem. 72, 3662 (1968).

15. K. Kawasaki and N.Hackerman, Jap. J. App. Phys. 6, 1184 (1967).

16. A. Soffer and M.Folman, Trans. Far. Soc. 62, 3559 (1966).

17. J. R. Zimmerman and L. A. Lasater, J. Phys. Chem. 62, 1157 (1958).

PHYSICAL PROPERTIES OF DRIED Na_2O-SiO_2 MONOLITHS

ROUNAN LI AND L. L. HENCH
Advanced Materials Research Center, University of Florida, One Progress Blvd., #14, Alachua, FL 32615

ABSTRACT

Dried monolithic gels of compositions XNa_2O-$(1-X)SiO_2$ (with X from 0 mol% to 7 mol%) were obtained by acid catalyzed sol-gel processing using tetramethylorthosilicate and $NaNO_3$. Optically clear monoliths in the range of 20 to 90 mm diameter by 3 to 20 mm thickness were routinely produced by controlling the processing schedule. Complete drying in air without cracking was achieved at 180°C from 10-14 days. The bulk density and optical properties of the gels, characterized by UV/VIS/NIR transmission, IR reflection and index of refraction, showed a compositional dependence on Na_2O similar to melt glasses of the same Na_2O content. However, the true density and microhardness decreased with Na_2O content in contrast to melt glasses.

INTRODUCTION

Binary Na_2O-SiO_2 glasses have been made by sol-gel processing [1-4]. Low gel-glass transformation temperatures dependent on the Na_2O content of the gel have been observed. Gel-derived 33 mol% Na_2O-67 mol% SiO_2 glass was obtained at temperatures as low as 500°C [1]. However, when the Na_2O content was more than 20 mol% the gel-derived glass had very poor durability and little usefulness. The production of large samples and reproducibility of Na_2O-SiO_2 gel-glass have also been major problems. Consequently, there is little information on the preparation, properties and durability of large monolithic Na_2O-SiO_2 gels. This is especially so for chemically durable gels in which the Na_2O content is less than 10 mol%. Therefore, the objectives of this paper are: (1) to prepare large monolithic dried gels with compositions XNa_2O-$(1-X)SiO_2$ (with X=0, 1, 3, 5 and 7 mol%); (2) to measure the physical properties of the gels and compare them with those of pure silica gel and melt glasses of same composition; (3) to select an optimum Na_2O-SiO_2 gel which has similar optical properties as pure silica gel but can be densified at a substantially lower temperature.

EXPERIMENTAL

Tetramethylorthosilicate $[Si(OCH_3)_4]$ was used as a precursor of polysilicic acid to form the gels. Before this precursor was mixed with water at room temperature, $NaNO_3$ was added. The proportions of $NaNO_3$ to $Si(OCH_3)_4$ was selected to yield XNa_2O-$(1-X)SiO_2$ compositions with X=0, 1, 3, 5 and 7 mol% after the loss of water and methanol. Either nitric, hydrochloric or acetic acid was added to the mixture as a catalyst to accelerate the hydrolysis and produce a stronger gel. After efficiently stirring for 15 minutes at 25°C, the sol was cast into PS (polystyrene) containers, sealed and put into a drying oven with programmable controls.

Different sol pH values, time and temperature of gelation and drying were investigated. Likewise, various methods of drying were studied in order to control the rate of evaporation of the liquid and the rate of shrinkage of the gels. A final drying schedule of 10-14 days in air was used. Results of the studies of processing variables are reported in another publication [5].

True densities were determined using a Quanta Chrome Micropycnometer (MPY-1) and a simple mercury displacement technique was used for bulk density measurements. Microhardness was measured using a diamond pyramid indenter on a Kentron Tester with a 100g load. Porosity and surface area were measured using N_2 absorption with a Quanta Chrome Autosorb-6. The transmission spectra were made with a Perkin-Elmer Lambda UV/VIS/NIR Spectrophotometer in which ϕ30x4mm dried gels with as-cast surface finishes were used. IR spectra were obtained using the above samples, with a Nicolet 20 SXB FTIR/TGS, and diffuse reflection stage scanning between 250-1600 cm^{-1}. The indices of refraction were measured using an oil immersion technique with an Olympus Vanox Microscope.

RESULTS

Monolithic xerogels with composition XNa_2O-(1-X)SiO_2 (with X=0, 1, 3, 5 and 7 mol%) were obtained successfully with sizes up to 90 mm diameter and 20 mm thickness. True and bulk densities, microhardness, porosity and surface area are listed in Table I. Figure 1 shows the transmission UV/VIS/NIR spectra and Fig. 2 the IR spectra for dried gel monoliths with Na_2O content(L) from 0-7 mol%. The densities of dried gels along with the melt glasses of the same compositions are plotted in Fig. 3. Figure 4 compares the indices of refraction for the various Na_2O compositions of dried gels and melt glasses.

Table I. Bulk and True Densities, Microhardness, Porosity and Surface Area of the L-X [XNa_2O-(1-X)SiO_2] Gels

Code	Bulk Density (g/cc)	True Density (g/cc)	Micro Hardness (Kg/mm^2)	Surface Area (M^2/g)	Total Pore Volume (cc/g)	Average Pore Radius (A)
L-0	1.16	2.2717	42.00	760	0.4811	12.67
L-1	1.18	2.2141	41.86	729	0.4543	12.47
L-3	1.19	2.2036	40.07	662	0.4167	12.58
L-5	1.21	2.1987	39.96	572	0.3695	12.92
L-7	1.26	2.1651	35.22	520	0.3337	12.81

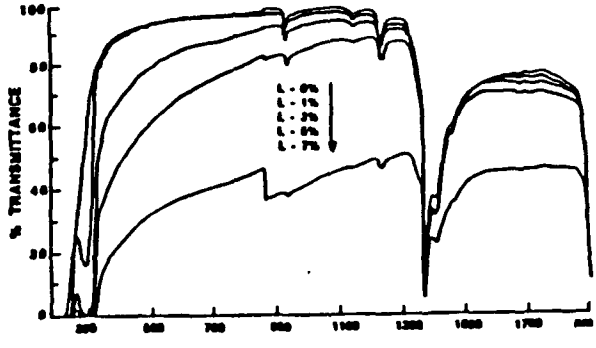

Fig. 1. Optical transmission of the Na_2O-SiO_2 gels in ultraviolet, visible and near infrared (L = mol% Na_2O).

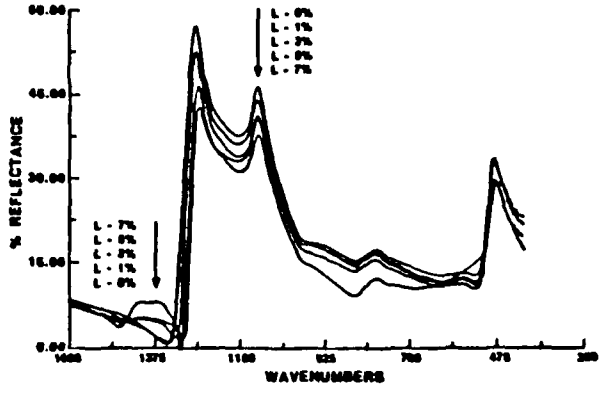

Fig. 2. IR reflection spectra of XNa_2O-(1-x)SiO_2 gels (with X = 0, 1, 3, 5 and 7 mol%).

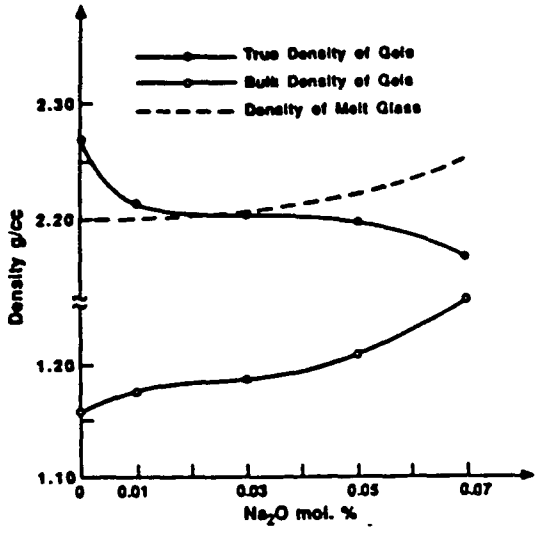

Fig. 3. Density of the gels and melt glass.

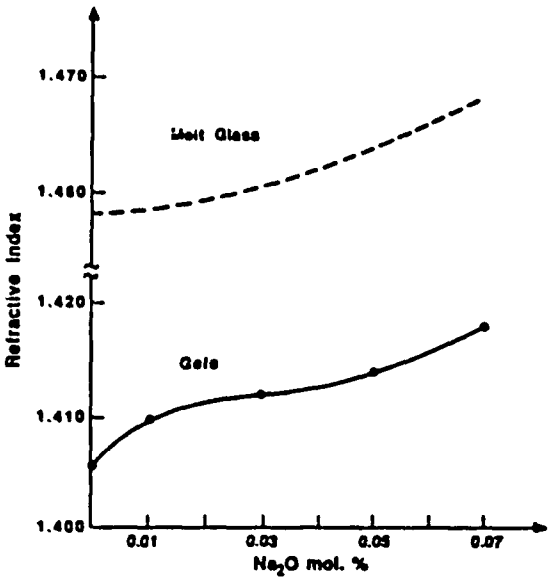

Fig. 4. Refractive index of the gels and melt glass.

DISCUSSION

Density of melt derived soda silicate glass is a minimum value for the pure network former and increases as modifier ions are added [6]. However, a dried gel differs from a glass by its texture. The gel is essentially an agglomerate of elementary particles, the size of which may be of the order of 10nm [7], aggregates of particles formed by primary particles, so-called secondary particles, as well as micro- and macro-pores.

In contrast with the effect of alkali ions on the true density of Na_2O-SiO_2 glasses, Table I, shows that the true densities of the gels decreased with increasing Na_2O content. This indicates that the primary network structure of gel particles is more open than that of a melt glass of the same composition. During sol-gel processing, the sodium ions apparently were more effective in forming non-bridging oxygen bonds within the tetrahedra. It is possible that Na^+ can replace either the organometallic radical or the hydroxyl radical in the reaction products. The size of secondary particles decreased with increasing Na_2O content. The closer packing caused the total pore volume to decrease as well as increase the bulk densities. Microhardness decreased with increasing Na_2O content, indicating that it is only related to the primary network structure.

The transmission spectra of the samples (Fig. 1) showed that the UV cutoff occurred at longer wavelengths than that of the fused silica glass [8], but not appreciably. The spectra of pure silica gel and 3 mol% Na_2O-97 mol% SiO_2 gel were very close to each other. The IR spectra (Fig. 2) was almost the same as that obtained previously on small samples [2]. The band at about 1090 cm^{-1} was attributed to the stretching vibration of the Si-O-Si bonds [2]. The band at 475 cm^{-1} was attributed to the rocking vibration of the Si-O-Si bonds, and the band located at 785 cm^{-1} was attributed to the ring structure of the tetrahedra [2]. When the content of Na_2O increased, the intensity of the peaks at 1090 cm^{-1}, 475 cm^{-1} and 785 cm^{-1} decreased. Thus, the IR spectra was generally the same as observed for Na_2O-SiO_2 melt glasses [9].

The refractive index of Na_2O-SiO_2 binary glasses increases with Na_2O content [10] (Fig.4). The data in Fig. 4 shows that the refractive index of

the XNa_2O-$(1-X)SiO_2$ gels also increases with an increase in Na_2O content. However, in glass, the refractive index depends simply on the density of the glass as required by the Lorenz-Lorentz relationship. In a gel refractive index depends on bulk density rather than true density as discussed in more detail elsewhere [5].

CONCLUSION

1) Dried monolithic gels with composition XNa_2O-$(1-X)SiO_2$ (with X from 0 mol% to 7 mol%) were obtained successfully by catalyzed organometallic sol-gel processing.

2) The comparison of the ultrastructure and properties of Na_2O-SiO_2 gels with pure silica gel and melt glasses of the same compositions show that a 3 mol% Na_2O-97 mol% SiO_2 gel has optical properties that are similar to a pure silica gel but can be densified at a substantially lower temperature.

ACKNOWLEDGEMENTS

The Authors gratefully acknowledge the partial financial support of AFOSR Contract No. F49620-85-C-0079.

REFERENCES

1. L.L. Hench, M. Prassas and J. Phalippou, J. Non-Cryst. Solids 53, 183-193 (1982).

2. M. Prassas, L.L. Hench, J. Phalippou and J. Zarzycki, J. Non-Cryst. Solids 48, 79-95 (1982).

3. M. Prassas, J. Phalippou and L. L. Hench, J. Non-Cryst. Solids, 63, 375-389 (1984).

4. S.H. Wang and L.L. Hench, in Better Ceramics Through Chemistry, edited by C. J. Brinker, D. E. Clark and R. R. Ulrich (Elsevier Science Publishes, New York, (1984) pp. 71-78.

5. Rounan Li and L.L. Hench, to be published.

6. W.D. Kingery, H.K. Bowen and D.R. Uhlmann, in Introduction to Ceramics (John Wiley and Sons, New York, 1976) pp. 595-596.

7. J. Zarzycki, in Glass Current Issues edited by A.F. Wright and J. Dupuy (Nijhoff Publishes, Dordrecht/Boston/Lancaster, 1985).

8. R.H. Doremus in Glass Science (John Wiley and Sons, New York, 1973) p. 320.

9. I. Simon, in Modern Aspects of the Vitreous State, V.1, edited by J.D. Mackenzie (Butterworth & Co. Ltd., 1960) p. 137.

10. G.W. Morey, in The Properties of Glass (Reinhold Publishing Corporation, New York, 1938) p. 229.

CORRELATIONS BETWEEN PROCESSING PARAMETERS, ULTRASTRUCTURE, AND STRENGTH OF GEL-SILICA

JON K. WEST, RANDY NIKLES, GUY LATORRE
University of Florida, Advanced Materials Research Center, One Progress Blvd., #14, Alachua, FL 32615

ABSTRACT

The effect of various processing parameters during the aging of sol-gel derived silica are evaluated. Improvement in the physical properties of the wet gel-silica are shown to be well correlated to their aging temperatures and time. Changes in the pore structure also show correlations with aging process parameters.

INTRODUCTION

Gel-silica processing offers the potential of rapidly producing high quality optical silica components. This new type of optical material can be classified into two types of ultrapure gel-silica: Type V and Type VI [1]. Type VI is a fully stable ultraporous silica with applications in electronics, electro-optical interconnects and waveguides [2]. Type V silica is fully dense, water free and contamination free with an extremely wide transmission window in the UV-VIS-NIR [3].

The importance of maximizing sol-gel process yields cannot be overemphasized. The ability to control the ultrastructure and the mechanical properties during processing would allow improvements in the overall process. The initial goal is to correlate aging process variables with the resulting ultrastructure and mechanical strength of the gels. Later studies are planned to use gels of improved mechanical properties in drying and stabilization process optimization.

GEL-SILICA PROCESSING

The process starts with a chemical reaction of TMOS (tetramethoxysilane) with nitric acid catalyst, and H_2O (deionized) to form the sol. Once mixed and cast the sol is aged. During that time, the sol forms a highly porous solid called a gel with pore radii ranging from 10 Å to 20 Å. Next, during the drying step, the liquor surrounding the structure is driven off, the pores collapse, and lose their liquid content. In the final portion of the process, the gel is heated to 1150°C to 1200°C and fully dense glass is formed. This study is focussed on the aging part of this gel-silica process.

During the aging step the strength of the gel increases. This increase is determined as a function of aging time and temperature. It is expected that gel strength will increase with increased aging temperature and as the log of aging time. The method of determining strength was by four point bend testing. The data collected from these tests should give an understanding of the times and rates of certain chemical changes in the aging process. The data should show whether the expected logarithmic trend is seen experimentally.

EXPERIMENTAL

The sols were prepared by mixing controlled quantities of the precursor, water, and acid ratios. After one hour of stirring, the solution was vacuum filtered, then poured into rectangular polystyrene molds 2 3/4" deep, 2 1/2" wide, and 8 3/4" long. Each mold contained 240 ml of solution. The containers were sealed and placed into various control conditions. All mixing and casting was done in a hood. The 160 casts were separated into 6 temperature groups of 25°C, 45°C, 60°C, 75°C, 90°C and 105°C. Each group was then equally distributed over a time period of one, two, four, eight, sixteen, twenty-five and thirty-two days. After each set of samples was aged at their predetermined temperature and time intervals, they were placed in a refrigerator at ∿0°C. The cold environment was intended to retard the aging process until testing was completed.

The stress testing procedure was based on ASTM standard C 158-80 [4]: Flexure Test of Glass. The four point fixture was placed in an Instron Model 1123 with cross head speed of five mm/min. The grams force ranged from 1000 grams to 5000 grams. Each sample was measured in length before testing, with width, height and microhardness measured after testing. The samples were then returned to the 0°C environment to preserve their structure before the porosity was measured. The porosities were measured on dry gels after an identical drying schedule with a maximum temperature of 200°C. The microhardness measurements were made with a Vickers indenture on the wet gels. These values were used to quantify the plastic depressions made by the four-point-bend fixture. The values of the Vickers Hardness Number (VHN) were used to calculate the reduction of cross head deflection by a small fraction. The modified deflection value was the basis for the elastic modulus calculations.

RESULTS AND DISCUSSION

Figure 1 shows the average elastic modulus modeled as a logarithmic function of aging time and temperature from room temperature to 75°C. The elastic modulus was calculated using a modified deflection, f, based on the microhardness values. The VHN is related to the surface area, SA, of the indenture and the load as follows:

$$SA = \sqrt{2} \quad \frac{L}{VHN} \qquad (1)$$

where L = load in kg

This relation was used to estimate the actual deflection of the test bars by subtracting the small plastic depression Δ caused by the test fixture touching the wet gels:

$$\Delta = \frac{1}{2b} \quad (\sqrt{2} \cdot \frac{L}{VHN} - b \cdot t) \qquad (2)$$

where

b = width of test sample

t = width of supports = 6.35 mm

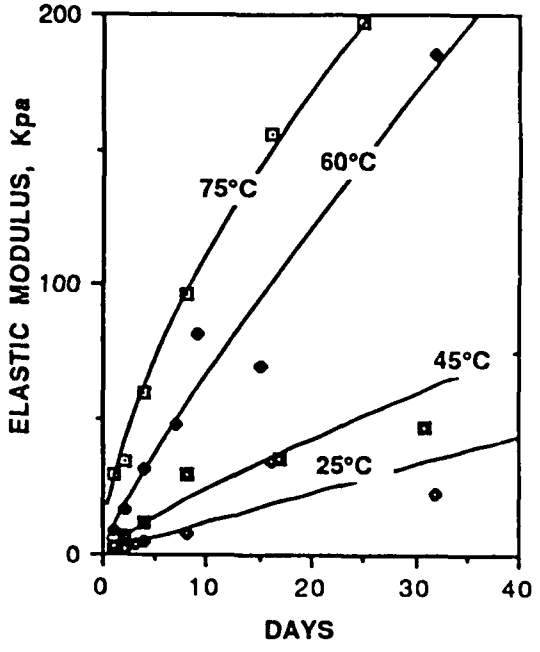

Figure 1. Elastic modulus below 90°C.

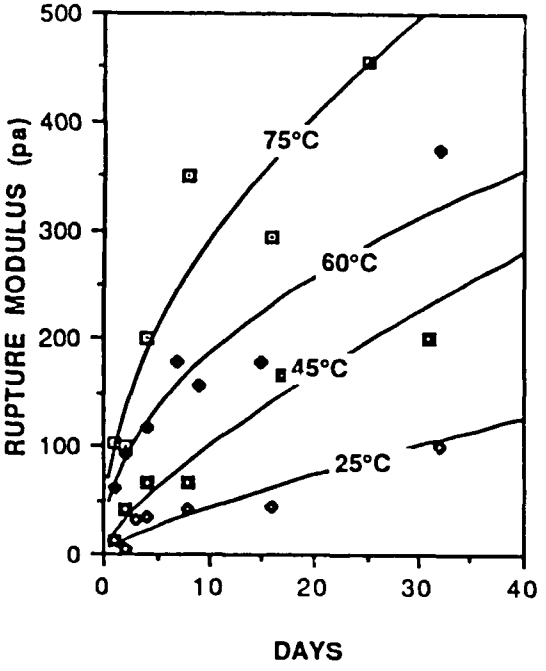

Figure 2. Rupture modulus below 90°C.

The deflection, f, of the sample is related to the elastic modulus E [5] as follows:

$$E = \frac{3La l^2}{2(f-\Delta)bd^3} \qquad (3)$$

where a = moment = 63.5 mm

b = width of sample

d = thickness

L = load in gm

l = distance between lower supports = 152.4 mm

f = deflection measured by cross head travel

Finally, the rupture modulus, S, is related to the rupture load L by:

$$S = \frac{3\ L\ a}{b\ d^2} \qquad (4)$$

where all of the variables have been defined as for equation (3).

Figure 2 shows the average rupture modulus for the same set of samples as Figure 1. The set of curves are logarithmic functions of aging time and temperature.

Figure 3 shows tne average elastic modulus modeled as a logarithmic function of aging time and temperature 90°C and 105°C.

Figure 4 shows the average rupture modulus modeled as a logarithmic function of the aging time and same temperature as Figure 3.

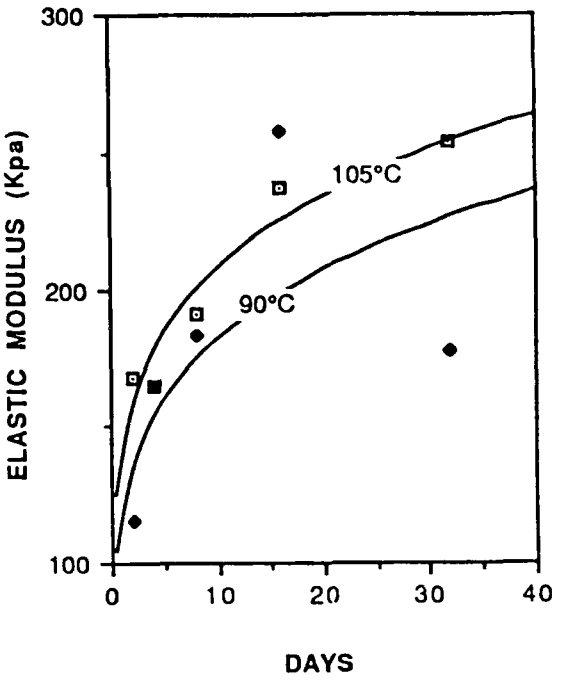

Figure 3. Elastic modulus above 90°C.

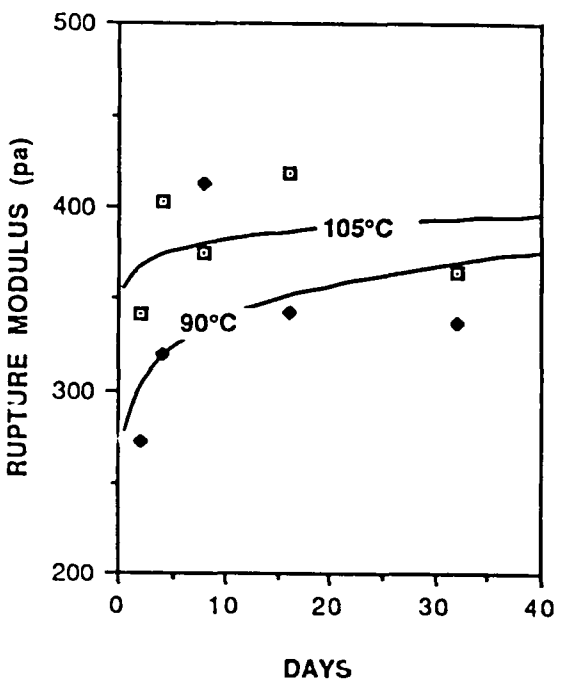

Figure 4. Rupture modulus above 90°C

Using linear interpolation of the VHN, the plastic depression Δ was calculated for 65 of the test samples. The value Δ appeared to be relatively constant. The stronger gels broke under higher loads which kept Δ constant:

mean Δ = 0.1169
Standard Deviation = 0.1165

This value was then used throughout the study.

Samples were difficult to maintain and process at these elevated temperature. The lower temperature samples were simply aged in the molds. However, high temperature, above 60°C, samples had to be gelled and transferred into other containers. Samples aged above 75°C were transferred into autoclaves after they were gelled.

Logarithmic regression curves are shown on the figures of Elastic Modulus and Rupture Modulus. The regression coefficient (r^2) values, strengths and standard deviations are shown in Table I and verify aging time as a logarithmic variable.

Finally, the ultrastructure was characterized as a function of aging time and aging temperature. Table I also shows that the pore volume and pore size for both increased with aging time and temperature.

CONCLUSIONS

The observed trend of increased strength was expected. However, the magnitude of the effect was much larger than expected. The improved microhardness, rupture modulus and elastic modulus correlate well to the increased aging time and temperature. These trends indicate clearly the need to investigate the effects this increase in mechanical properties would have drying. Gels aged for just a few days at temperatures over 100°C have

Table I. Ultrastructure and Strength as Function of Aging Time and Temperature with Regression Coefficients

Age Time (Days)	Age Temperature	n	Elastic Modulus Mean (Kpa)	Elastic Modulus Stand. Dev.	Rupture Modulus Mean (pa)	Rupture Modulus Stand Dev.	Surface Area (m^2/gm)	Pore Volume (cc/gm)	Pore Radius Å
2	25° C	1	2.1	-	4.8	-	-	-	-
3	25° C	4	4.0	0.6	32.5	19.3	-	-	-
4	25° C	4	4.7	0.7	33.2	10.7	-	-	-
8	25° C	4	8.2	0.3	40.7	10.2	-	-	-
16	25° C	4	34.9	41.1	43.6	36.2	-	-	-
32	25° C	3	22.7	0.9	101.4	42.8	-	-	-
			R^2 = 0.383		R^2 = 0.673				
1	45° C	6	2.8	1.4	12.4	8.2	771.7	0.485	12.6
2	45° C	5	6.5	1.6	41.5	11.3	-	-	-
4	45° C	4	11.9	1.9	65.3	4.2	-	-	-
8	45° C	5	29.5	20.8	65.8	37.1	773.4	0.496	12.85
17	45° C	4	35.6	1.6	167.3	8.8	-	-	-
31	45° C	4	47.6	7.6	200.4	80.8	-	-	-
			R^2 = 0.955		R^2 = 0.921				
1	60° C	5	8.7	2.8	61.3	14.5	745.6	0.479	12.89
9	60° C	3	82.1	21.5	157.2	52.9	735.9	0.474	12.87
15	60° C	6	69.9	10.0	179.2	52.0	791.5	0.510	12.9
32	60° C	4	185.1	16.8	375.7	436.5	780.1	0.535	13.7
			R^2 = 0.971		R^2 = 0.943				
1	75° C	4	29.9	23.7	103.5	35.0	807.6	0.544	12.45
8	75° C	5	96.2	56.2	350.5	254.2	854.1	0.532	12.46
16	75° C	4	155.9	38.4	294.3	78.5	781.8	0.493	12.6
25	75° C	4	196.8	32.4	456.9	216.2	801.4	0.545	13.6
			R^2 = 0.986		R^2 = 0.889				
2	90° C	6	115.9	56.3	272.4	134.1	799.9	0.475	11.8
4	90° C	6	165.4	42.6	320.4	161.2	834.0	0.519	12.4
8	90° C	5	183.2	19.6	413.7	99.3	862.0	0.608	14.1
16	90° C	6	259.9	58.9	343.7	113.6	822.0	0.726	17.7
32	90° C	6	178.0	18.1	337.6	95.5	751.2	0.890	23.7
			R^2 = 0.523		R^2 = 0.277				
2	105° C	6	167.7	17.2	342.5	70.5	794.5	0.498	12.52
8	105° C	6	191.2	27.5	375.8	45.8	658.2	0.937	28.47
16	105° C	6	237.1	73.4	418.6	118.5	792.6	0.768	19.37
32	105° C	6	253.4	48.7	365.5	63.6	797.5	0.761	19.08
			R^2 = 0.912		R^2 = 0.115				

strength that can gained. The logarithmic plateau seen in the 90° and 105° samples indicate particle growth may have stop and equilibrium with particle deterioration may be occurring. This effect is discussed in an aging model presented by Iler [6,7] evaluated by Orcel and Hench [8].

The model of the aging process is the dissolution of the smaller particles which is then redeposited onto the larger particles. The model predicts that this process is thermally activated and was found to be so in a study of multicomponent sol-gel by Orcel and Hench [9] and in this study.

As the surface area of the particles increase it takes more and more redoposition to generate an effect. Thus the strength is a logarithmic function of time.

ACKNOWLEDGEMENTS

This work was funded by AFOSR contract No. F49620-85-C-0079. Thanks is extended to student laboratory assistants Dan Bartlett, John Ringelberg and Fang Wang.

REFERENCES

1. L.L. Hench, S.H. Wang and J.L. Nogues, to be published in Proceedings of SPIE Meeting, Los Angeles, CA, 1988.

2. R.V. Ramaswamy, T. Chia, R. Srivastava, A. Miliou and J.K. West, to be published in Proceedings of SPIE Meeting, Los Angeles, CA, 1988.

3. S.H. Wang, L.L. Hench and C. Campbell, to be published in the Proceedings of the 3rd Annual Ultrastructure Conference, San Diego, CA., 1987.

4. ASTM Standard C158-80, Flexure Testing of Glass (Determination of the Modules of Rupture) pp. 25-31.

5. Lionel S. Marks, Mechanical Engineers' Handbook, Fourth Edition (McGraw-Hill, N.Y., 1941) pp. 455.

6. Ralph K. Iler, Chemistry of Silica, (John Wiley and Sons, NY, 1979).

7. Ralph K. Iler in Science of Ceramic Chemical Processing, edited by L.L. Hench and D.R. Ulrich (John Wiley and Sons, NY, 1986) pp. 3-19.

8. L.L. Hench, G. Orcel, and J.L. Nogues, in Better Ceramics Through Chemistry II, edited by C.J. Brinker, D.E. Clark, and D.R. Ulrich (Mater. Res. Soc. Proc. 73, Pittsburgh, PA, 1986) pp. 35-47.

9. G. Orcel and L.L. Hench, in Science of Ceramic Chemical Processing, edited by L.L. Hench and D.R. Ulrich (John Wiley and Sons, NY, 1985) pp. 224-230.

SOL-GEL PROCESSING OF LARGE SILICA OPTICS

L. L. Hench*, M. J. R. Wilson*, C. Balaban** and J. L. Noguès**

* Advanced Materials Research Center, Univ. of Florida, One Progress Blvd., Box 14, Alachua, Florida 32615

** GELTECH, Inc., One Progress Blvd., Box 18, Alachua, Florida 32615

Abstract

Since the first Ultrastructure Processing Conference the progress made in sol-gel science allowed the development of two new types of optical silica. A fully dense sol-gel derived silica, termed Type V Gel-Silica, can be made either with a colloidal or an organometallic process. An optically transparent porous silica, termed Type VI Gel-Silica can be made by the organometallic route and can be used for applications such as an optical element with a second phase impregnated within the pores or as a substrate for laser written waveguides.

The major progress was made in size scale-up by: 1) developing an understanding of the chemical mechanisms involved in sol-gel-glass processing, and 2) establishing careful process controls for each processing step. This progress allowed the production of optics of 75 and 100 mm in diameter or larger for both Type V and Type VI silicas respectively.

The physical properties of the organometallic derived Type V Gel-Silica are equal or superior to Types I-IV optical silicas and include: short UV cutoff, low optical absorption throughout the spectrum, high homogeneity, very few defects, low strain birefringence, and low coefficient of thermal expansion.

Both the colloidal and the organometallic methods can be used to produce complex net shapes by direct casting at ambient temperature. This unique property of the sol-gel process can be used to make optics with special shapes and surface features such as lightweight mirrors, Fresnel lenses and aspheric optical components.

Introduction

In the first Ultrastructure Processing Conference in 1983, J. D. Mackenzie summarized numerous potential advantages and disadvantages of sol-gel processing [1]. The advantages cited were largely based upon the intimate mixing possible with chemically based processing compared with powder processing. The disadvantages primarily centered around the difficulties in controlling this new generation of molecular based processing and potential costs.

The objective of this paper is to summarize and present, six years later, the progress made in achieving the advantages and minimizing the disadvantages in the sol-gel processing of one important application, sol-gel derived silica optics. The potential advantages discussed are: Homogeneity, Purity, Coefficient of Thermal Expansion, As-Cast Shapes and Surface Features, and Unique Properties of Silica Ultrastructures such as for Doping Applications and Laser Enhanced Densification.

The possible disadvantages discussed in this paper are inherent to size scale-up. They can be in most cases overcome by well defined processing including: Control of Drying, Elimination of Casting Defects, and Precise Atmosphere Control. The consequence of overcoming most of these problem areas is the ability to make new types of silica optics with sizes of 100 mm and larger using organometallic based sol-gel silica processing.

Silica Optics Processing

Silica optics are preferred for many optical systems, such as intracavity laser optics, because of the characteristics listed in Table 1. Development of a successful sol-gel derived process for making silica optics requires achieving all the features listed in this table. It also requires achieving significant improvements in at least some of the most important properties over what is presently produced commercially.

There are presently four major methods of manufacturing silica optics, as summarized in Table 2 [2,3]. The first two processes involve melting naturally occurring quartz crystals at high temperatures. The resulting materials are termed *Fused Quartz*. Deficiencies of fused quartz optics can include: substantial amounts of cation impurities (Type I), hydroxyl impurities (Type II), inhomogeneities, seeds, bubbles, inclusions, and microcrystallites. The relative extent of these defects depends on the grade of fused quartz. The higher the grade, the fewer the defects but the higher the cost and the more difficult the production of large optics.

Both Types III and IV are termed synthetic *Fused Silica*. The cation impurity content of fused silica optics is substantially lower than fused quartz optics due to the higher purity of the raw materials [3]. It is difficult for the chemical reactions indicated in Table 2 for these types of silica to go to completion, consequently water contents up to a few thousands ppm are present in Type III silica, and Cl ion contents of a few hundreds ppm can be retained as an unreacted residue in both Type III and Type IV silicas. Other defects are somewhat lower for fused silicas than for fused quartz [3]. The nature of the chemical processes involved in the production of Types III and IV silicas makes the direct manufacture of near net shape optics impossible. Price increases considerably as the quality of fused silica and the size of the optics increase.

During the last few years chemically based sol-gel processes have been developed and lead to the manufacture of Types V and VI silicas as described in Table 2 [3-6]. These processes offer the potential for improving many features of silica optics listed in Table 1. Additional advantages over Types I to IV silicas are also possible, as described in Table 3.

Two primary sol-gel processing methods for silica optics have reached commercialization; 1) hydrolysis and condensation of an organometallic precursor [3-5], and 2) gelation of a colloidal alkali silicate powder suspension [6]. The silicas resulting from these sol-gel processes are termed Type V when the final product is fully dense with no residual porosity. If the densification process is not accomplished entirely the organometallic method produces a porous optical material named Type VI silica.

The ultrastructure of the gel and the final densification conditions are considerably different for the organometallic vs the colloidal methods of manufacture of sol-gel silicas, as summarized in Figure 1. An organometallic based sol-gel silica, such as Gelsil™†, has a totally interconnected porosity with a dried bulk density of 1.2 g/cm^3, an average pore diameter of 2.5 nm and a specific surface area of 700-800 m^2/g prior to densification [3]. Because of the very small pore size and the very narrow distribution of pores the gel is optically transparent. The uniformity of the ultrastructure results in densification at a very low temperature, 1150°C, without a change in mean pore radius. Densification takes place almost entirely by decreasing the connectivity (genus) of the uniform pore network [7], and is very sensitive to pore size, as shown in Figure 2.

Since there is no pore growth by Ostwald ripening, the organometallic derived monoliths remain optically transparent throughout the processing schedule shown in Figure 1, after they pass the opaque stage in drying [8]. Examples of a large 100 mm organometallic sol-gel derived optical silica monolith after drying is shown in Figure 3a. Samples of organometallic derived Type VI and Type V silica plano-plano optical components are shown in Figures 3b and 3c, respectively.

The colloidal sol-gel optics process developed by R. D. Shoup [6] involves nucleation and polymerization of potassium silicate by colloidal silica in the presence of a hydrolytic organic reagent. By varying the ratio of colloidal species to soluble silicate the gel pore diameter can be controlled between 10 to 300 nm with a relatively narrow size distribution. As a result, strong silica gel structures are formed by the colloidal process with large pores, >200 nm diameter, that can resist capillary pressures encountered during drying. Microwave drying can be used for these ≥80% porous colloidal gels in minutes to hours, depending on body dimensions, without cracking.

The large pore structures produced in the colloidal sol-gel method help in the removal of alkali ions by an aqueous dealkalization process. The large pores also facilitate gaseous removal of chemisorbed impurities prior to densification, yielding low water levels and alkali and transition metal impurity of a few hundreds of ppm. Total density is achieved after 30 minutes at 1500°C and high quality optical silica is achieved after 10 minutes at 1720°C. Examples of Type V silica glasses made by the colloidal gel-silica process are shown in Figures 4 and 5.

Factors in Size Scale-up

Scale-up of sol-gel processing has been considered potentially one of the greatest uncertainties. In order to achieve large optical components by the sol-gel route it is essential to control: 1) Drying Rates, 2) Defects in the as-cast gel monoliths, and 3) Removal of chemisorbed water prior to pore closure in densification. Control of these factors is less sensitive in the colloidal method because of the large pores in the structure.

1) Drying Control: A critical step in the drying of organometallic derived sol-gel optics is the rate of removal of water during the "opaque stage". As shown by Wilson and Hench in this proceedings [8], it is during the transition between filled pores and pore emptying that substantial bulk strains are developed in the gel monoliths.

The rate of water removal must be slowed during this critical period to avoid cracking. The gel monolith is relatively insensitive to the rate of drying prior to and after the opaque stage.

2) Defect Control: Imperfections in a gel will cause stress risers during drying and further processing steps. Consequently, even if a gel monolith has sufficient strength to withstand a given level of bulk strain the presence of stress risers will induce fracture. These imperfections can take many forms and are usually created during casting of the sol and are incorporated in the solid when gelation occurs. Several examples of bubbles, which are particularly damaging stress risers, are shown in Figure 6. In Figure 6a a stress field is beginning to develop around the bubble, in Figure 6b we can see a crack initiating from a bubble, in 6c three cracks have initiated, and in 6d a complex crack front originates from the interaction of stress fields around two bubbles.

Elimination of bubbles involves careful deareation of the sol prior to casting, using a casting technique which does not introduce air, avoiding gas generating chemical additives in the sol formula, and avoiding containers which nucleate bubbles at the interface.

3) Atmosphere Control: Tightly bound hydroxyl ions on the surface of pores must be removed prior to pore closure during densification for both organometallic and colloidal sol-gel silicas. Surface dehydroxylation occurs from 200°C to 1000°C for organometallic derived gels and up to 1300°C for colloidal silica monoliths. It is usually necessary to enhance the dehydroxylation process by flowing halogen-containing gases through the pore network before closure. In this particular case the atmosphere control treatment should include the removal of any halogen left in the structure of the glass. If densification is attempted without hydroxyl removal, foaming and bloating result due to expansion of the gases formed and trapped in the closed pores. Because of the very small size of pores in organometallic derived gels and the absence of pore growth during densification it is especially critical to have complete hydroxyl removal for these materials if they are to achieve full density. It is important to recognize that more internal SiOH groups are retained in an acid catalyzed organometallic derived gels at high temperature than base catalyzed gels [9]. The internal SiOH groups polarize the silica tetrahedra [10] which probably is responsible for a decrease in the viscosity of the silica gel network. Consequently viscous flow, responsible for pore closure and reduction of pore network connectivity, takes place at a lower temperature. Thus it is essential to optimize hydroxyl removal for acid catalyzed gels when the pore network has as large a connectivity as possible; i.e. at as low a

temperature as possible, e.g. below 900°C for small pore organometallic derived gels (Figure 2).

Control of drying rates, elimination of casting defects and rigorous atmosphere control can yield large sol-gel silica optical components as shown in Figures 3, 4 and 5.

Potential Advantages of Sol-Gel Silica Optics

1) Homogeneity: One of the primary incentives for use of chemically based ultrastructure processing of materials is improvement of homogeneity. The fact that organometallic precursors can be hydrolyzed with water on a molecular scale of mixing yields the possibility that the glass structure derived from an organometallic gel may have a molecular level of homogeneity. However, as indicated above macroscopic defects must be eliminated first in order to achieve high levels of homogeneity. Also, processing controls must be developed to eliminate fluctuations in the density and index of refraction during densification.

Successful processing controls have been achieved for organometallic derived optics up to 75 mm for Type V silica and 100 mm for Type VI silica (Figure 3). Results from optical property measurements show no evidence of bubbles, no striae, a superior index of refraction homogeneity of about 1-6 10^{-6}, and very low strain birefringence of 4-6 nm/cm. These characteristics of organometallic derived sol-gel silica (Gelsil™) are equal or superior to Types I-IV optical silicas. Figure 7a is an example of an earlier generation organometallic gel-silica monolith that was homogeneous as a gel but developed large index of refraction gradients during densification. This type of inhomogeneity can be eliminated, as shown in Figure 7b.

2) Purity and Properties: Another major incentive for low temperature chemically based processing is achieving a higher level of purity than traditional glass and ceramic processing methods. The organometallic sol-gel glasses have very few cation and hydroxyl impurities. An important consequence of the elimination of impurities is the improvement of transmission throughout the optical spectrum. Figure 8 compares the ultraviolet optical transmission of two commercial UV grade optical silicas (Type III) with a typical spectrum from an organometallic derived gel-silica (Type V). The vacuum UV cutoff wavelength is substantially improved for the gel-silica material. Recent quantum mechanical calculations of West et al have shown that the greater transmission in the UV can be attributed to a lower alkali and OH radical content in the gel-silica [11]. Results from the quantum mechanics

calculations are compared in Figure 9 with the improvement in gel-silica transmission over the last three Ultrastructure Processing Conferences, as the OH radical content of the gel-silica glasses has been progressively eliminated. The ultraviolet transmission of colloidal based silica is poorer than organometallic derived gel-silica due to a higher level of impurity inherent to the alkali-silicate based colloidal process.

Elimination of OH radicals from gel-silica optics also results in elimination of absorption bands in the near IR, as shown in Figure 10. This figure shows the difference between Type V gel-silica and Type III silica which exhibits absorption bands at 1400 nm and 2200 nm, and a very broad absorption band at 2730 nm. Reliability of production of low OH radical content in Type V gel-silicas (Gelsil™) has also been recently achieved.

3) Coefficient of Thermal Expansion: A very low coefficient of thermal expansion (CTE) is an especially important physical characteristic of optical silica. The organometallic process leads to the production of a Type V silica having a lower CTE than other types of silica. Figures 11 and 12 compare the thermal expansion and the CTE values of a Type V silica (Gelsil™) optics with the NBS silica reference and Type III and IV commercial silicas over the temperature range of 25°C to 700°C. The organometallic sol-gel optical silica have lower values of thermal expansion and CTE than the other types of silica [12].

4) As-Cast Shapes and Surface Features: Another area of potential advantage of sol-gel optics processing is that of obtaining net shapes and surfaces, or at least near-net shapes and surfaces, through casting sols at low temperature into molds of predetermined configurations. Advantages offered by this type of processing are listed in Table 3. A lightweight mirror with integrally cast face plate and honeycomb backing made by gelation of silica organometallic precursor is shown in Figure 13. This configuration has been successfully dried and a sample of similar size (75 mm in diameter) and shape has been successfully densified. A net shape honeycomb mirror backing made by the colloidal route is shown in Figure 4 and a complex mold casting of colloidal silica gel-glass is shown in Figure 5.

Another application of net shape casting is the replication of specific surface features. For example, Figure 14 shows the surface characteristic graphs obtained on a Sloan Dektak/FLM profilometer of a plastic Fresnel lens master and the corresponding gel-silica Fresnel lens. The lens master was machined in a polymer and the

organometallic sol-gel silica positive replica was made by direct casting against it. Figure 15 shows a microscope photograph of a dry organometallic sol-gel silica part. It can be seen from this photograph and the profilometry graphs that the replication of the surface details is very good. The precision of the master was maintained through densification into a Type V gel-silica. The advantages of the silica Fresnel lens over a polymer lens is the very low thermal expansion coefficient and the thermal and radiation stability of the silica compared to a polymer.

5) Porous Type VI Gel-Silica and Applications: The extremely small scale of interconnected porosity in organometallic derived gel-silica results in optical transparency to UV wavelengths as far as 250 nm. The transparent porous structure can be impregnated with a second phase thereby achieving an optical composite. Examples of optical polymers which have been put into Type VI silica (Porous Gelsil™) are shown in Table 4. Results from some of these studies have been discussed elsewhere [3,13]. The colloidal based silica processing produces gels with large pore size which are not optically transparent and therefore cannot be used to make Type VI optical silica.

Another unique application of the Type VI structure is to use it as the substrate for laser densification. Optical waveguides have been made using laser writing of higher density tracks on the porous gel-silica substrate [14]. The higher density tracks have a greater index of refraction than the porous matrix and therefore can serve as a planar waveguide. The prime advantage of the laser written waveguide is that it matches the index of refraction of silica fiber optics, which is not the case for ion-exchanged or diffusion based waveguides.

Conclusions

Since the first Ultrastructure Processing Conference the progress made in sol-gel science allowed the development of two new types of optical silica. A fully dense sol-gel derived silica, termed Type V Gel-Silica, can be made either with a colloidal process or an organometallic process. The colloidal method results in optically opaque gels due to large pores of >200 nm in diameter with ≥80% porosity requiring 1500-1720°C densification temperatures. The organometallic process results in optically transparent gels with 45% pores of only 2.5 nm in diameter and require a densification temperature of only 1150°C. An optically transparent sol-gel derived porous silica, termed Type VI Gel-Silica can be made by the organometallic route. This new type of silica can be used for applications such as an optical element with a second phase impregnated within the pores or as a substrate for laser written waveguides.

The major progress was made in size scale-up. This was achieved by: 1) developing an understanding of the chemical mechanisms involved in each of the seven sol-gel-glass processing steps, and 2) establishing careful process controls for each processing step. It is the precise control over the chemical mechanisms and rates of reactions that allows the production of optics of 75 and 100 mm in diameter or larger for both Type V and Type VI silicas respectively.

The physical properties of the organometallic derived Type V Gel-Silica are equal or superior to Types I-IV optical silicas and include: short UV cutoff, low optical absorption throughout the spectrum, high homogeneity, very few defects, low strain birefringence, and low coefficient of thermal expansion.

Both the colloidal and the organometallic methods of optical gel-silica manufacture can be used to produce complex net shapes by direct casting at ambient temperature. This unique property of the sol-gel process can be used to make optics with special shapes and surface features such as lightweight mirrors, Fresnel lenses and aspheric optical components.

Acknowledgements

The authors gratefully acknowledge financial support of Air Force Office of Scientific Research Contracts #F49620-88-C-0073, F49620-85-C-0079 and F49620-86-C-0120 and the encouragement of D. R. Ulrich throughout this research. Two of the authors (LLH and MJRW) also acknowledge financial assistance of the State of Florida High Tech and Industries Council.

Note: † Gelsil™ is a trademark of GELTECH, Inc.

References

1) J. D. Mackenzie, in: Ultrastructure Processing of Ceramics, Glasses, and Composites, eds. Larry L. Hench and Donald R. Ulrich (Wiley, New York, 1984) p. 15.

2) M. Grayson, ed., Encyclopedia of Glass, Ceramics, Clays and Cement (Wiley, New York, 1985).

3) L. L. Hench, S. H. Wang and J. L. Noguès, SPIE Vol. 878 Multifunctional Materials (1988) p. 76.

4) S. H. Wang, C. Campbell and L. L. Hench, in: Ultrastructure Processing of Advanced Ceramics, eds., John D. Mackenzie and Donald R. Ulrich (Wiley, New York, 1988) p. 145.

5) L. L. Hench, G. Orcel and J. L. Noguès, in: Better Ceramics Through Chemistry, Vol. 73, eds., C. Jeffrey Brinker, David E. Clark and Donald R. Ulrich (Materials Research Society, Pittsburgh, 1986) p. 35.

6) R. D. Shoup, in: Ultrastructure Processing of Advanced Ceramics, eds., John D. Mackenzie and Donald R. Ulrich (Wiley, New York, 1988) p. 347.

7) W. Vasconcelos and L. L. Hench, in: Proceedings 4th Ultrastructure Processing Conference, Tucson, AZ, February 1989.

8) M. J. R. Wilson and L. L. Hench, in: Proceedings 4th Ultrastructure Processing Conference, Tucson, AZ, February 1989.

9) G. Orcel, J. Phalippou and L. L. Hench, J. Non-Cryst. Solids 88 (1986) p. 114.

10) J. K. West, personal communication.

11) J. K. West et al, in: Proceedings 4th Ultrastructure Processing Conference, Tucson, AZ, February 1989.

12) C. Balaban, J. L. Noguès, To be published.

13) J. L. Noguès, S. Majewski, J. K. Walker, M. Bowen, R. Wojcik, and W. V. Moreshead, J. Am. Ceram. Soc. 71, 12, (1988) p. 1159.

14) R. V. Ramaswamy, T. Chia, R. Srivastava, A. Miliou, and J. K. West, SPIE Vol. 878 Multifunctional Materials (1988) p. 86.

Table 1: Features of Silica Optics

1) Excellent optical transmission from the ultraviolet (160 nm) to near infrared wavelengths (3600 nm)

2) Excellent refractive index homogeneity

3) Isotropic optical properties

4) Small strain birefringence

5) Very low coefficient of thermal expansion (CTE) of about 0.55 10^{-6} /°C

6) Very high thermal stability

7) Very high chemical durability

8) Small numbers of bubbles or inclusions

9) Ability to be polished to high standards

Table 2: Methods of Silica Optics Manufacture

Fused Quartz

Type I: Electric melting of natural quartz crystals

$$SiO_2 \text{ (quartz)} \xrightarrow[\text{vacuum}]{\text{heat}} SiO_2 \text{ (glass)}$$

Type II: Flame fusion of natural quartz crystals

$$SiO_2 \text{ (quartz)} \xrightarrow[\text{oxy-hydrogen}]{\text{heat}} SiO_2 \text{ (glass)}$$

Fused Silica

Type III: Vapor-phase hydrolysis of pure silicon tetrachloride carried out in a flame

$$SiCl_4 + O_2 + 2\,H_2 \rightarrow SiO_2 \text{ (glass)} + 4\,HCl$$

Type IV: Oxidation of pure silicon tetrachloride which is fused electrically or by means of a plasma

$$SiCl_4 + O_2 \rightarrow SiO_2 \text{ (glass)} + 2\,Cl_2$$

Gel-Silica

Type V: Gelation of alkali silicate colloidal solutions with fully densification (1500 to 1720°C)
or
Hydrolysis and condensation of organometallic precursor with fully densification (1150 to 1200°C)

$$Si(OR)_4 + 4\,H_2O \rightarrow Si(OH)_2 + 4\,(ROH)$$

$$Si(OH)_4 \rightarrow SiO_2 \text{ (dense gel-silica)} + 2\,(H_2O)$$

Type VI: Hydrolysis and condensation of organometallic precursor with partial densification (600 to 950°C)

$$Si(OR)_4 + 4\,H_2O \rightarrow Si(OH)_4 + 4\,(ROH)$$

$$Si(OH)_4 \rightarrow SiO_2 \text{ (porous gel-silica)} + 2\,(H_2O)$$

Table 3: Potential Advantages of Gel-Silica Optics

Net Shape/Surface Casting

- complex geometries
- light weight optics
- aspheric optics
- surface replication (e.g. Fresnel lenses)
- internal structures
- reduced grinding
- reduced polishing

Improved Physical Properties (Type V)

- lower coefficient of thermal expansion (CTE)
- lower vacuum ultraviolet cutoff wavelength
- higher optical transmission
- no absorption due to H_2O or OH bands
- lower solarization
- higher homogeneity
- fewer defects

Transparent Porous Structures (Type VI)

- impregnation with organic polymers
- graded refractive index lenses (GRIN)
- laser enhanced densification
- controlled chemical doping
- control of variable oxidation states of dopants

Table 4: Optical Composite Made from Type VI Silica (Porous Gelsil™)

NON-LINEAR OPTICAL POLYMERS

PBT [Phenylenebenzobisthiazole]
MNA [2-Methyl-4-Nitroaniline]

ORGANIC FLUORS

B-PBD [2-(4'-t-Butylphenyl)-5-(4"-Biphenylyl)-1,3,4-Oxadiazole]
P-TP [p-Terphenyl]
P-QP [p-Quaterphenyl]

WAVELENGTH SHIFTER

3-HF [3-Hydroxyflavone]

OTHER ORGANICS

Laser Dyes
Liquid Crystals

Figure Captions

Figure 1 Processing sequence for sol-gel silica optics.

Figure 2 Temperature dependence on pore network connectivity of organometallic gel-silicas with differing mean pore radii. Data courtesy of W. Vasconcelos, U. of Florida.

Figure 3 Organometallic sol-gel silica monoliths: (a) Dried, (b) Porous plano-plano optical component (Type VI Gelsil™), (c) Fully dense plano-plano optical component (Type V Gelsil™).

Figure 4 Lightweight mirror backing made by colloidal gel-silica process: (a) after drying, (b) after densification. Photo courtesy of R.D. Shoup, Corning Glass Works.

Figure 5 Near net-shape colloidal gel-silica component: (a) after drying, (b) after densification. Photo courtesy of R.D. Shoup Corning Glass Works.

Figure 6 Bubbles in a gel-silica monolith: (a) acting as a stress riser, (b) initiating a crack, (c) initiating 3 cracks, and (d) initiating a complex crack front.

Figure 7 Interferometry analysis of dense organometallic gel-silicas (Type V Gelsil™): (a) improperly densified with severe index gradients, (b) ideal densification with good homogeneity.

Figure 8 Ultraviolet optical transmission of a dense organometallic gel-silica (Type V Gelsil™) compared with two commercial Type III silicas.

Figure 9 Improvements in UV transmission of organometallic gel-silicas with time compared with quantum mechanics predictions of UV cutoff wavelength.

Figure 10 Near IR transmission of a dense organometallic gel-silica (Type V Gelsil™) compared with a Type III silica.

Figure 11 Thermal expansion of a dense organometallic gel-silica (Type V Gelsil™) compared with NBS silica reference and Types III and IV silicas.

Figure 12 Coefficient of Thermal Expansion (CTE) of a dense organometallic gel-silica (Type V Gelsil™) compared with NBS silica reference and Types III and IV silicas.

Figure 13 Lightweight sol-gel silica mirror with integral faceplate made by the organometallic route. Photo courtesy of J. West, M.J.R. Wilson, J. Parramore and B.F. Zhu, U. of Florida.

Figure 14 Profilometry graphs of Fresnel lenses: (a) Polymer master, (b) Replication in organometallic gel-silica.

Figure 15 Microscope photograph of a dry organometallic gel-silica Fresnel lens.

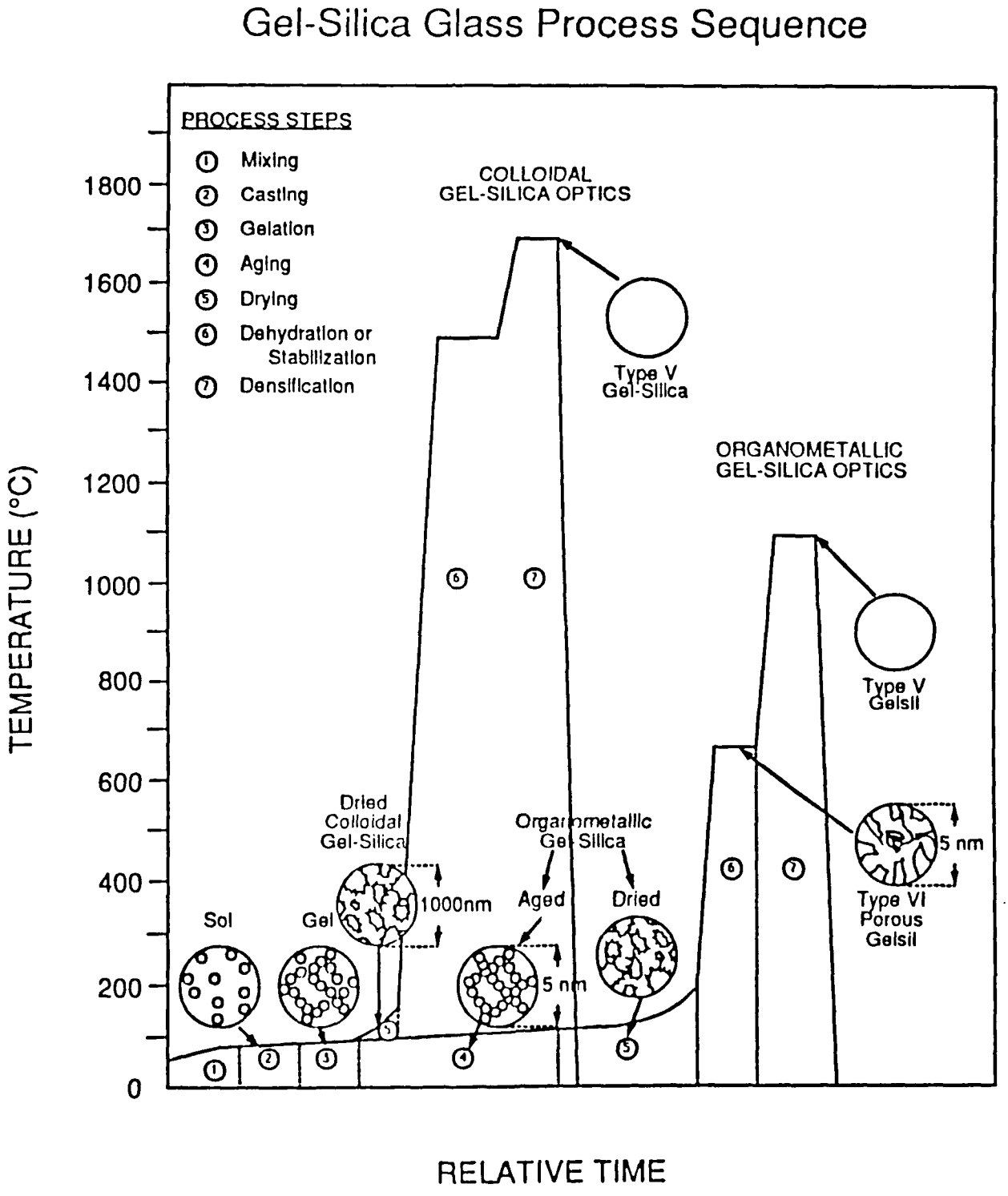

Figure 1: Processing sequence for sol-gel silica optics.

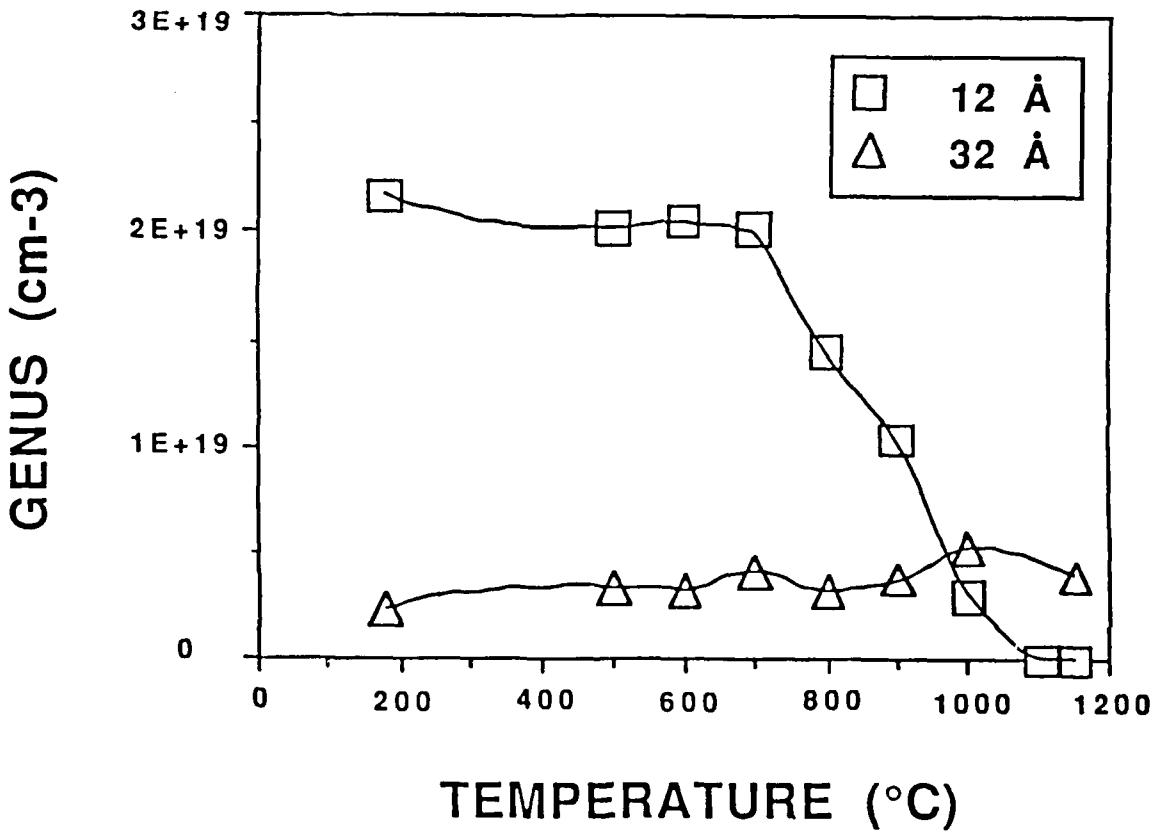

Figure 2: Temperature dependence on pore network connectivity of organometallic gel-silicas with differing mean pore radii. Data courtesy of W. Vasconcelos, U. of Florida.

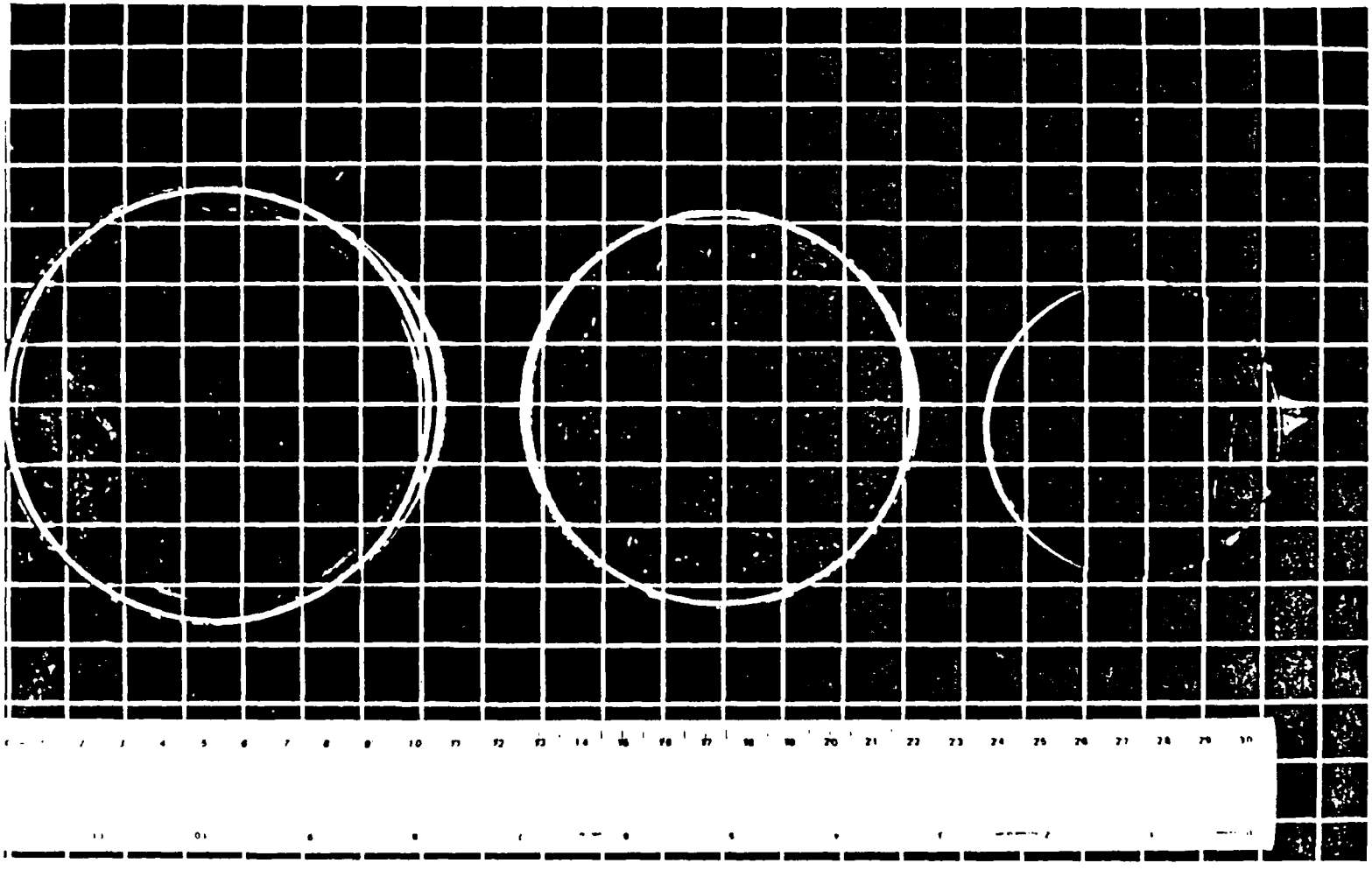

Figure 3: Organometallic sol-gel silica monoliths: (a) Dried, (b) Porous plano-plano optical component (Type VI Gelsil™), (c) Fully dense plano-plano optical component (Type V Gelsil™).

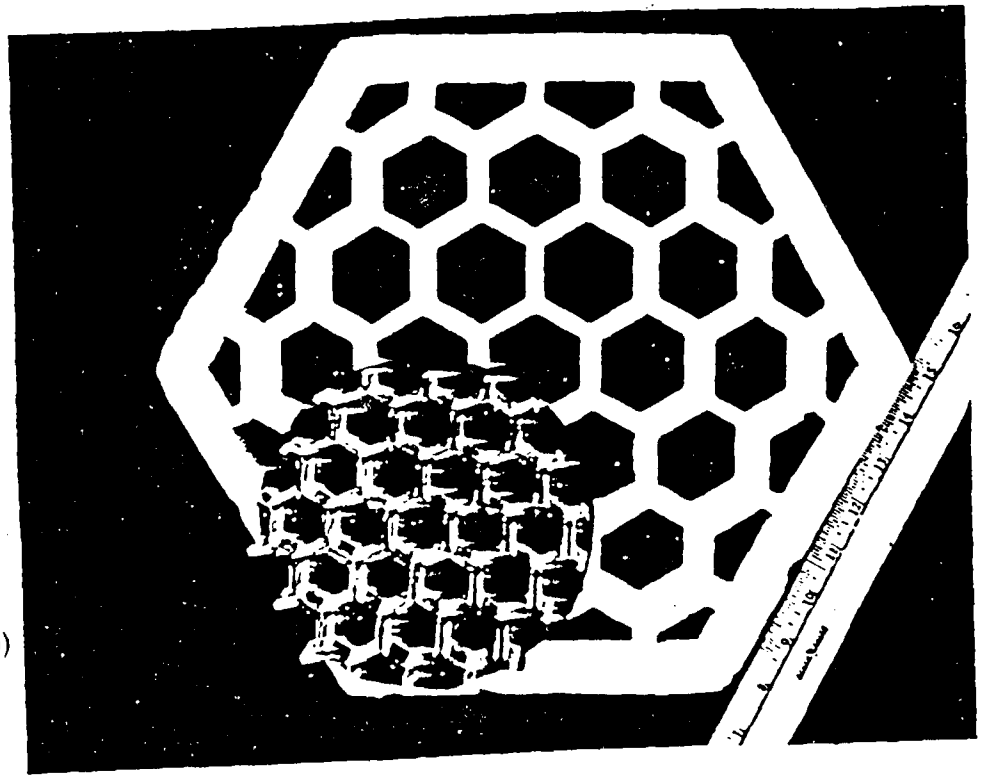

Figure 4: Lightweight mirror backing made by colloidal gel-silica process: (a) after drying, (b) after densification. Photo courtesy of R.D. Shoup, Corning Glass Works.

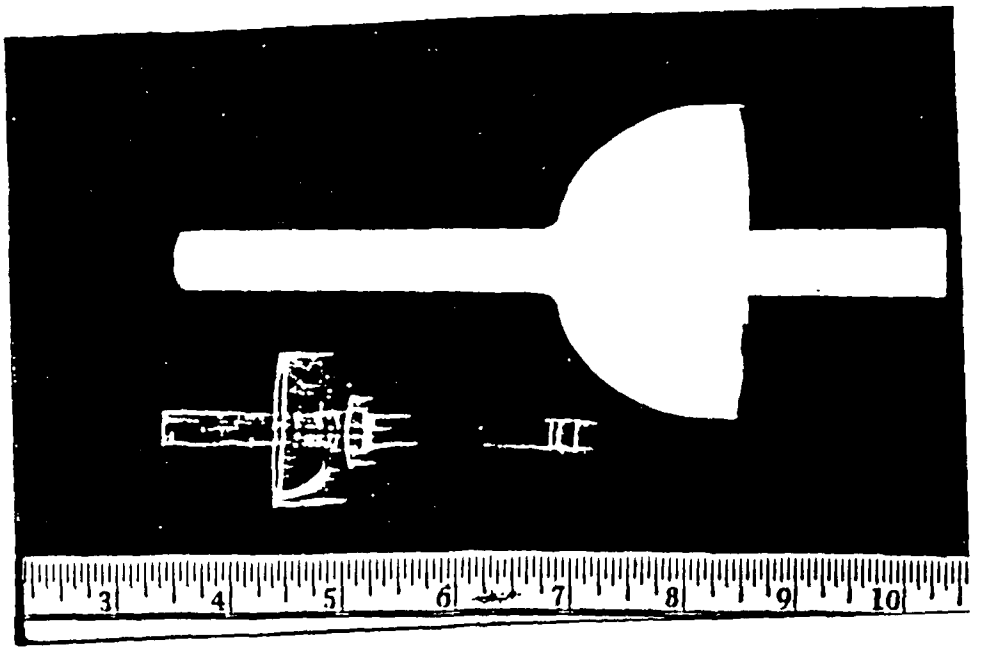

Figure 5: Near net shape colloidal gel-silica component: (a) after drying, (b) after densification Photo courtesy of R.D. Shoup Corning Glass Works.

(a)

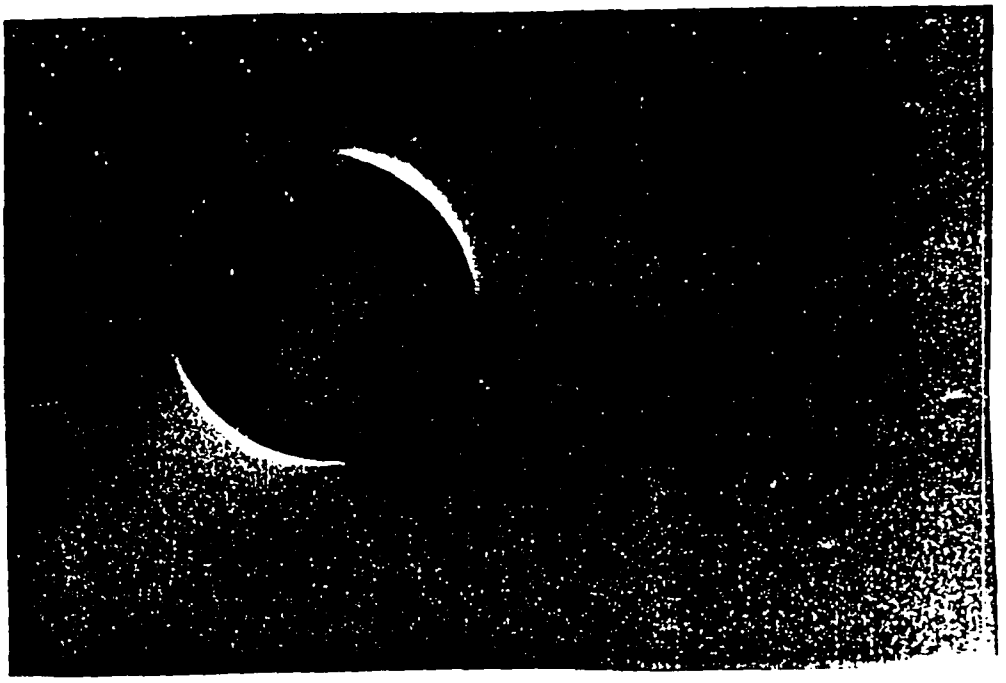

(b)

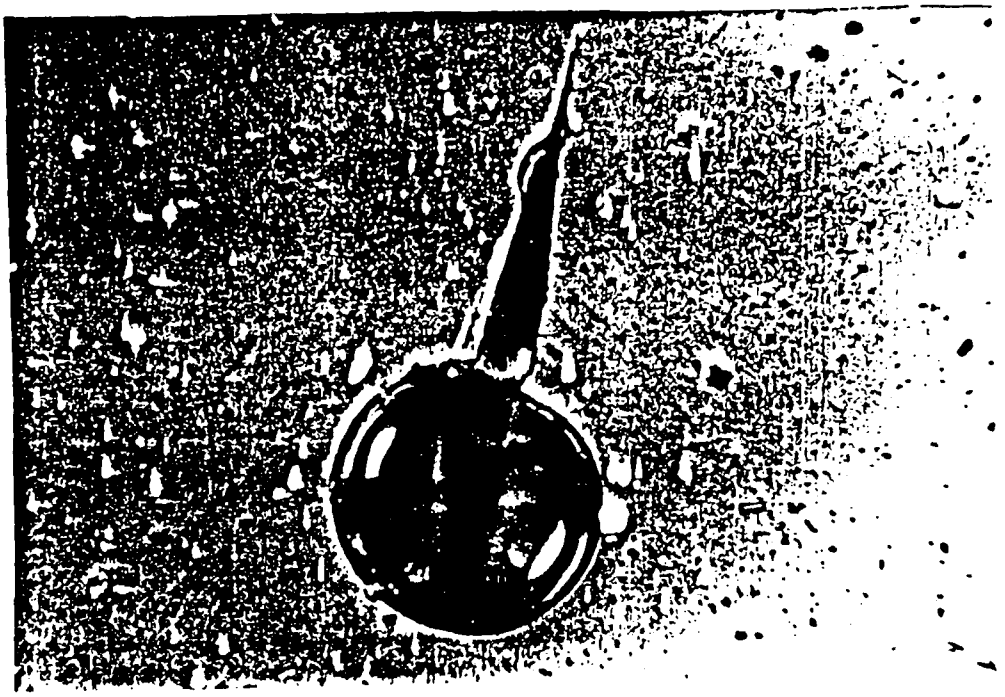

Figure 6: Bubbles in a gel-silica monolith: (a) acting as a stress riser, (b) initiating a crack, (c) initiating 3 cracks, and (d) initiating a complex crack front.

(c)

(d)

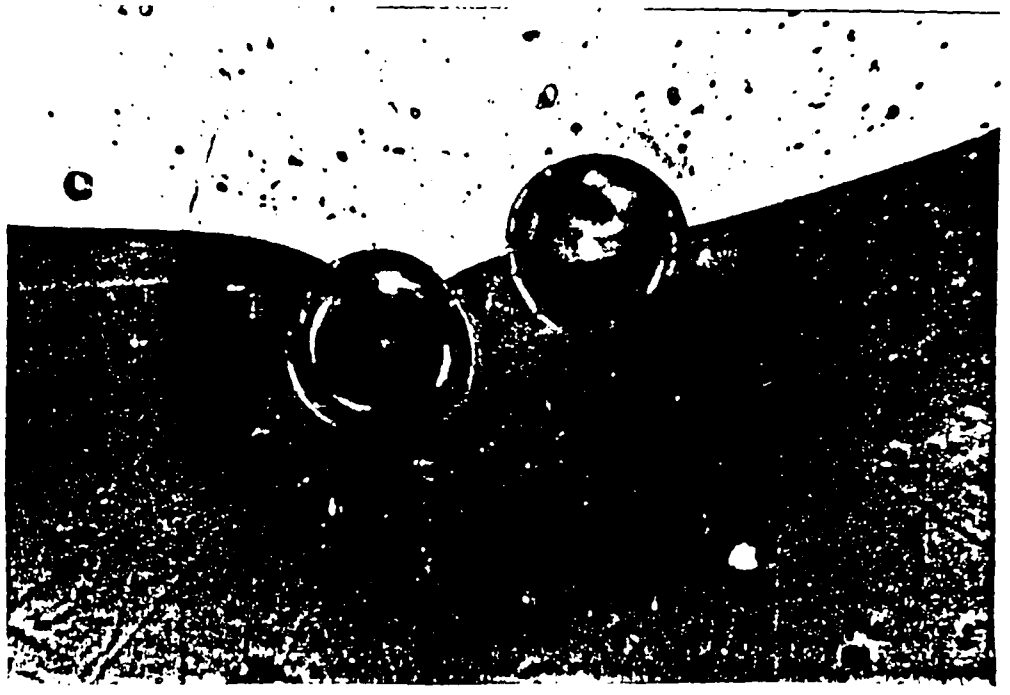

Figure 6: Bubbles in a gel-silica monolith: (a) acting as a stress riser, (b) initiating a crack, (c) initiating 3 cracks, and (d) initiating a complex crack front.

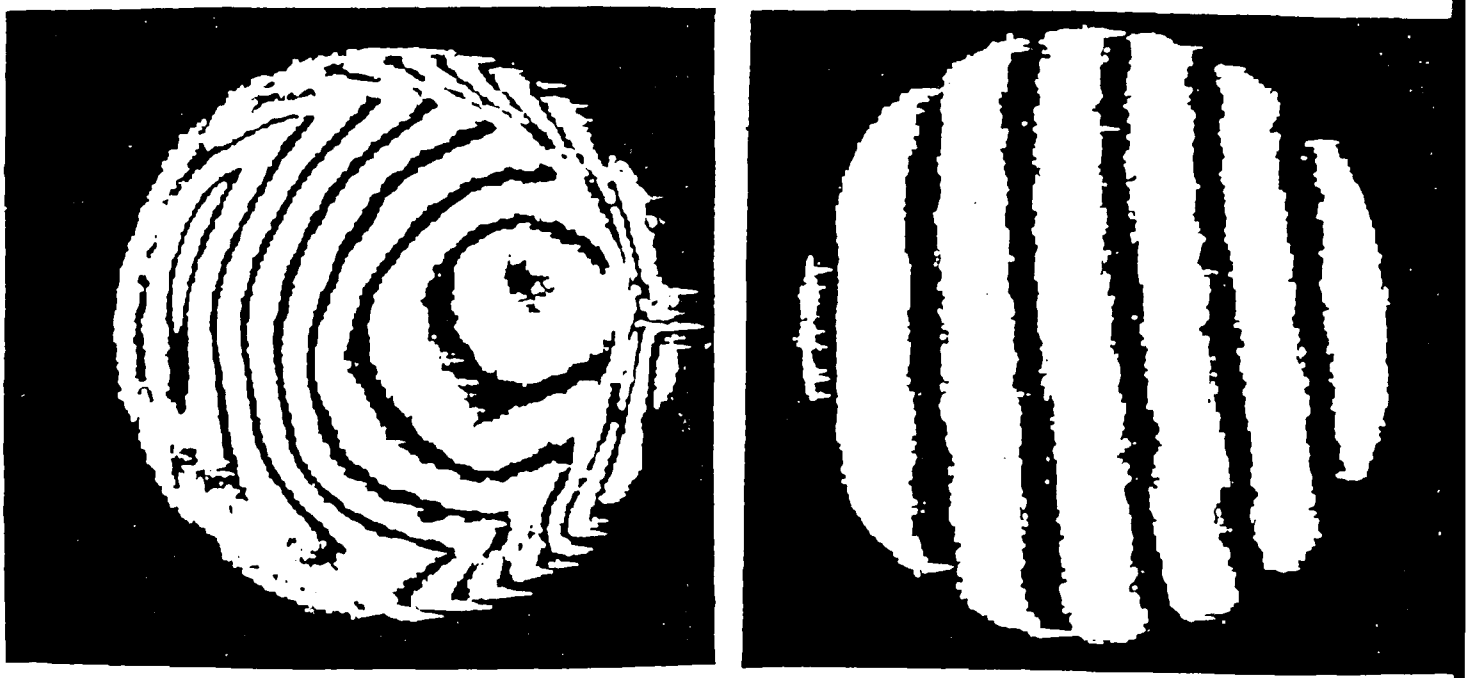

(a) (b)

Figure 7: Interferometry analysis of dense organometallic gel-silicas (Type V Gelsil™): (a) improperly densified with severe index gradients, (b) ideal densification with good homogeneity.

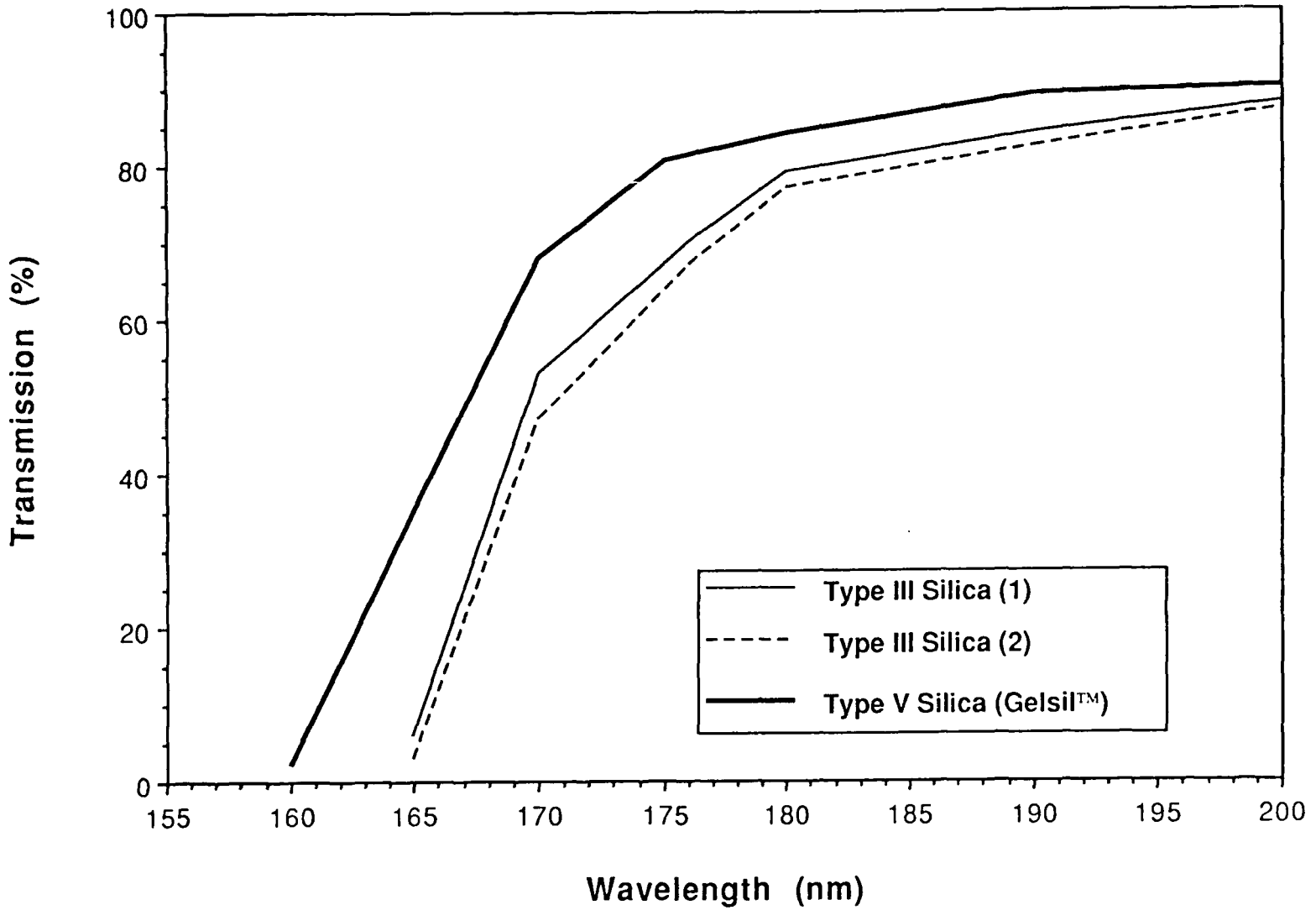

Figure 8: Ultraviolet optical transmission of a dense organometallic gel-silica (Type V Gelsil™) compared with two commercial Type III silicas.

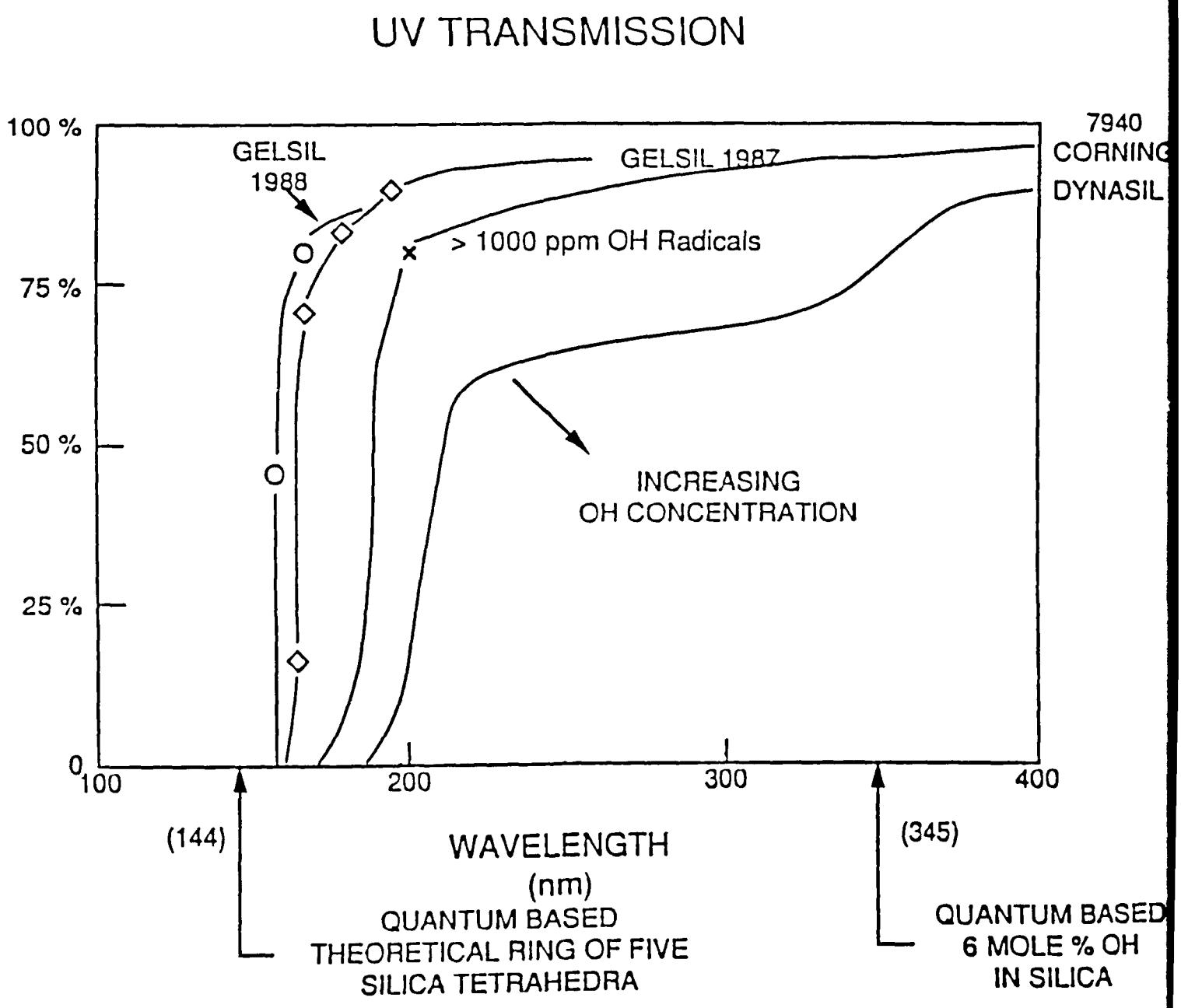

Figure 9: Improvements in UV transmission of organometallic gel-silicas with time compared with quantum mechanics predictions of UV cutoff wavelength.

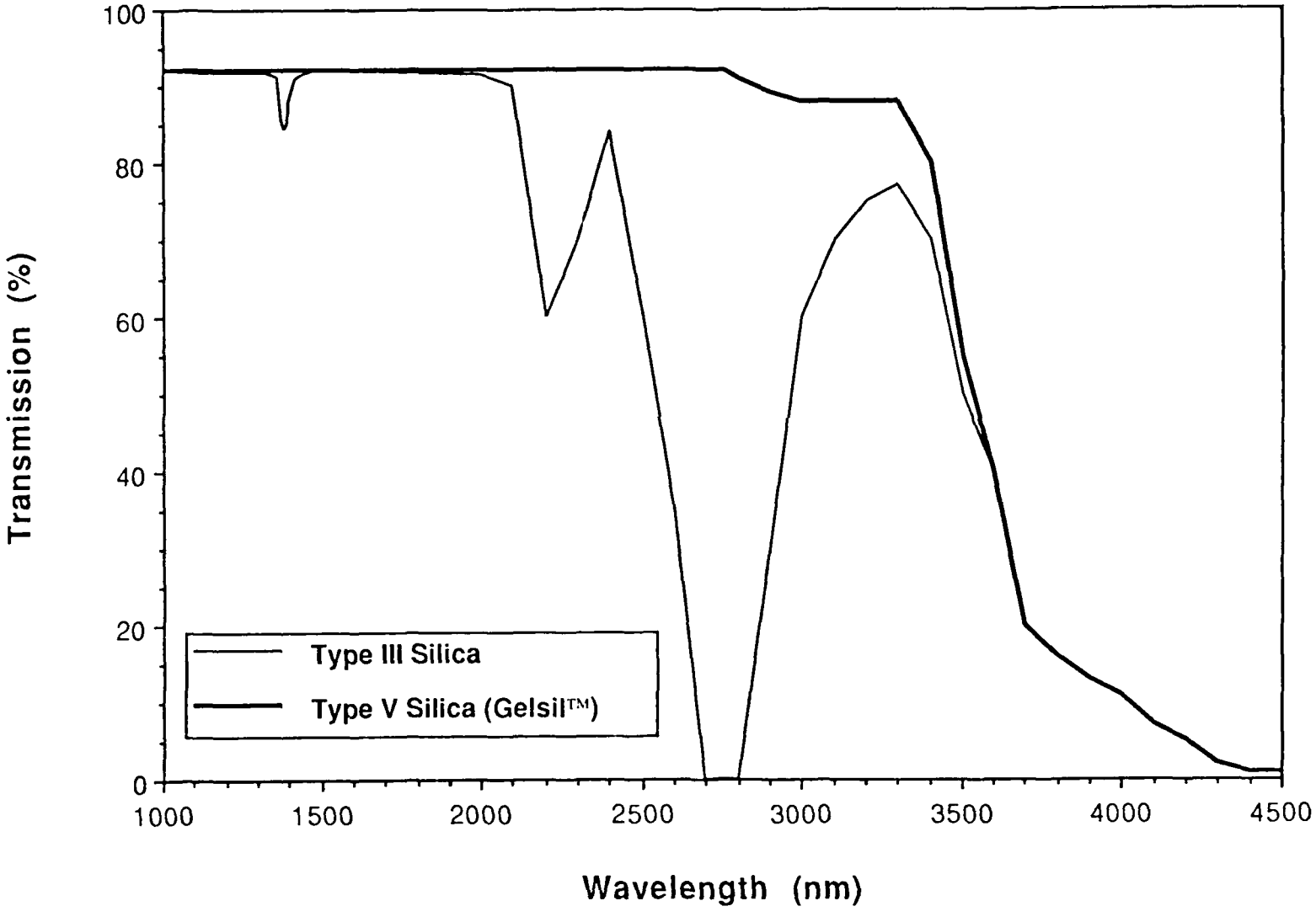

Figure 10: Near IR transmission of a dense organometallic gel-silica (Type V Gelsil™) compared with a Type III silica.

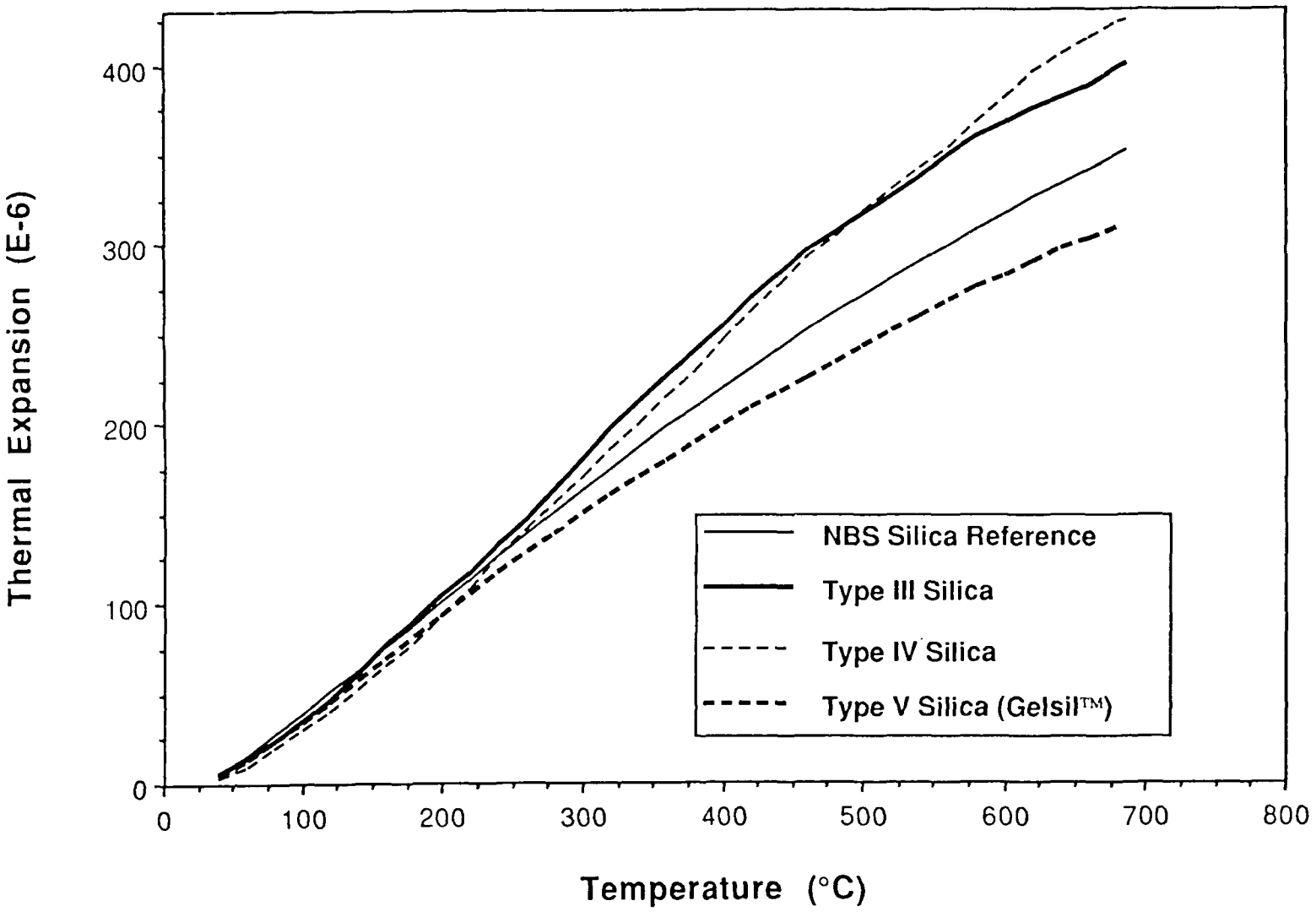

Figure 11: Thermal expansion of a dense organometallic gel-silica (Type V Gelsil™) compared with NBS silica reference and Types III and IV silicas.

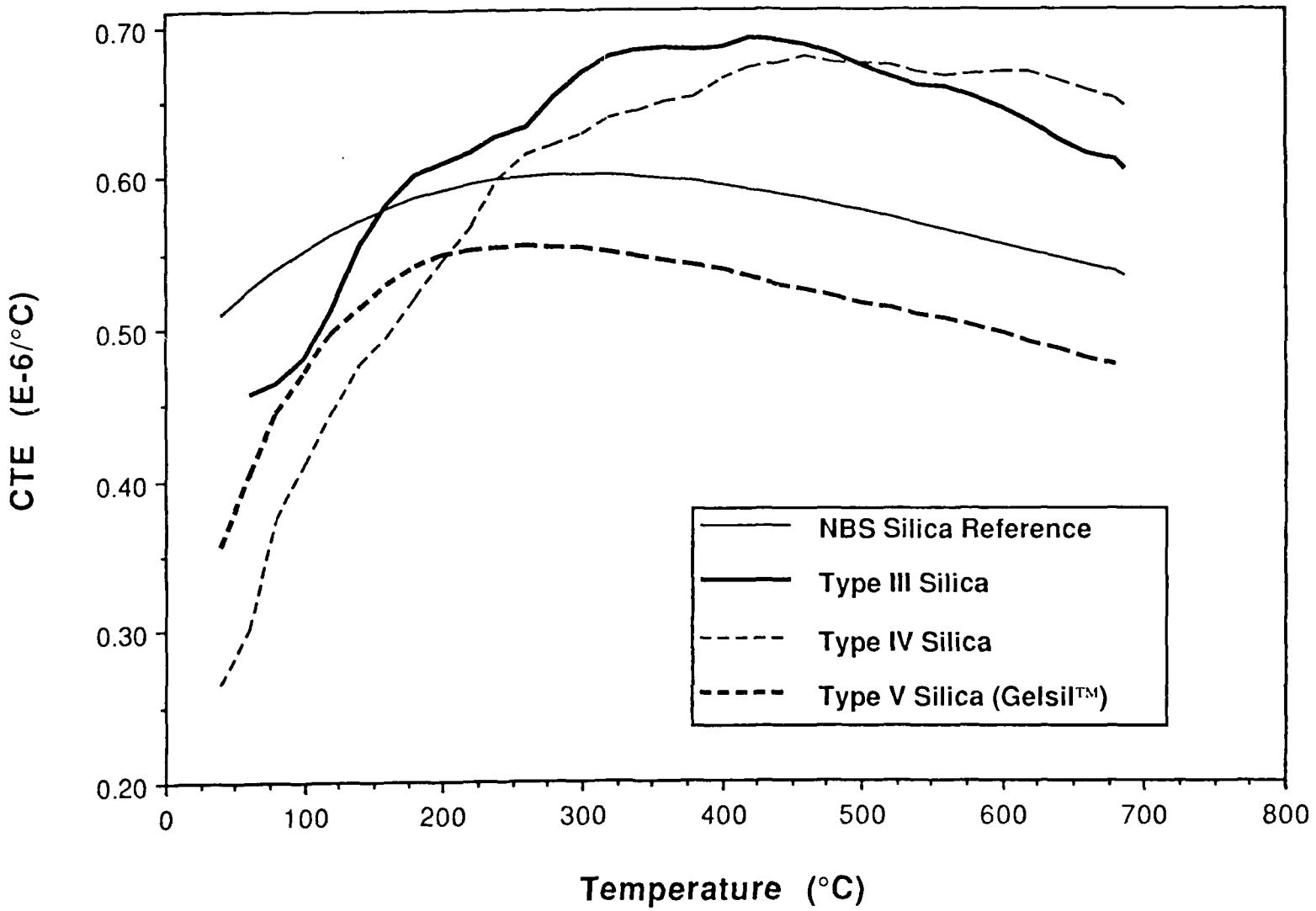

Figure 12: Coefficient of Thermal Expansion (CTE) of a dense organometallic gel-silica (Type V Gelsil™) compared with NBS silica reference and Types III and IV silicas.

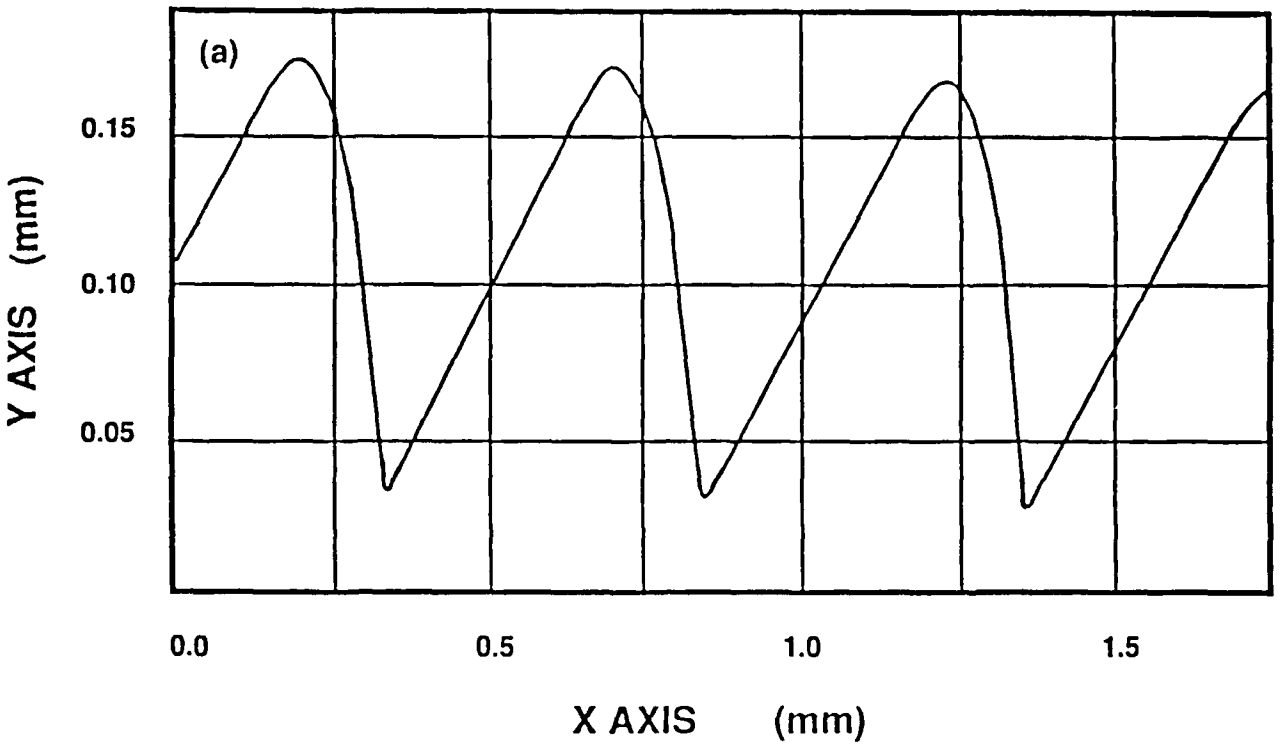

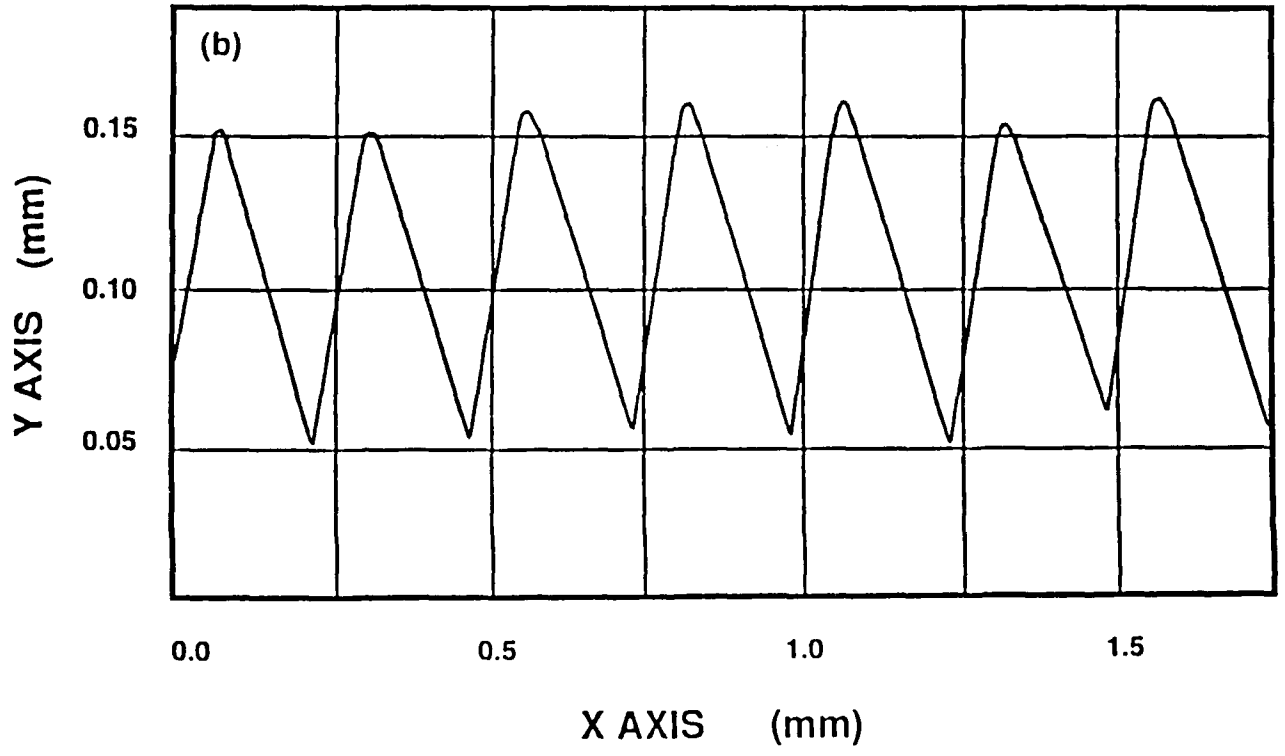

Figure 14: Profilometry graphs of Fresnel lenses: (a) Polymer master, (b) Replication in organometallic gel-silica.

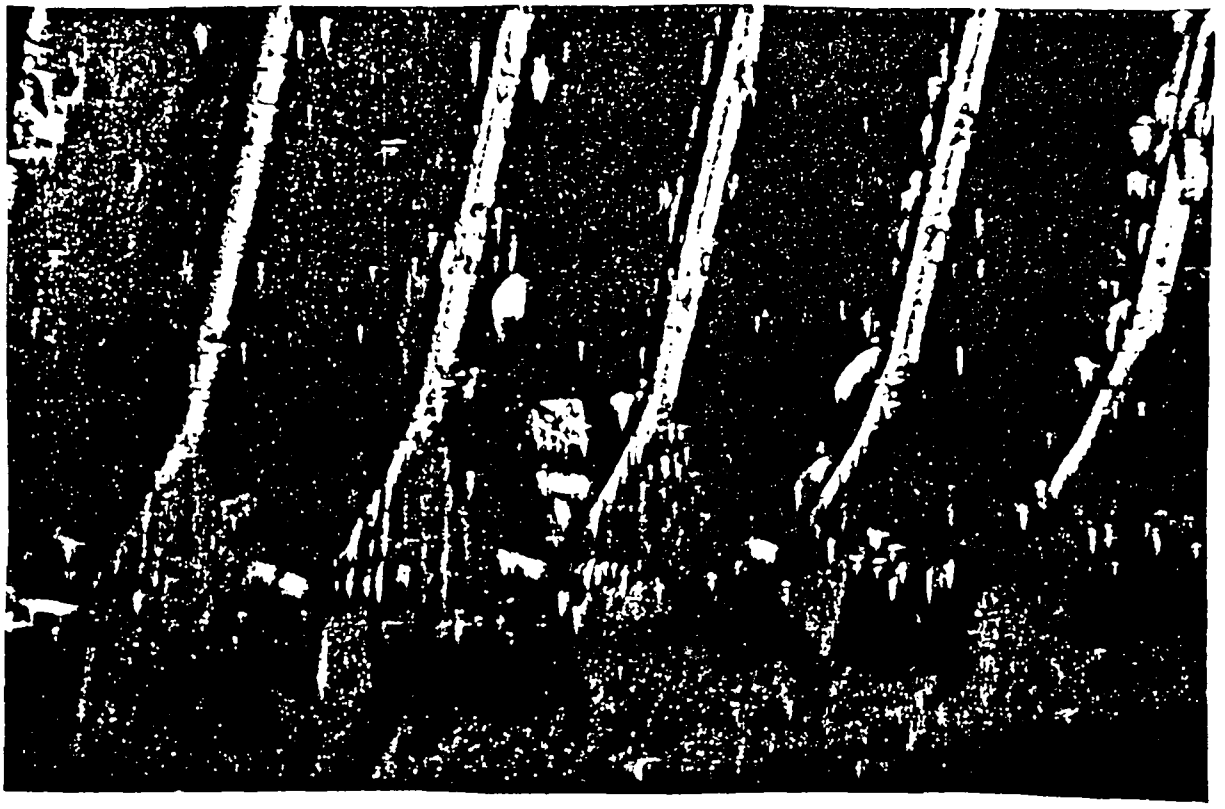

Figure 15: Microscope photograph of a dry organometallic gel-silica Fresnel lens.

A TOPOLOGICAL MODEL OF THE SINTERING OF SOL-GEL SILICA

W.L.VASCONCELOS, R.T.DeHOFF, L.L.HENCH
Department of Materials Science and Engineering,
University of Florida, Gainesville, Florida, 32611, USA

Abstract

Topological modeling is applied to a set of silica gel monoliths made by acid catalysis of TMOS. The samples were dried at 180 °C and partially densified in the range of 500 °C to 1150 °C. The evolution of the ultrastructure was characterized in terms of both metric and topological parameters. Relationships between the structural parameters and physical properties are discussed.

1. Introduction

Sol-gel research has grown markedly due to potentially unique applications for that class of materials [1-8]. Of foremost importance in the sol-gel area is control over properties based upon knowledge of the structural state. The presence of initial porosity in the gel and its change as densification proceeds is an opportunity for control of the structure.

Since densification is the increase in bulk density that occurs in a material as a result of the decrease in volume fraction of pores, this parameter (volume fraction, V_V) has been traditionally used to characterize a structure during sintering. Rhines [9] added to the metric parameters the topological concepts which provide complementary information about the sintering process [10-12]. In topological terms the densification process can be divided into three stages, according to the genus [9] (which is defined as the maximum number of non-self reentrant closed curves which may be constructed on the surface without dividing it into two separate parts [10]):

First stage: growth of weld necks while the genus remains constant.

Second stage: the genus decreases to zero as the pores become isolated.

Third stage: the genus remains constant at zero while the number of pores goes to zero.

In this work topological concepts are used to describe the evolution of the ultrastructure of optical components made by densification of sol-gel derived silica monoliths.

2. Topological Modeling

In order to carry out a topological evaluation of the structural changes that occur during densification, two models are proposed. The necessity of modeling arises because of the current impracticability of applying the technique of serial sectioning to a nanometer scale structure. The first model assumes a prismatic geometry in which the pores are tetrahedra connected by triangular prisms (Fig.1). The second model uses a cylindrical geometry (Fig.2). Correlating the volume of pores (V_V), the surface area of pores

(S_V), the average branch size (L), and the average pore diameter (D) to a particular geometry, one obtains a unique set of solutions that yield the number of branches (B_V), number of nodes (N_V), the genus (G_V), and the coordination number of pores (CN), as shown in Figs 1 and 2. The average pore size (D) reported for the cylindrical model is the mean lineal intercept of the pore phase [13]:

$$D = 4\ V_V / S_V. \qquad (1)$$

The prismatic model associates a volume to both the nodes and the branches of the pores, while the cylindrical model considers that all the volume is associated with the branches which form the porosity [14].

3. Experimental Procedure

Samples of silica-gel monoliths were prepared using TMOS, DI-water, and acid catalyzed by HNO_3. After aging at 60 °C for 23 h and at 75 °C for 23 h, the samples were dried at 115 °C for 93 h and at 180 °C for 12 h. The samples were densified in a dry-air (< 3 ppm H_2O) atmosphere at temperatures in the range of 500 °C to 1100 °C and in a chlorine atmosphere at 1150 °C. The (densification) heating rate was 20 °C/h and the maximum temperature was held for 1 h before cooling to room temperature .

After the densification experiments the samples were tested in an automatic N_2 adsorption apparatus, Autosorb-6 (Quantachrome), for pore volume and area of pores. The true density was obtained in a Helium micropycnometer (Quantachrome). Four point flexural testing was performed in a MTS-810/442 mechanical tester in ambient air at a cross head speed of 0.016 mm/min with a gauge length of 4 cm. Details of these and other tests, photographs of samples, and description of other topological models are in ref.14.

4. Results and Discussion

As shown in Fig.3, the models assume 4 as the average coordination number of pores (CN) in the dried stage. That initial stage usually corresponds to a maximum number of branches, nodes, and genus. In a sol-gel processed material the interconnected structure is developed during gelation, aging, and drying [15-17]. In topological terms these processes correspond to the first stage of densification. As the genus decreases, during the second stage of densification, the number of nodes remains constant and the number of branches decreases. The pyramidal model (Fig.3a) assumes that when CN reaches 2, further elimination of branches leads to disappearance of nodes, and therefore both B_V and N_V decrease, keeping CN constant at 2 during the third stage of densification. At this stage G_V is equal to 1 and it is kept constant during the third stage. The cylindrical model assumes a constant number of nodes for the entire process, and the coordination number varies from 4 to 0, as shown in Fig.3b. Both models can be incorporated in a generalized model [14] considering the *zeroth* Betti number (number of separate parts, P_V) in the expression $G_V = B_V - N_V + P_V$. During the third stage of densification, as the number of nodes and branches decrease, CN actually goes to zero. The temperatures indicated in Fig.3a correspond to the processing temperatures of the silica-gels.

The temperature dependence of the structural evolution is shown in Fig.4. Both models show the tendency towards decrease in genus and number of pores at increasingly higher temperatures. The models indicate the limit temperature for the beginning of the third stage of densification in the range of 1000 °C to 1150 °C. Despite differences in the numeric values of N_V, G_V, and B_V associated with the pyramidal and cylindrical models, they describe the structure in a very similar way, which is consistent with a topological description.

Because the number of nodes is constant during the second stage and the genus is constant during the third stage of densification, the number of branches seems to be a convenient parameter to follow the evolution of the structure. In order to make it numerically easier to compare the different topological states a topological index (fraction of removed branches) is defined as follows:

$$\beta = 1 - (B_V / B_V^o), \quad (2)$$

where B_V^o corresponds to the number of branches of an arbitrary reference state. If the dried state is chosen as reference, β for the dried sample is zero and β for the fully dense material is equal to 1. Thus the topological index β can be associated with the densification process changing from 0 to 1 with time. The rate of topological change will therefore be $d\beta/dt$.

The choice of the initial coordination number (CN^o) does not affect the evaluation of B_V, but it influences the numerical values of N_V and G_V. β for the beginning of the third stage of densification is given by [14]:

$$\beta_{(G_V=0)} = 1 - (2 / CN^o). \quad (3)$$

However a sensitivity analysis of the topological models shows that variations in CN^o (from 3 to 24), do not affect the description of the structural evolution in a fundamental manner [14], and the CN^o of 4 used in this work seems to be a convenient factor, besides representing a coordination thermodynamically and geometrically feasible.

The variation of flexural strength as a function of V_V shows relatively scattered data (Fig.5a). The flexural strength correlates better with β, as shown in Fig.5b (for cylindrical model).

The application of the cylindrical topological model to structures of different pore sizes (24 Å and 64 Å average diameter) is shown in Fig.6. While B_V for 24 Å structures decreases sharply after about 800 °C, B_V for the 64 Å structure remains roughly the same (in fact it increases slightly) over a much broader temperature range. An explanation for the apparently larger thermal stability of the large pore size structure is the smaller driving force for sintering associated with the smaller pore-solid surface area present in the large pore structure. The shape of the curves in Fig.6 is influenced by variations in the true density with temperature, as described elsewhere [14].

Much larger structures ($G_V \approx 10^6$ cm^{-3}), such as those studied by Rhines and DeHoff [11], show similar paths of topological evolution during densification (particularly a decrease in G_V as V_V decreases) indicating the broad spectrum of applications of the topological concepts. The path of microstructural evolution as seen in Fig.7 for silica-gel is also similar to the path associated with the sintering of larger structures [11].

5. Conclusion

Application of topological modeling to the densification of sol-gel derived nanometer scale structures reveals the same principles as determined for the sintering of larger scale powder structures. The topological evolution of the structure can be related to physical properties and presents potentially useful information which is complementary to the traditional metric parameters.

Acknowledgments

The authors acknowledge the US-AFOSR (Contract F49620-88-C-0073). One of the authors (WLV) is indebted to the support of UFMG (Federal University of Minas Gerais) and CAPES (Brazilian Agency of Post-Graduation).

References

[1] L.L.Hench and D.R.Ulrich (Eds.) Ultrastructure Processing of Ceramics, Glasses and Composites, Wiley, New York, 1984.

[2] L.L.Hench and D.R.Ulrich (Eds.) Science of Ceramic Chemical Processing, Wiley, New York, 1986.

[3] D.R.Ulrich, J.Non-Cryst.Solids 100 (1988) 174.

[4] H.Dislich, J.Non-Cryst.Solids 73 (1985) 599.

[5] J.D.Mackenzie, J.Non-Cryst.Solids 73 (1985) 631.

[6] G.W.Scherer, J.Non-Cryst.Solids 73 (1985) 661.

[7] J.Wenzel, J.Non-Cryst.Solids 73 (1985) 693.

[8] D.R.Uhlman, B.J.J.Zelinsky and G.E.Wnek, in: Better Ceramics Through Chemistry, eds. C.J.Brinker, D.E.Clark and D.R.Ulrich, Materials Research Society, Vol.32 (North-Holland, New York, 1985) p.59.

[9] F.N.Rhines, Plansee Proc., 3rd Seminar, Reutte, Tyrol (1958) 38.

[10] R.T.DeHoff, in: Quantitative Microscopy, eds. R.T.DeHoff and F.N.Rhines (McGraw-Hill, New York,1968) p.291.

[11] F.N.Rhines, R.T.DeHoff and J.Kronsbein, A Topological Study of the Sintering Process, Final Report for the US Atomic Energy Commission, 1969.

[12] F.N.Rhines and R.T.DeHoff, in: Sintering and Homogeneous Catalysis, eds. G.C.Kuczynski, A.E.Miller and G.A.Sargent (Plenum, New York, 1984) p.49.

[13] R.T.DeHoff, in: Encyclopedia of Materials Science and Engineering, ed. M.B.Bever (Pergamon, Oxford, 1986) p.4633.

[14] W.L.Vasconcelos, PhD Thesis, University of Florida, Gainesville, 1989.

[15] L.L.Hench, in: ref.1, p.52.

[16] C.J.Brinker, E.P.Roth, D.R.Tallant and G.W.Scherer, in: ref.1, p.37.

[17] L.C.Klein, T.A.Gallo and G.J.Garvey, J.Non-Cryst.Solids 63 (1984) 23.

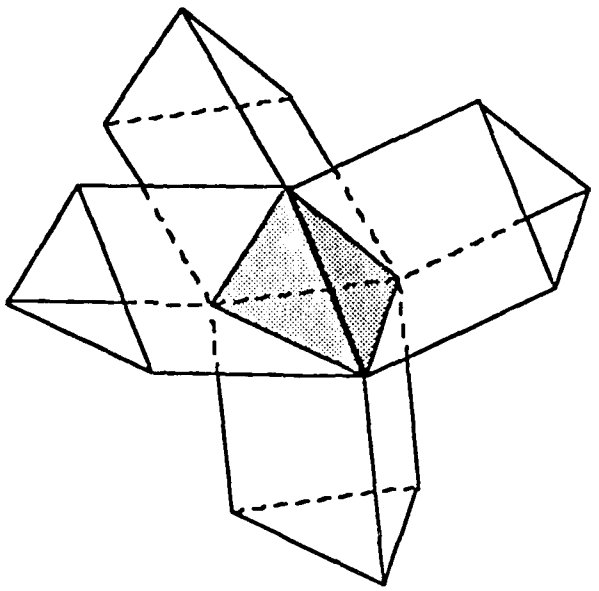

$$D = \frac{144(1-Vv)}{\sqrt{6}\,Sv}\left(\frac{\sqrt{6}}{12} + \sqrt{\frac{3}{72} + \frac{\sqrt{6}}{72(1/Vv-1)}}\right)$$

$$L = \frac{4(1-Vv)}{Sv}$$

$$Nv = \frac{\sqrt{2}\,Sv}{9\,DL}$$

$$Bv = \frac{8}{3\sqrt{3}\,D^2 L}\left(Vv - \frac{\sqrt{3}}{8}NvD^3\right)$$

$$Gv = Bv-Nv+1$$

Fig.1. Tetragonal geometric model.

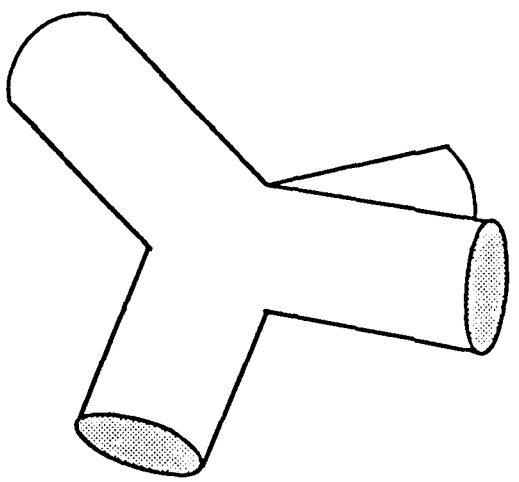

$$D = \frac{4Vv}{Sv}$$

$$L = \frac{4(1-Vv)}{Sv}$$

$$Bv = \frac{Sv^3}{16\pi Vv(1-Vv)}$$

$$Nv = \frac{Bv^o}{2}$$

$$Gv = Bv-Nv+1$$

Fig.2. Cylindrical geometric model.

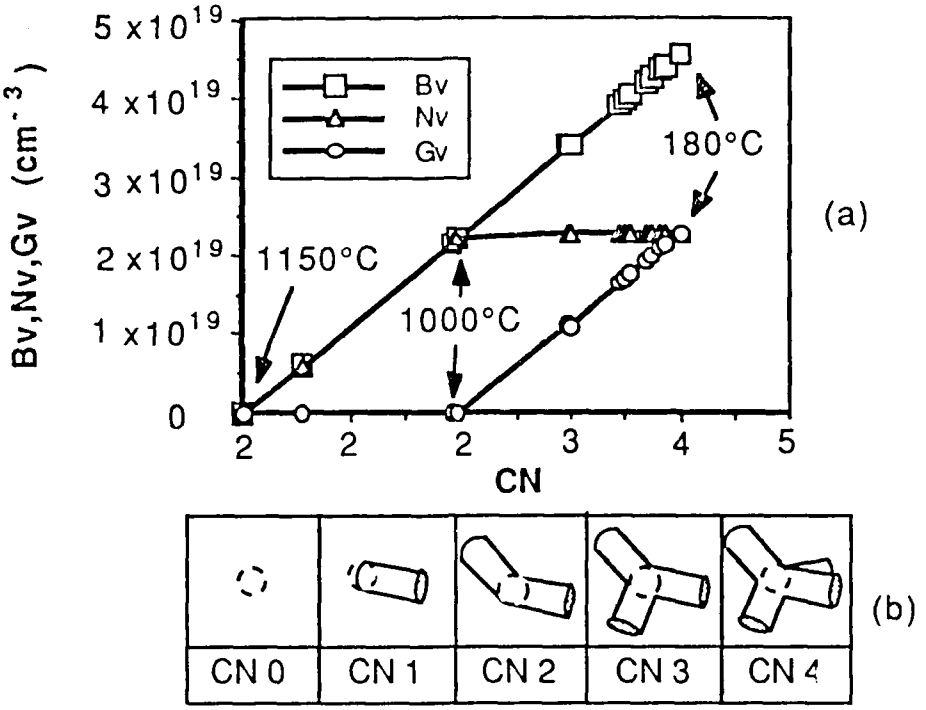

Fig.3. (a) Variation of the number of branches (Bv), number of nodes (Nv), and genus (Gv), as a function of the coordination number (CN). (b) Schematic of the evolution of the pore coordination number.

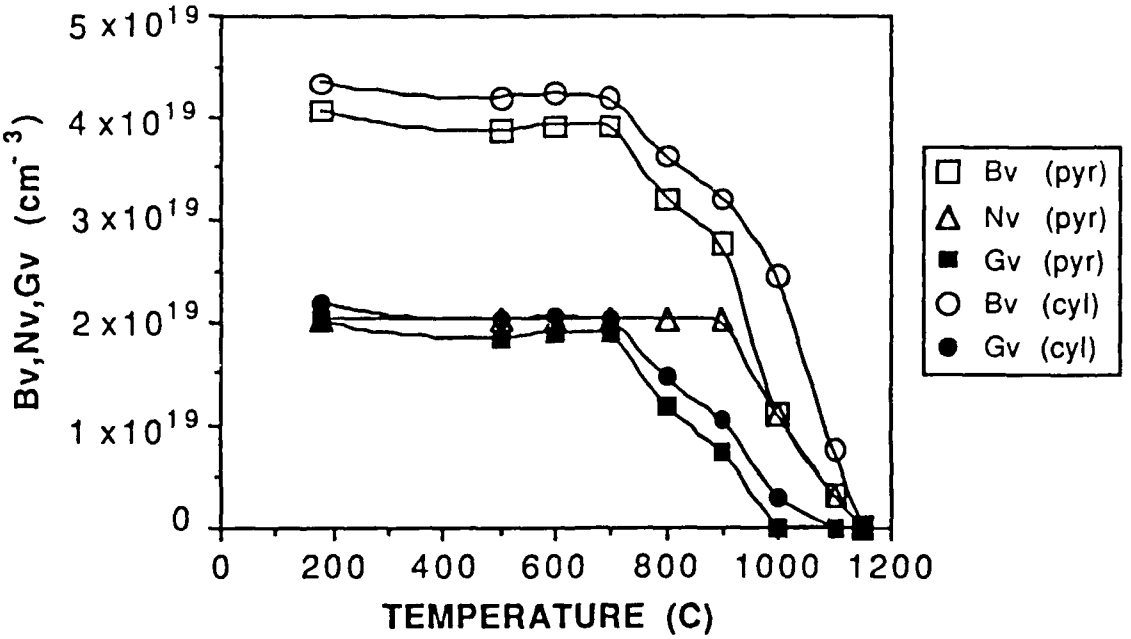

Fig.4. Variation of the number of branches (Bv), number of nodes (Nv), and genus (Gv) as a function of temperature of an organometallic silica-gel monolith.

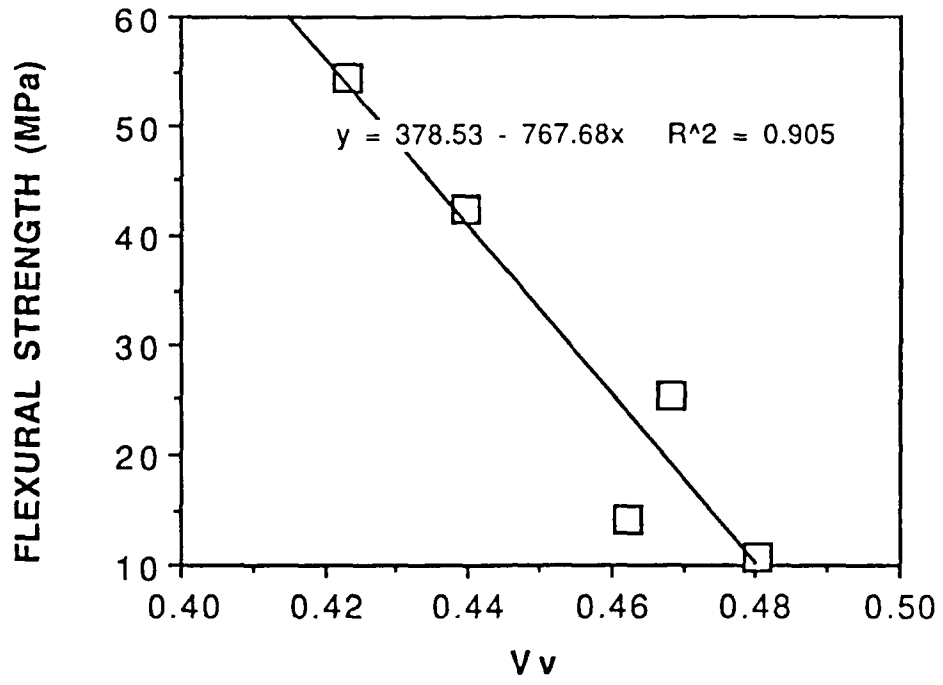

(a)

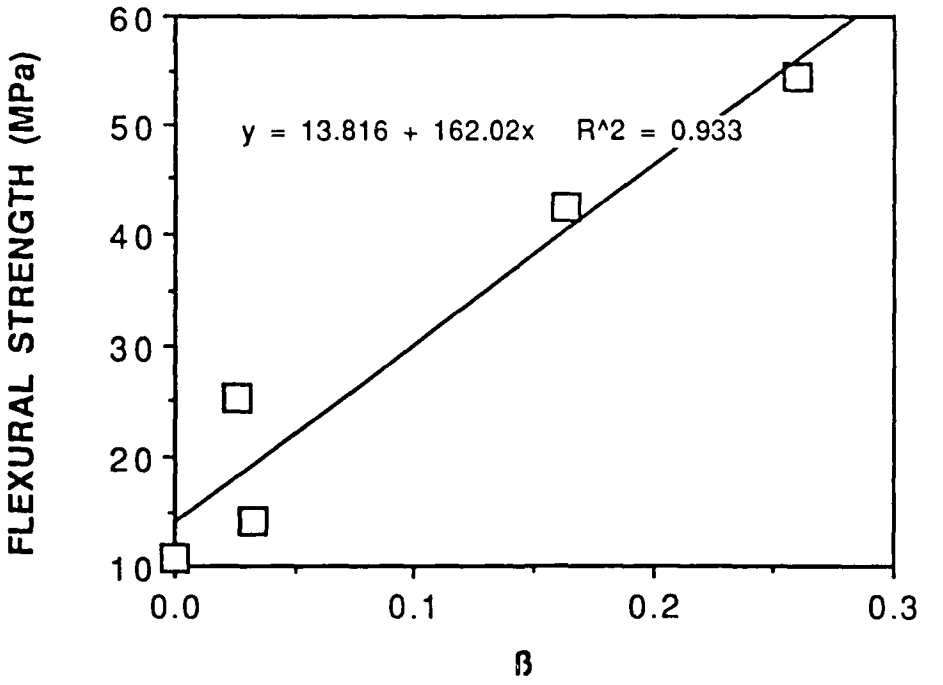

(b)

Fig.5. (a) Variation of the flexural strength as a function of the volume fraction of pores (Vv), and (b) as a function of the topological index ß.

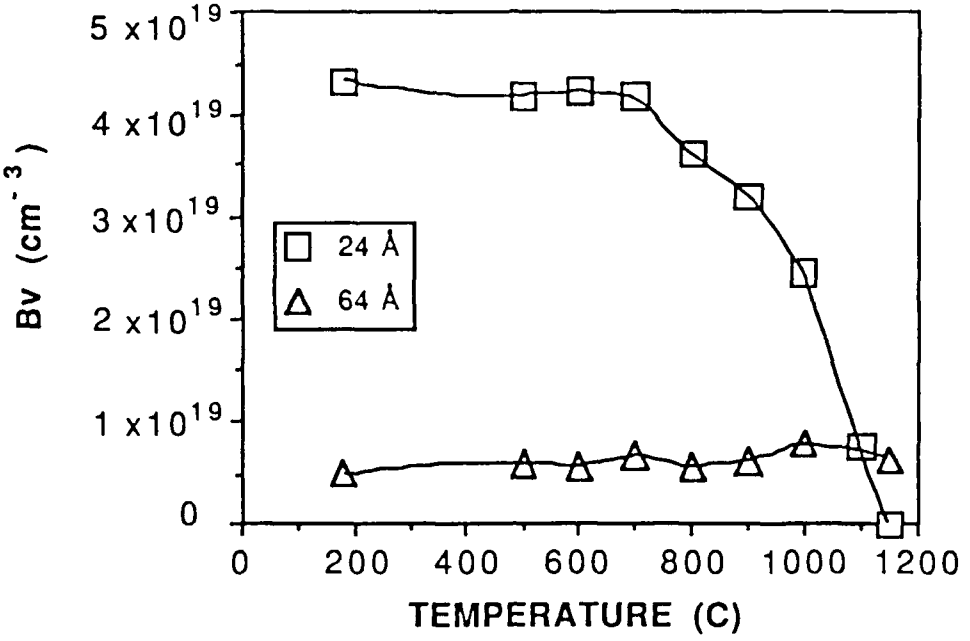

Fig.6. Variation of the number of branches (Bv) as a function of temperature for structures of 24 Å and 64 Å of pore diameter.

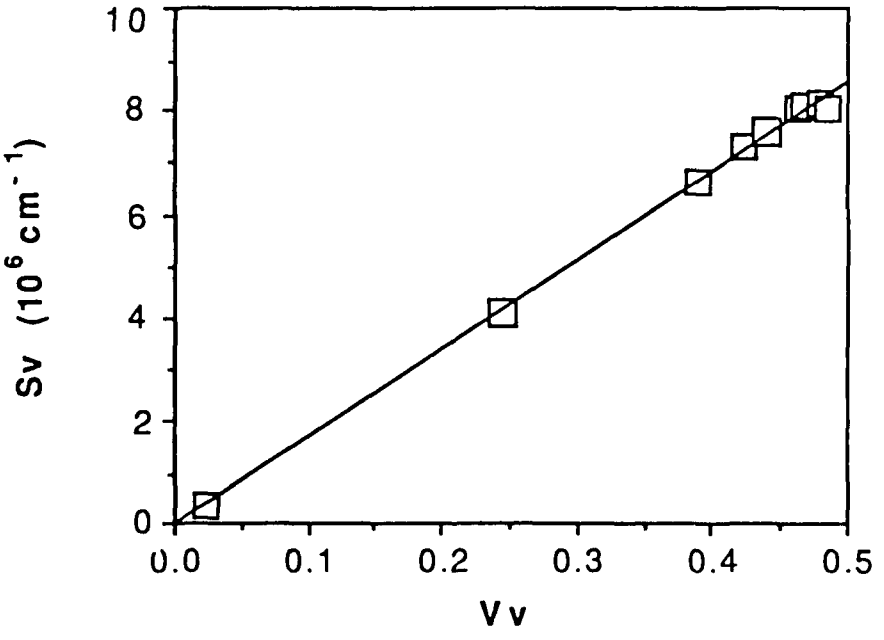

Fig.7. Relation between surface area of pores (Sv) and volume fraction of pores (Vv).

Processing, properties and applications of sol-gel silica optics

Jean-Luc R. Noguès and Anthony J. LaPaglia

GELTECH, Inc., One Progress Blvd., Box 18, Alachua, Florida 32615, (904)462-2358

ABSTRACT

For many years the market share maintained by U.S. optics manufacturers has been declining continuously caused in part by intense competition principally from countries in the Far East, and in part by the lack of a highly trained cadre of opticians to replace the current generation.
This fact could place in jeopardy the defense system of the United States in case of international war. For example, in 1987, optical glass component imports accounted for approximately 50 percent of the Department of Defense (DOD) consumption.
GELTECH's sol-gel technology is a new process for making a high quality optical glass and components for commercial and military uses. This technology offers in addition to being a local source of optics, the possibility to create new materials for high-tech optical applications, and the elimination of the major part of grinding and polishing for which the skill moved off-shore.
This paper presents a summary of the sol-gel technology for the manufacture of high quality optical glass and components. Properties of pure silica glass made by sol-gel process (Type V and Type VI silicas) are given and include: ultraviolet, visible and near infrared spectrophotometry, optical homogeneity and thermal expansion. Many applications such as near net shape casting or Fresnel lens surface replication are discussed. Several potential new applications offered by the sol-gel technology such as organic-inorganic composites for non linear optics or scintillation detection are also reported in this paper.

1. SOME TRENDS OF THE U.S. OPTICAL INDUSTRY

In 1985, the optics production capacity for defense applications was estimated to be able to supply 87 percent of the optical component military needs but the production capacity was dropping regularly by over 20 percent per year. The possibility to reverse this trend and to increase the production capacity of U.S. manufacturers looked difficult and long, due to shortages of skilled opticians and long lead times for raw materials.

In 1987, the Department of Defense's Joint Logistics Commanders anticipated in peacetime a requirement of approximately 100,000 optical components per month of the types used for direct applications in military systems.[1] In case of mobilization, the requirement for military optical components were found to be much greater.

The same year, optical glass component imports already accounted for more than 50 percent of the Department of Defense (DOD) consumption. The potential of converting commercial production capacity to military production appeared inadequate to support the rapid increase in optical elements needed to meet emergency defense requirements and would ruin the development of the commercial optical industry.

During the last few years the increasing need of optical elements was boosting the imports from all over the world with a large predominance from the small countries of the Pacific Rim (Korea, Taiwan, Malaysia, Hong-Kong) where labor rates are perhaps one-tenth those of the U.S..

Figure 1 presents the trends of imports and exports of all optical elements over a time period from 1978 to 1986. This figure shows that the imports increased by more than a factor 2 over a few years while the exports were decreasing slightly. This means that the U.S. manufacturer share of the market of optical components was decreasing drastically over the years. This trend applies for all optical market segments such as for example laser applications and figure 2 presents the estimated sources of laser optics by world regions. It was estimated in 1984 that 62 percent of the laser optics used in the U.S. were from domestic source, the projection for 1990 predicts a U.S. market share of about only 37 percent.[2] Because the need for this type of optical component is expected to increase by over 40 percent, the decrease in market share becomes even more dramatic.

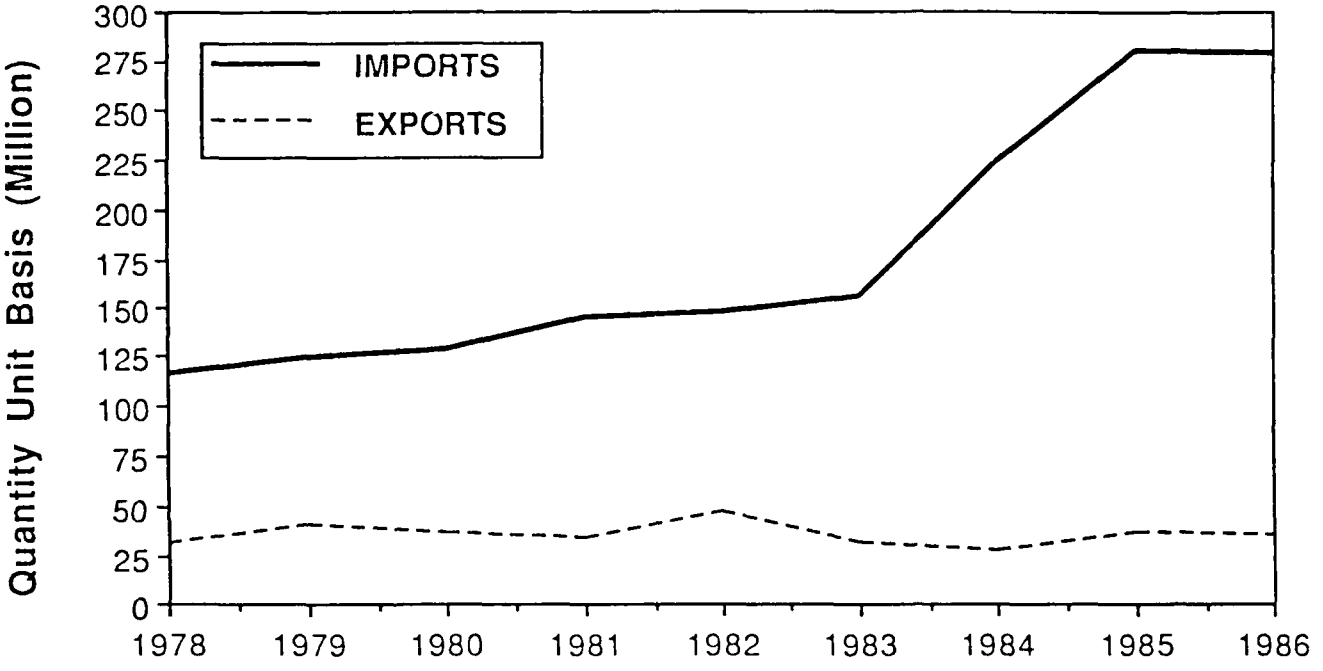

Fig. 1. U.S. Trade balance (All optical elements)

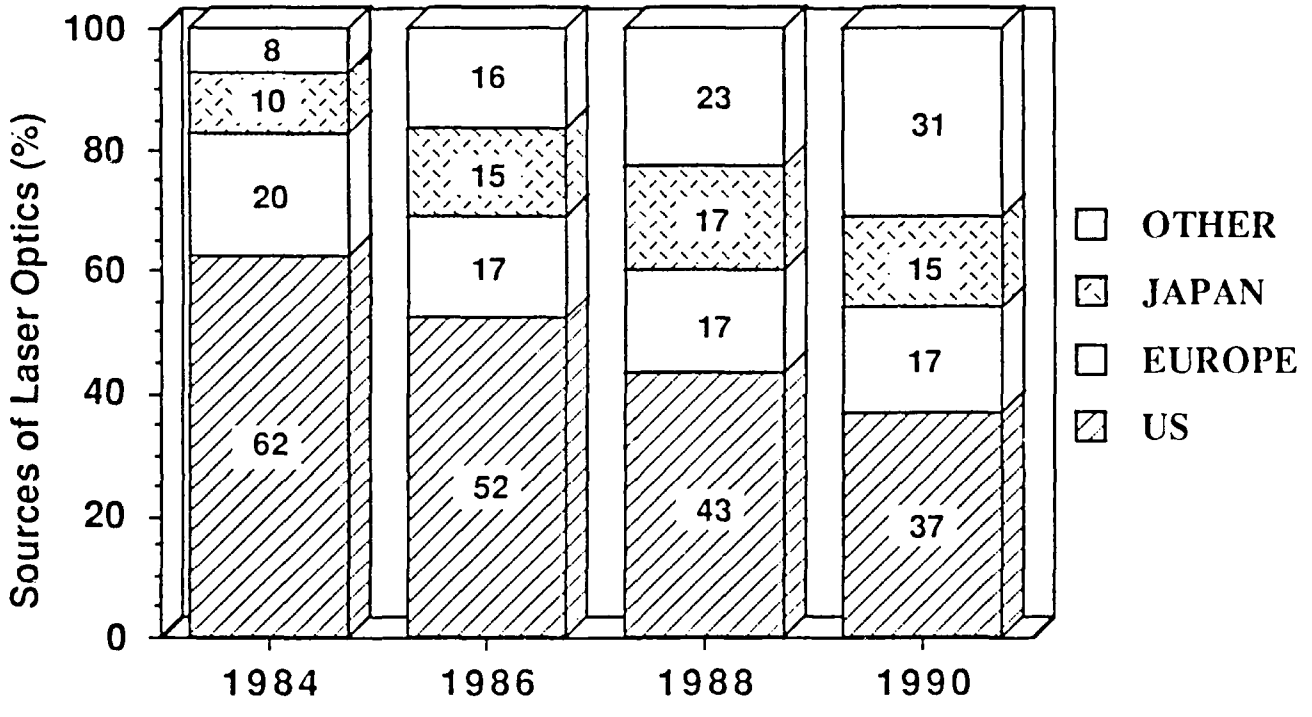

Fig. 2. Estimated sources of laser optics by world region

Today, most optical companies are reliant to some degree, between 36 and 70 percent function of the type of components, on imports of materials, parts and production equipment. In general, imports are used because of three main reasons: availability of materials or equipment, lower prices, and sole sources due to the extinction of U.S. suppliers or the set up of subsidiaries in the Far East in an attempt to reduce production costs and increase competitiveness.

Every phase of the business from raw materials to finished optical products has been impacted. For the past few years more than 70 percent of the glass used by U.S. optical component producers were imported and this percentage is expected to increase in the near future. The percentage of optical components from overseas rises up to 98 percent for some specific optical applications. Another consequence of these circumstances is that the overall employment in the optical industry has declined by over 40 percent in only five years.

In summary, the need of optical components in the United States is growing very rapidly but the market share maintained by U.S. optical manufacturers has been declining continuously for many years caused in part by intense competition principally from countries in the Far East and in part by the lack of a highly trained cadre of opticians to replace the current generation. The requirement of large imports of military optical components represents a real threat which could place in jeopardy the defense system of the United State.

Today the U.S. optical manufacturers have to try to reverse these trends and have to define new strategies for the future if they want to keep or increase their market share, and at the same time decrease the dependency of the U.S. on foreign suppliers. An identification of the key elements in the optical industry is at this point necessary to understand better the factors leading to the decline of the U.S. optical industry.

The manufacture of optical components involves three broadly defined stages of production. The first stage is the raw glass production mainly by melting various raw materials in high temperature furnaces. The second stage begins with the annealing of the blocks, slabs or gobs manufactured in stage 1 and continues with the cutting, slicing and even pressing of the raw glass to produce blanks or preforms. Both stages are capital intense operations and require large volume production to achieve cost economies. The third stage of optical element production is the finishing stage. It is a very labor intense stage which requires special skilled personnel and represents up to 80-90 percent of the component cost. At this stage the blanks are ground to near net shape and further polished to the adequate standard for each specific optical application. The process to manufacture optical elements is in fact high capital and high labor intense operations. Today the U.S. equipment park is old and the skilled personnel is not replaced after retirement. To be competitive on the market place very large investments (equipment and personnel) are an indispensable necessity but with the purchasing of large quantities of optical components offshore, domestic manufacturers could not generate enough profits to modernize their capital equipment and simultaneously form an apprenticeship program to develop a new generation of opticians. This route, to be very successful in the optical industry, looks very difficult and many companies are investigating other alternatives.

Some companies are doing very well in the optical business because they developed a specialty in a high-tech segment of the market and they are trying to stay in front of the progress. Examples of high-tech segments include laser development, infrared materials and optoelectronic applications. Other small companies are devoting their effort to develop niche marketing applications but they are always vulnerable to smaller and more aggressive niche marketers.

Another way to be successful in the optical application business is to look for new technologies such as sol-gel processes, diamond turning, gradient index optics, replication, molding, and other novel solutions. In this paper we will focus on Sol-Gel Technology as a new manufacturing process which can offer smart solutions to the crucial problem of the U.S. optical component manufacture industry. This work addresses in particular the manufacture of pure silica for commercial and military optical applications.

2. SOL-GEL TECHNOLOGY BACKGROUND

The sol-gel technology for forming glasses and glass-ceramics received a great deal of attention during the last two or three decades because of the recognized advantages inherent in the method.[3-5] The three main advantages of the sol-gel process are:

1. The possibility of obtaining glasses difficult to prepare with a high degree of homogeneity by conventional methods of fusion. The good homogeneity is obtained at the beginning of the process by mixing the different liquid precursors together at relatively low temperature. This mixing allows an homogeneity of the various elements at a molecular level and this homogeneity can be kept in many cases through the complete processing.

2. The possibility of obtaining high purity due to the chemical aspects of the raw materials which can be supplied in an electronic grade for the majority of them.

3. The potential of molding to near net shape by casting at low temperatures the sol into molds of predetermined shapes.

The first two advantages allows for the preparation of excellent materials for high-tech applications such as advanced optics, optoelectronic devices and tailored ceramics. The third advantage allows for the preparation of parts at lower manufacturing costs and opens the possibility of the manufacture of elements with special surface features. Table 1 shows a list of potential advantages offered by the sol-gel technology toward the preparation of glasses and glass ceramics.

Table 1. Some advantages of the sol-gel processing

Better homogeneity
Better purity
Lower temperature of preparation
New noncrystalline solids
New crystalline solids
Special products such as films
Near net shape casting
Surface feature optics

The sol-gel process can be divided in three main steps:

1. Gel formation.
2. Drying.
3. Consolidation (densification, sintering).

In the first step, the necessary ingredients are mixed to produce a sol. By destabilization or hydrolysis and polycondensation of the sol, the three dimensional network of the future glass is formed and the solution sets into a stiff gel called wet gel. After an aging step necessary to develop the formation of the initial texture of the material, the aged wet gel is dried. This crucial step consists of eliminating the interstitial liquid from the gel body. This induces a drastic modification of the texture of the gel which leads often to the destruction of the monolith aspect of the material. The dry gel is then heat-treated to convert the porous solid into an homogeneous glass free of porosity.

The sol-gel technology is very complex and many processes have been developed for very specific applications. The following parts of this paper address the production of pure gel-silica monolithic glass for optics applications.

3. GEL-SILICA PROCESS

A large amount of the optics used in the world are made in pure silica glass because of its very good optical transmission, refractive index homogeneity, low coefficient of thermal expansion, very good thermal and chemical stability, and its ability to be polished to high standards.

There are presently four major methods of manufacturing silica optics. The first two methods involve melting at high temperatures natural quartz crystals. These processes produce Type I and Type II *Fused Quartz* which provides for average optical properties due to substantial amounts of cation and hydroxyl impurities, defects, seeds, bubbles, inclusions, and microcrystallites.

The other two processes produce Type III and Type IV *Fused Silicas*. They are made by vapor-phase hydrolysis and oxidation of pure silicon tetrachloride respectively. The higher purity of the raw materials allows cation impurity contents substantially lower than in fused quartz. These two processes lead to a higher quality of glass than Types I and II but do not permit the direct manufacture of neat net shape optics.[6]

The sol-gel processing of pure silica glass has the potential of producing a high quality optical glass due to the high purity of raw materials and at the same time the production of near net shape parts which require a minimum of finishing.

The pure silica sol-gel process described in this paper includes several steps: mixing, casting, gelation, aging, drying, densification, and requires total control of each process variable to be successful. Figure 3 gives a synoptic of the entire gel-silica process.

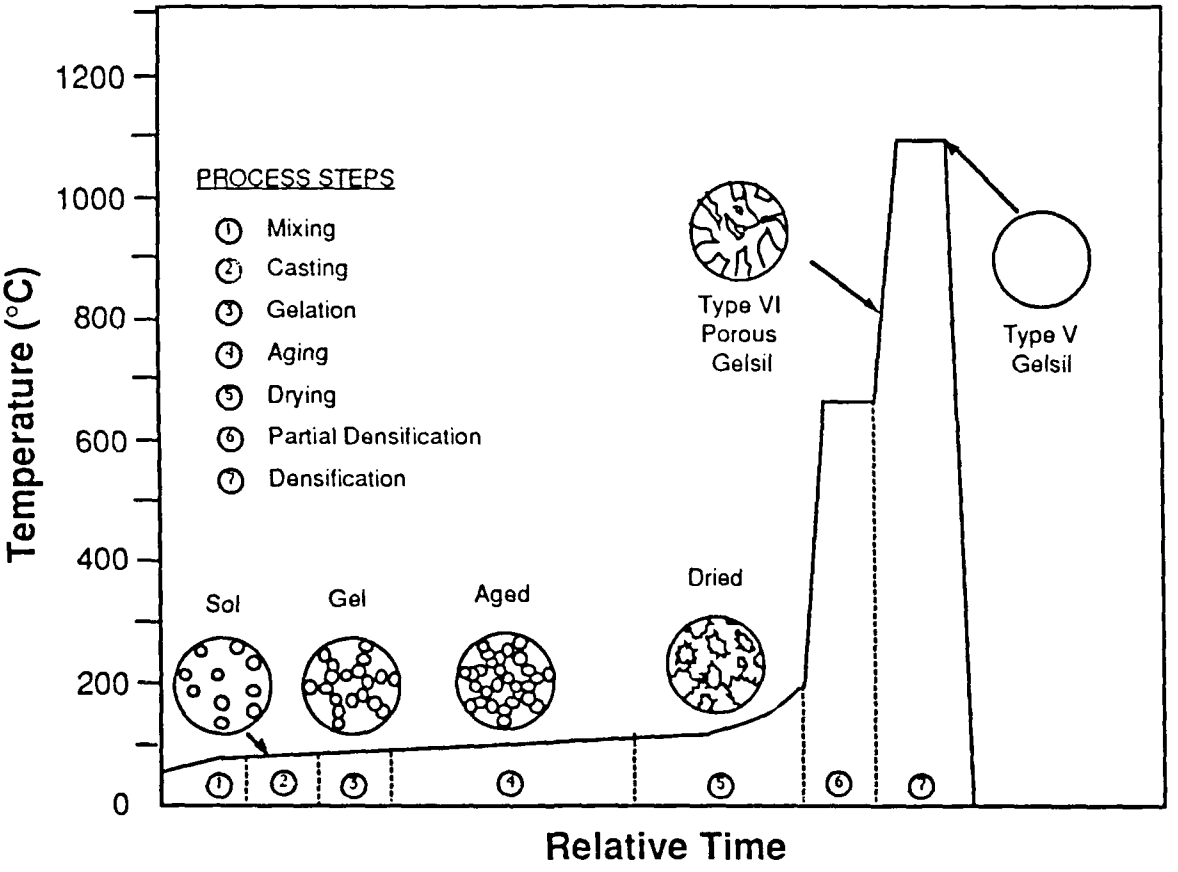

Fig. 3. Gel-silica process sequence

Alkoxide silicon precursors are choosing over colloidal suspension raw materials because of their higher level of purity. Typical silica precursors are tetraethylorthosilicate (TEOS) and tetramethylorthosilicate (TMOS) which can be produced in the USA in various levels of purity. The silica sol is prepared by adding the silica precursor to deionized water. Hydrolysis of the silica precursor and condensation reactions occur during this mixing step:

Hydrolysis: $Si(OR)_4 + 4\,H_2O \longrightarrow Si(OH)_4 + 4\,ROH$ (1)

Condensation: $Si(OH)_4 \longrightarrow SiO_2\,(gel) + 2\,H_2O$ (2)

After complete homogeneity of the sol is reached, the solution is cast into molds of specific shapes. The polycondensation reaction continues and the silica particles randomly link together and form a three-dimensional network. This mechanism increases the viscosity, the sol loses its freedom of movement and becomes a rigid, wet gel having the shape and surface quality of the mold. This phenomena is called gelation.

During the aging step, the polycondensation reaction continues to build the glass network giving at the same time enough strength to the gel to resist and support without cracking the tremendous stresses developed during the drying step. During this drying step, the by-products of the hydrolysis and condensation reactions are eliminated and the final product is an ultraporous monolithic body with the shape and surface details of the original mold.

The last step of this process corresponds to the densification of the dried gel via elimination of the porosity by heat treatment. During the first part of this densification treatment (up to 600°C) the organic impurities present in the pore of the gel are eliminated in order to leave a pure silica material which can be heated up for full densification after an additional dehydration period. This dehydration treatment is necessary to drop the residual hydroxyl group content lower than 5 ppm in the fully dense pure gel-silica glass (Type V). When the process of densification is stopped before reaching complete densification, a partially dense pure gel-silica glass (Type VI) is produced and can be used for some very novel applications as described below.

The glasses manufactured by this specific process developed in GELTECH, Inc. are identified as Dense Gelsil™ (Type V silica) and Porous Gelsil™ (Type VI silica) for the fully dense and partially dense glass respectively. Details of the production processes of these two gel-silicas were published elsewhere.

4. PROPERTIES AND APPLICATIONS OF GEL-SILICAS

4.1 Properties of dense gel-silica (Type V Silica)[7]

One of the primary reasons for use of alkoxide derived silica glass is an improvement of purity and homogeneity. The high purity of the raw materials in addition to a lower temperature process have permitted the manufacture of gel-silica glass with a very high optical transmission throughout the optical spectrum and in particular an outstanding ultraviolet transmission cut-off. Figure 4(a) presents a comparison of the optical transmission in the ultraviolet wavelength range for Type V silica and a Type III silica available on the market. Figure 4(b) shows the elimination of the absorption bands in the near infrared for Type V silica in comparison with Type III silica which exhibits peaks at 1400 nm and 2200 nm, and a very broad absorption band at 2730 nm.

The quality of the raw material in addition to a very well controlled process allows for the manufacture of glass with an index of refraction homogeneity of about $1\text{-}6\text{x}10^{-6}$, no evidence of bubbles, no striae, very low strain birefringence of 4-6 nm/cm, and very low residual hydroxyl group concentration.

A very low coefficient of thermal expansion and very good thermal stability are also important physical properties for pure silica optical glass. The alkoxide derived process leads to the manufacture of Type V silica having a lower expansion than the National Institute of Standards and Technology (NIST) silica standard and Types III and IV commercial silicas over the temperature range of 25°C to 700°C as shown in figure 5. Figure 6 shows the good thermal stability of Type V silica over the same range of temperature.

The overall properties measured on alkoxide derived Type V silica are generally equivalent to or superior to the best grades of Types I to IV commercial optical silicas. This Type V silica represents a potential alternative to all the different types of pure silica commercially available today and used for civilian or military applications. The Type V silica production is not an equipment or labor intensive operation, does not require any special equipment available only from overseas, and decreases part of the dependency of the United States on foreign suppliers.

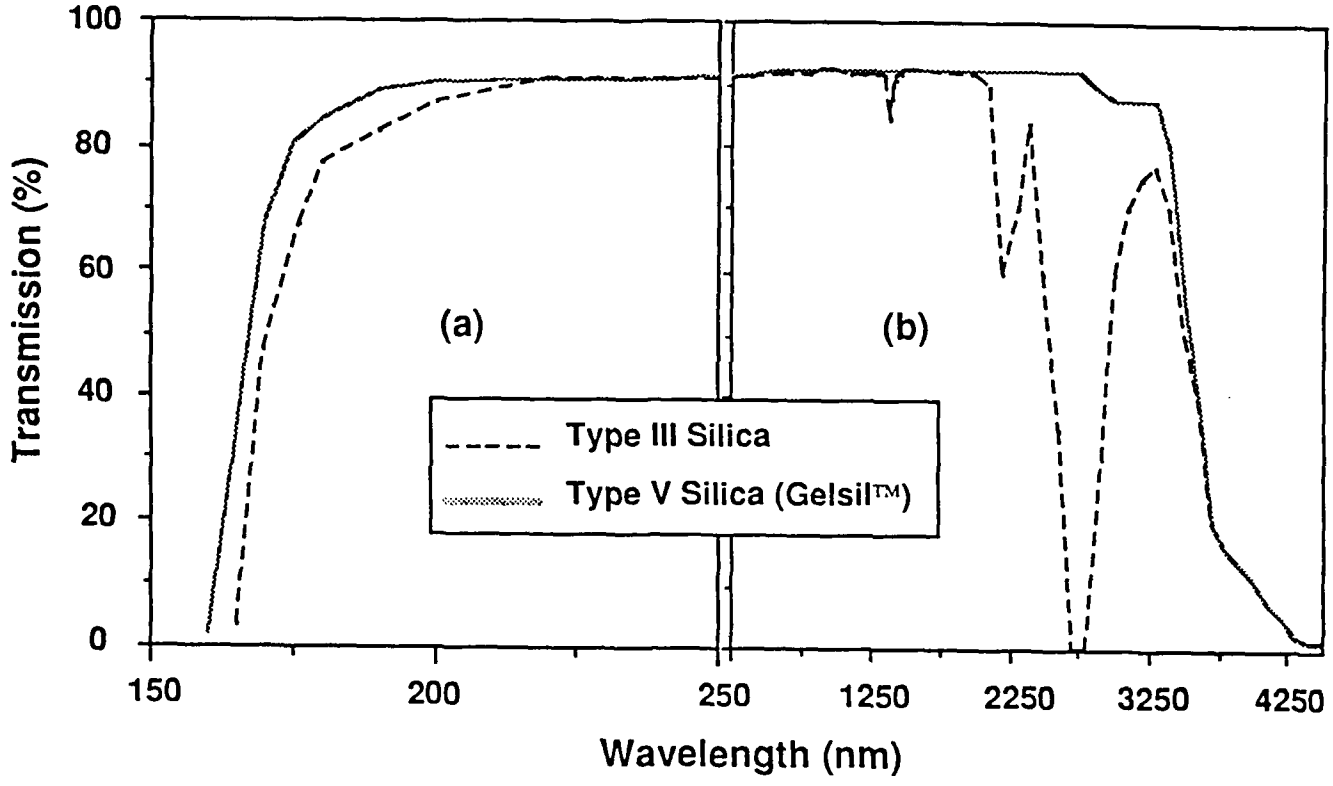

Fig. 4. Optical transmission of various silicas

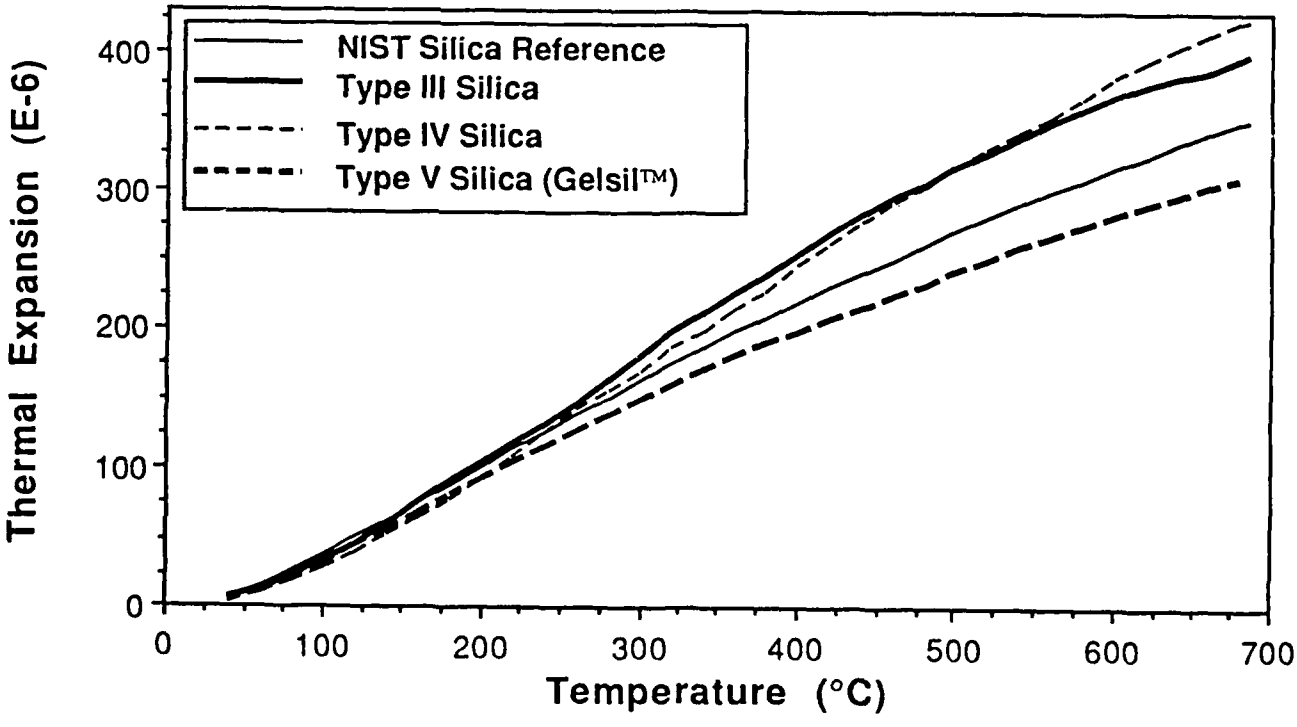

Fig. 5.Thermal expansion of various silicas

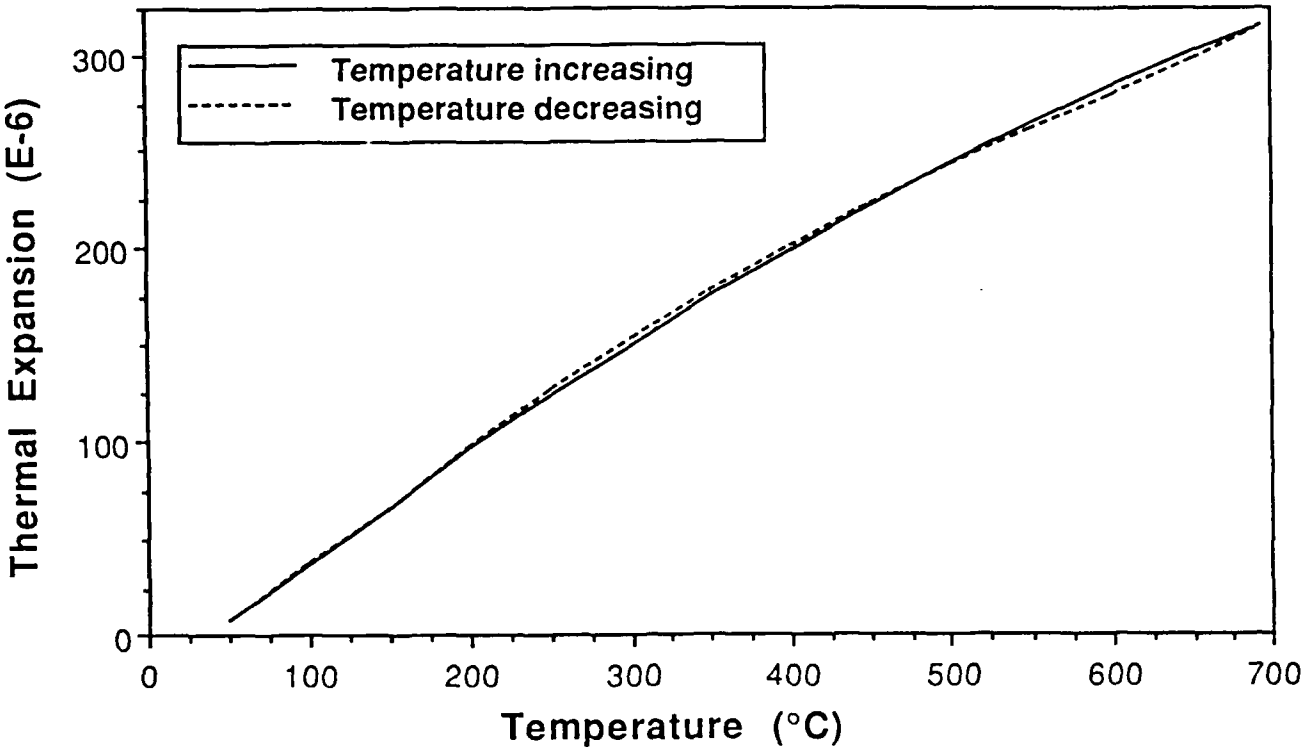

Fig. 6. Thermal stability of dense gel-silica (Type V)

4.2 Properties of porous gel-silica (Type VI Silica)[8]

An important feature of the alkoxide derived silica process is that with sufficient control of the kinetics and ultrastructure, it is possible to produce an optically transparent pure silica which has a substantial residual porous volume (Type VI silica). This Type VI silica is transparent because the pores have a very small average diameter of about 2.5 nm and do not induce too much light scattering. The transmission spectra of a porous gel-silica is shown in figure 7. This spectrum shows that the samples still transmits 50 percent of light at wavelength as low as 290-300 nm, and displays the typical absorption bands principally due to the residual hydroxyl groups and their overtones.

The properties of this material are a function of the final maximum temperature of densification. This feature in addition to the possibility to be able to change the pore diameter during the process allows for the manufacture of tailored porous gel-silica for specific applications.

There is very little change in the average diameter of the interconnected pores during the densification but their number decreases rapidly as the temperature increases. Consequently the ultrastructure and physical properties of the gel change dramatically during the consolidation treatment. Figure 8 shows the decrease in total porous volume and specific surface area, determined by quantitative nitrogen absorption-desorption measurements, of gel-silica samples over a temperature range of 200°C and 900°C. Figure 9 presents the increase in bulk density and microhardness over the same range of temperature.

For a practical range of densification temperature from 600°C to 900°C, the porous gel-silica presents the following ranges of characteristics:

Total pore volume:	0.4 to 0.2 cc/g
Specific surface area:	620 to 290 sq. m/g
Bulk density:	1.3 to 1.5 g/cub. cm
Microhardness:	100 to 285 Kg/sq. mm

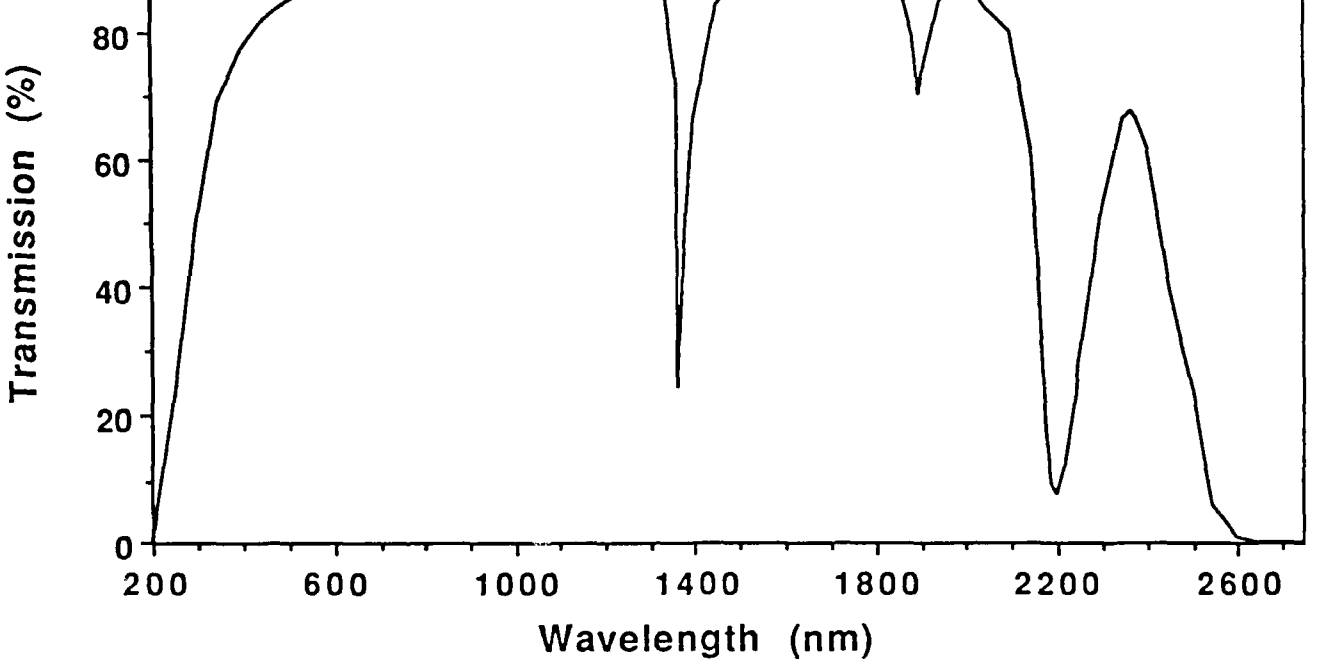

Fig. 7. Optical transmission of porous gel-silica (Type VI)

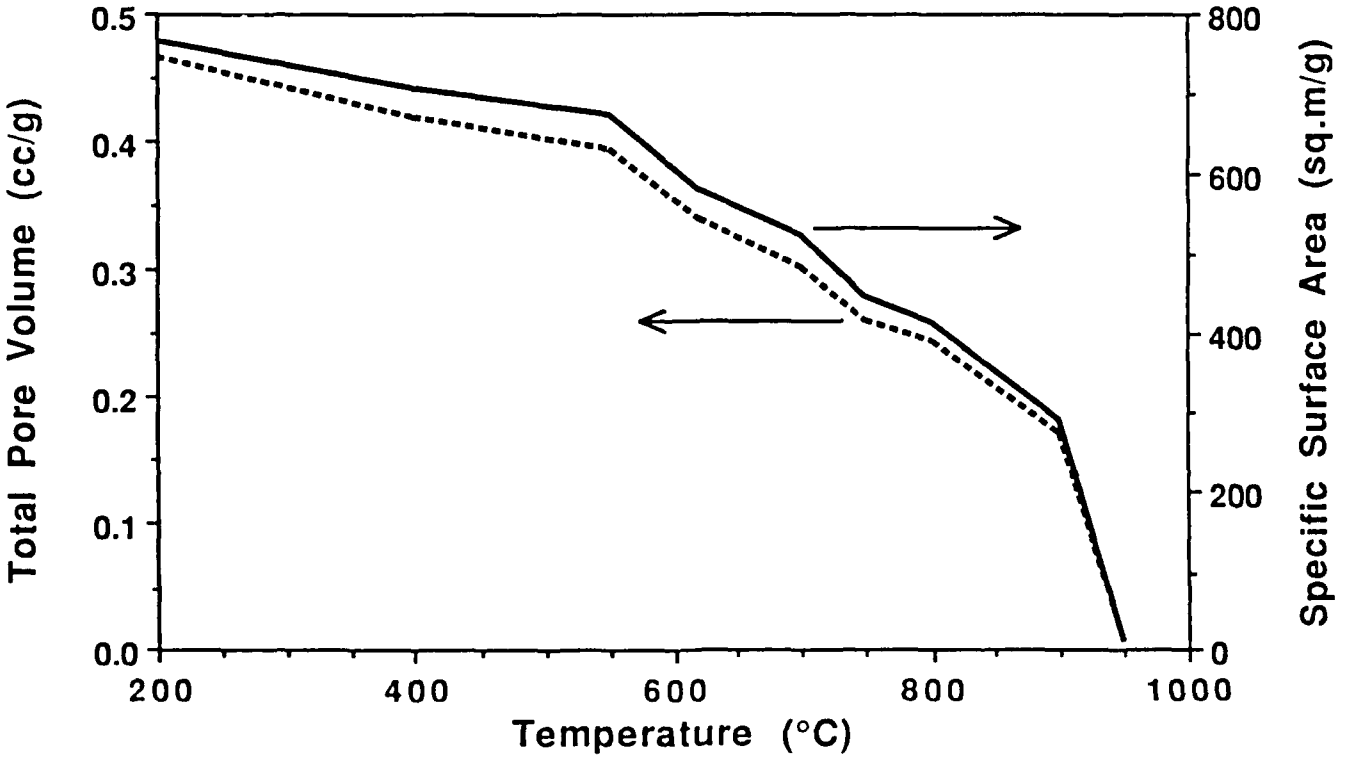

Fig. 8. Ultrastructure characteristics of porous gel-silica (Type VI)

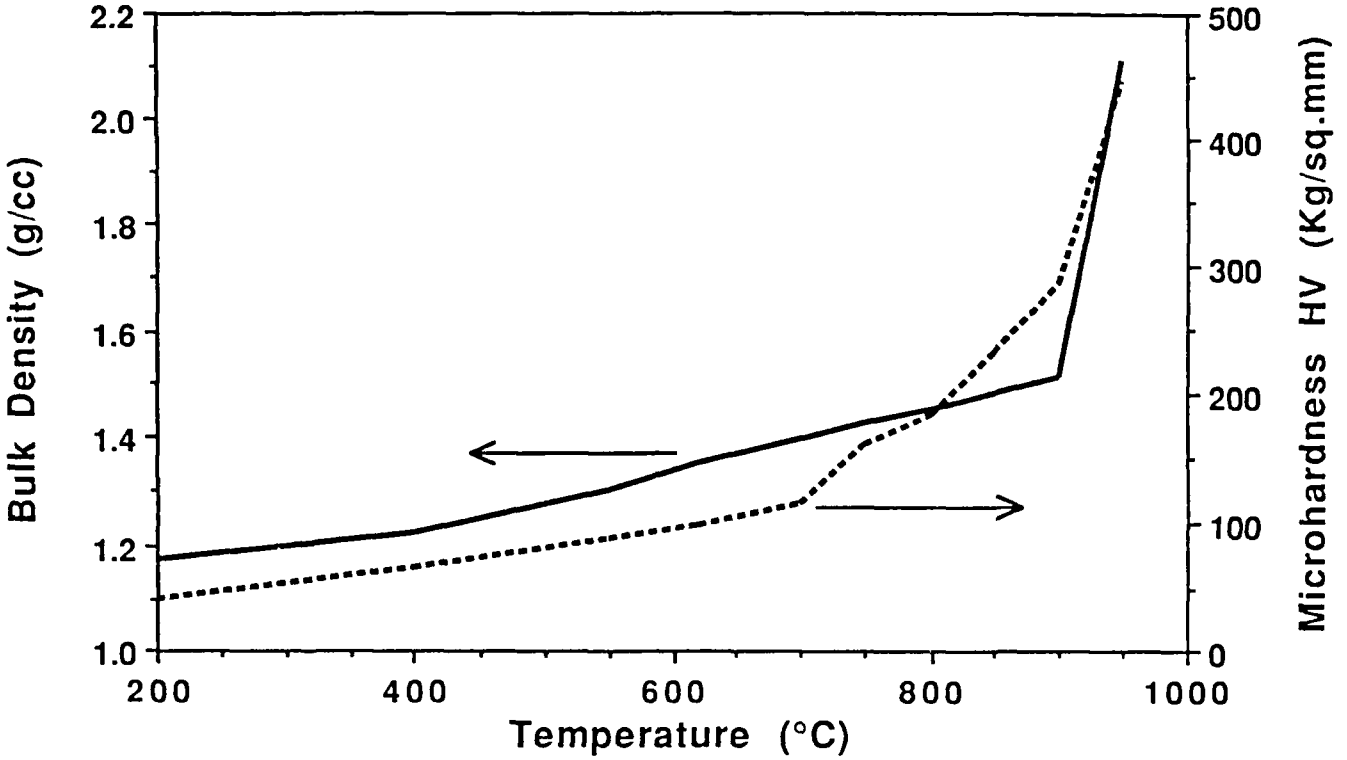

Fig. 9. Physical characteristics of porous gel-silica (Type VI)

The physical properties of porous gel-silica (Type VI) described above are attractive for many potential applications. The low density can be interesting for lightweight optical component applications. The interconnected residual porosity of the components makes them desirable for thermally cooled optics or for molecular filtration devices. This type of porous glass can be used as substrates for diffusion to produce graded refractive index optics (GRIN) or as substrates for silica waveguides. The type of applications where the most investigations were accomplished is for the production of composites by doping or impregnation of a second phase into the interconnected pore network. This technique allows the production of nano-scale composites because of the size of the pore of about 2 to 10 nanometers in diameter. Many composites had already been prepared and successfully tested at laboratory scale. These composites include the impregnation of the porous gel-silica matrices with organic fluors, wavelength shifters[9], non-linear optical polymers or compounds, laser dyes, liquid crystals, etc. Details of properties and specific potential applications of porous gel-silica are published elsewhere.[10]

Another unique application of Type VI silica is for pure silica optical waveguide substrates.[11] By laser densification, optical waveguides have been made using laser writing of higher density tracks on the porous gel-silica substrate. The higher density tracks have a greater index of refraction than the porous matrix and therefore can serve as a planar waveguide. The major advantage of this type of waveguide is that it matches the index of refraction of silica fiber optics, which is not the case for ion-exchanged or diffusion based waveguides.

This Type VI porous silica represents a new material with tremendous potential possibilities of developments for optical and optoelectronic applications.

5. AS-CAST SHAPES AND SURFACE FEATURES

Another area of potential advantage of sol-gel optics processing is that of obtaining net shapes and surfaces, or at least near-net shapes and surfaces, directly through casting sols at low temperature into molds of predetermined configurations.

As explained in the first part of this paper, the grinding and polishing of a lens from the raw glass represents up to 80-90

percent of its cost. If this third stage of the optics manufacture could be eliminated the production cost of optical components would be dramatically reduced. The concept of grinding and polishing elimination is already used for manufacture by the pressing of lenses, but this technique can be used only for low temperature glasses and low quality optics, and definitely not for pure silica and high quality components. However, it is for the pure silica glass and high quality components that the cost of grinding and polishing is the most expensive.

The concept of casting to shape is an old concept used all around us for the manufacture of many products but its application to the sol-gel process is a challenge due to the high level of shrinkage, the fragility of the gel during the first steps of the process, and the relatively high temperature of the densification. The complexity of this process requires control and a high understanding of each process variable. The synoptic of the casting to shape concept is presented in figure 10.

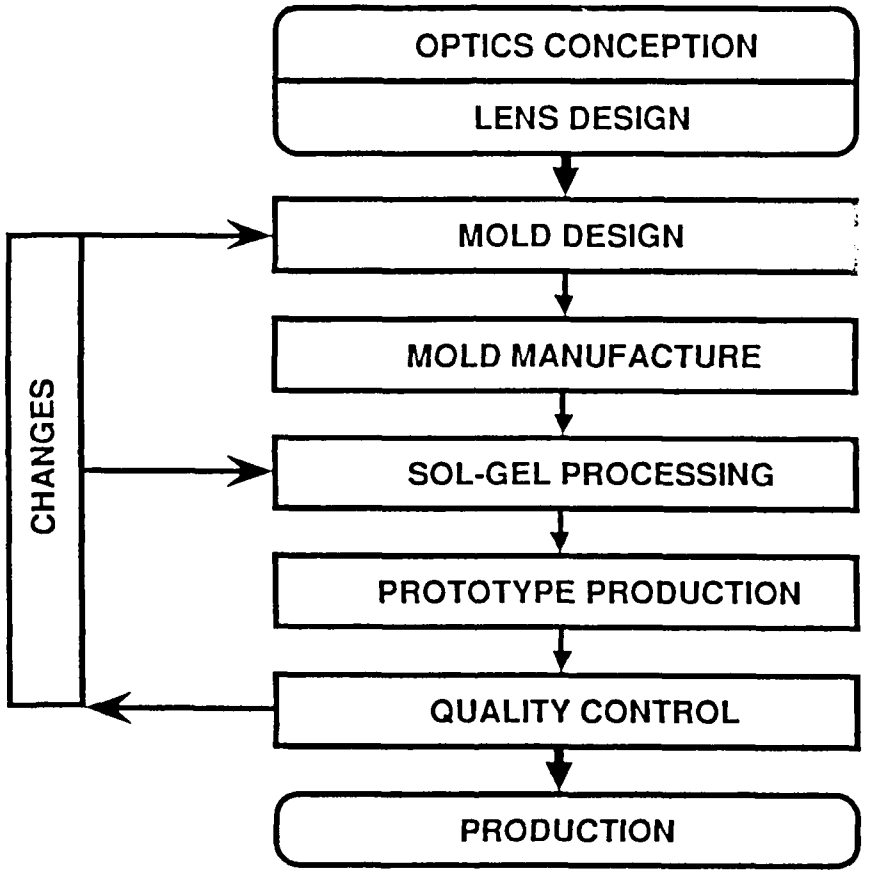

Fig. 10. The different steps of the casting to shape concept

The first step of the casting to shape processing is the design of a mold from the design of the lens to produce. This design is done based on a multitude of data on the shrinkage of the gel during the process as a function of its shape and its dimensions (diameter, thickness, radius of curvature, etc.). All this data on shrinkage is necessary to build a computer model and reduce the number of iterations to achieve the production of parts with the initial dimensional tolerances.

The second step consists of modifying the sol-gel process to be able to age, dry and densify the gel without cracking after casting the sol into the manufactured mold.

Each different optical component requires the design of a specific mold and an adaption of the sol-gel process. But these operations have to be done only once and their cost amortized over a large number of parts, whereas the cost of grinding and polishing is directly proportional to the number produced.

Fig. 11. Plano/convex gel-silica lenses (Dried and dense)

Figure 11 shows the photograph of plano-convex lenses produced by casting to shape without any additional processing. Their dimensions are in good agreement with the dimensional limits of commercial lenses.

This concept of casting to shape is even more important and more economic when the optical element presents a complex shape such as aspheric or cylindrical. The advantages of near net shape casting includes the ability to form internal cavities using a modification of the normal sol-gel process.

Another application of net shape casting is the replication of specific surface features. For example, Fresnel lens were manufactured by directly casting the sol into a mold having a surface with the negative indentation of the surface to reproduce. Microscopy and profilometry shown that the replication of the surface details is good and was maintained through full densification. The advantages of the silica Fresnel lens over a polymer lens is the very good chemical and thermal stability in addition to superior optical properties. The surface feature replication is a new possibility for optical components and will offer many new developments for optics and optoelectronic applications.

6. CONCLUSIONS

The trends of the optical industry shows that the market share maintained by U.S. manufacturers has been declining continuously and dramatically over the years. With the increasing need of optical components and the tremendous level of imports to fill this need, the dependency of the U.S. to foreign suppliers, especially for defense applications, represents a real threat.

The sol-gel technology can represent a good alternative by offering the U.S. a source of high quality optical components. This technology in not as capital and labor intensive as the conventional manufacturing process and should allow U.S. sol-gel optics producers to set up easily production facilities and to be competitive enough to reverse todays trends.

The specific sol-gel process described in this paper allows the production of a dense gel-silica (Type V) with excellent optical, physical and structural characteristics, generally equivalent to or superior to the best grades of commercial available Type I to IV optical silicas. In addition this process permits the production of a new material called porous gel-silica (Type VI) which presents good optical and physical properties, and could be used for many novel applications.

Both Types V and VI silica offer the advantage of near net shape casting and surface feature replication which can eliminate to a large extent the need of grinding and polishing, and the production of optics with surface details such as Fresnel lens.

Even though new technologies such as sol-gel process are under investigation in order to try reverse actual optical market trends, it is easy to prognosticate that domestic manufacturers can look forward to at least a few more painful years. The future of the optical business will certainly be challenging.

7. ACKNOWLEDGMENTS

The authors gratefully acknowledge financial support of Air Force Office of Scientific Research Contracts #F49620-86-C-0120 and F49620-88-C-0010 and the encouragement of D. R. Ulrich throughout this research.

8. REFERENCES

1. R. P. O'Shaughnessy, et al., Joint Precision Optics Technical Group's Final Report, Department of Defense's Joint Logistics Commanders, Precision Optics Study, June 1987.
2. R. Cunningham, "Trough the Looking Glass", Lasers & Optonics, 7 [5] 45-51 (1988).
3. L. L. Hench & D. R. Ulrich, eds., Ultrastructure Processing of Ceramics, Glasses, and Composites, John Wiley & Sons, NY, 1984, and Science of Ceramic Chemical Processing, John Wiley & Sons, NY, 1986. J. D. Mackenzie & D. R. Ulrich, eds., Ultrastructure Processing of Advanced Ceramics, John Wiley & Sons, NY, 1988.
4. C. J. Brinker, D. E. Clark, and D. R. Ulrich, eds., Better Ceramics Through Chemistry, Vol. 32, North-Holland, NY, 1984; Better Ceramics Through Chemistry II, Vol. 73, North-Holland, NY, 1986; and Better Ceramics Through Chemistry III, Vol. 121, North-Holland, NY, 1988.
5. V. Gottardi, ed., Proceedings of the International Workshop on Glasses and Glass Ceramics from Gels, J. Non-crystal. Solids, 48 [1], (1982); H. Scholze, ed., Proceedings of the Second International Workshop on Glasses and Glass Ceramics from Gels, J. Non-crystal. Solids, 63 [1&2], (1984); J. Zarzycki, ed., Proceedings of the Third International Workshop on Glasses and Glass Ceramics from Gels, J. Non-crystal. Solids, 82 [1-3], (1986); and S. Sakka, ed., Proceedings of the Fourth International Workshop on Glasses and Glass Ceramics from Gels, J. Non-crystal. Solids, 100 [1-3], (1988).
6. M. Grayson, ed., Encyclopedia of Glass, Ceramics, Clay and Cement, John Wiley & Sons, NY, 1985.
7. L. L. Hench, M. J. R. Wilson, C. Balaban, and J. L. Noguès, "Sol-Gel Processing of Large Silica Optics", Presented at the Fourth International Conference on Ultrastructure Processing of Ceramics, Glasses, and Composites, Tucson, AZ, February 1989.
8. L. L. Hench, S. H. Wang, and J. L. Noguès, "Gel-Silica Optics", SPIE - Multifunctional Materials, R.L. Gunshor, ed., Vol. 878, 76-85 (1988).
9. J. L. Noguès, S. Majewski, J. K. Walker, M. Bowen, R. Wojcik, & W. V. Moreshead, "Fast, Radiation Hard Scintillating Detector, A Potential Application for Sol-Gel Glass", J. Am. Ceram. Soc., 71 [12] 1159-63 (1988).
10. J. L. Noguès and W. V. Moreshead, "Porous Gel Silica, a Matrix for Optically Active Components", Presented at the Fifth International Workshop on Glasses and Glass Ceramics from Gels, Rio de Janeiro, August 1989.
11. R. V. Ramaswamy, T. Chia, R. Srivastava, A. Miliou, & J. West, "Gel-Silica Waveguides", SPIE - Multifunctional Materials, R.L. Gunshor, ed., Vol. 878, 86-93 (1988).

Note: † Gelsil™ is a trademark of GELTECH, Inc.

POROUS GEL SILICA, A MATRIX FOR OPTICALLY ACTIVE COMPONENTS

Jean-Luc R. Noguès and William V. Moreshead

GELTECH, Inc., One Progress Blvd, Box 18, Alachua, Florida 32615 (USA)

Abstract

The sol-gel process has been used to prepare optically active components in a silica matrix. In most cases this involves introducing an optically active material such as an organic dye into the initial sol prior to gelation. An alternative sol-gel route involves first the preparation of porous, pure silica monoliths which can then be impregnated with the desired organic or inorganic material. Critical to the usefulness of this material is a knowledge of the properties, such as thermal stability, UV/vis/nIR spectra and pore size. In this paper the structural evolution of these porous silica monoliths prepared by the sol-gel process is presented as a function of process temperature. Sample preparation and thermal treatments are briefly described, and results of sample characterizations are given in detail. Results of this study and their implications for the usefulness of the materials will be discussed.

Subject index codes: a2, d10, o7, s5, s9.

1. Introduction

Over the past several years there has been an increasing interest in sol-gel techniques for the manufacture of glasses, glass-ceramics and ceramics. This new route has been utilized for a variety of products ranging from optical fibers and lenses to special coatings and to production of ultra-pure powders.

The purpose of this paper is to focus in a first part on the processing and the properties of porous gel-silica glass monoliths to be used as matrix for the preparation of optically active components and new kinds of optical devices. This new material presents many properties of the dense pure silica glass but presents in addition many unique characteristics which could lead to very special and novel developments in optics. Several applications such as microoptical arrays, scintillation detectors and optical waveguides are briefly described in the second part of this paper.

2. Porous gel-silica matrix preparation, processing, and properties

2.1. Experimental

Porous gel-silica samples used in this study were manufactured by hydrolyzing a silica precursor, tetramethylorthosilicate (TMOS, Petrarch, Inc.) with deionized water. After complete homogenization this sol was cast into 60 mm polystyrene petri dishes to gel and age. The wet gel was then dried to give a transparent gel-silica monolith.

Further heat treatment was done in static air to study the evolution in gel properties with temperature. The rate of heating was selected low enough to maintain the monolithic aspect of the gels and to avoid a temperature gradient inside the sample which can cause heterogeneity in gel properties. Isotherms at 620℃ and 800℃ were observed to evacuate solvent and by-products from the gel structure, and to observe the evolution in sample properties during a soak. Samples were removed from the furnace at a given temperature and quenched in air at room temperature.

Shrinkage during densification was measured in static air using a Dupont 943 Thermomechanical analyzer (TMA). The heating rate was 0.5℃/min.

The textural characteristics were measured using an Autosorb-6 from Quantachrome Corporation. The results were analyzed according to the BET theory and a cylindrical pore model was used for the calculations of the pore radius distribution.

The density measurements were done on oven-dried samples using a specific gravity bottle with mercury as the fluid.

The microhardness was measured using a LECO Model-700 Microhardness Tester with a diamond Vickers indenter.

UV-vis-nIR spectra were recorded on a Lambda-9 Spectrophotometer from Perkin-Elmer.

2.2. Results and Discussion

Figure 1 presents the TMA thermogram of a dry gel monolith between room temperature and 685℃, the maximum temperature of the equipment. The heat treatment cycle was repeated three times without removing the sample from the cell, and with recalibration of the zero position before each cycle.

After the first cycle to 685℃ the sample underwent a net shrinkage of 8.4% after returning to room temperature. After the second cycle the shrinkage was not negligible but was greatly reduced (0.5%). A third cycle resulted in a total shrinkage of 0.2%.

These results lead to an important conclusion regarding the usefulness of these materials as porous matrixes: further heating to a temperature close to, equal to, or higher than the maximum temperature to which the gel has been previously heated will induce new variations in the structure of the gel-silica. However, a sample can be considered to be thermally stable at temperatures well below this maximum temperature.

Changes in other gel characteristics and properties measured for this study during densification are in good agreement. The results are summarized in table 1. These changes are smooth and regular as the treatment temperature is increased to 950℃. At this temperature the behavior of the gel changes drastically and the material loses its characteristics for porous matrix applications. Although the magnitude of the changes are greater for the soak at 620℃ than for the soak at 800℃, the trends were similar.

The transmission spectra of samples stabilized at 620, 900 and 950℃ show the well-known absorption bands due to the silanol groups (Si-OH) and the molecular water (figure 2).[1-3] With the stabilization temperature increasing, two phenomena occur: 1) the absorption bands decrease in intensity corresponding to the release of "water" by the sample, and 2) the transmission cutoff in the ultraviolet range shifts to lower wavelengths. For the sample stabilized at 950℃ the spectrum presents only the major absorption bands of the Si-OH.

Figure 3 shows the variation of the OH radical concentration in the gel as a function of temperature. The calculation of this OH radical content was done using a formula derived from the one used for OH content determination in silica glasses [4] and applied to the absorption band at 1.36 μm of the first overtone of the fundamental absorption peak of Si-OH groups (2.73 μm). Since the extinction coefficient is not presently available to quantify the water content using this band, the results are plotted in arbitrary units. However, this figure shows that the OH radical content in the gel decreases rapidly with increasing temperature

The data collected in this study allow the definition of three different sequences during the sintering treatment.

1) Between room temperature and 900℃ there is a continuous evolution of the gel properties. This evolution is faster for the higher temperatures, especially between 800℃ and 900℃. This evolution occurs mainly by loss of water. The specific surface area and the total pore volume decrease as a result of condensation reactions which cause the network to become more and more interconnected without causing any change in the calculated average pore radius (figure

4). As interconnectivity increases the bulk density and microhardness increase by the same trend, as expected (Table 1). The trend in microhardness is illustrated in figure 3.

2) Between 900℃ and 950℃ the densification takes place more rapidly since the viscosity of the material is low enough to allow viscous sintering. Measured changes are much more dramatic.

3) Above 950℃, pores remaining in the sample begin to close resulting in bloating of the sample. At this stage the sample loses its transparency, its homogeneity and its ability to be used as porous matrix for optical components.

The ultrastructure data also shows that the sintering of this particular type of gel silica occurs without variation of the average pore size, maintaining or enhancing the optical transmission of the porous sample.

3. Potential applications of porous gel-silica matrices

The properties and characteristics of porous gel-silica, in particular porosity and transmission, make this material adequate for the development of new types of optical elements.[5] The porous phase of this gel-silica matrix can be filled with a second phase with very special properties to produce a composite material. The completely open porosity and the very small size of the pores allow the production of a nano-scale composite with good macro homogeneity. The doping phase can be either an inorganic material such as metallic cations or an organic compound which leads to the preparation of organic/inorganic composites. Examples of these two types of applications is briefly described below, as well as a possible direct application of the porous gel-silica matrix.

3.1. Microoptical arrays [6]

The basic components for digital optics have been identified as modulator and detector arrays, which in many cases require microlens arrays for imaging. Stacked planar optics is an attractive technology for digital optics, and can be used for many possible applications, such as optical computing, camera auto focus modules, or imaging bar lenses in photocopiers.

The basic unit of the array is the individual microlens which is a region with an index gradient embedded in a glass substrate as a result of selective doping. The actual manufacture of this type of lens is difficult and often leads to optical aberrations, limiting the number of components which may be stacked together.

Sol-gel technology offers the possibility to minimize spatial aberration by doping a porous gel-silica matrix or preform. The porous gel-silica is doped selectively with polarisable ions, e.g. Ba^{2+}, or glass structure modifiers, e.g. Pb^{2+}, and the dopant elements are trapped in the glass by subsequent densification to form a microlens array.

3.2. Scintillations detectors [7]

Organic plastic scintillators have been used for particle detection for about thirty years. They have two advantages: 1) Fluorescence decay times as short as 1 nanosecond, and 2) Light output proportional to energy deposition in the detector. It is well known, however, that plastic scintillators are rather sensitive to ambient radiation which results in strong absorption of light for doses as small as 10^5 rd.

Scintillating glasses have been developed slowly over the last twenty five years but never came into general use as particle detectors. Because of the high temperature used in the production of glass, organic fluors were excluded as dopants and only inorganic dopants such as cerium and terbium oxides could be used. The advantages of scintillating glasses are that they are heavier and less sensitive to radiation than plastic scintillators. On the other hand, their fluorescence decay times have been found to be rather long.

To meet the present day rate and radiation dose requirements it would be desirable to have a scintillator with the high radiation resistance of pure silica glass and the short fluorescence decay time of organic fluors. Because of the high radiation resistance of silica, sol-gel technology opens the exciting possibility of doping glass with fast organic fluors which would provide an important advancement in particle detection. Although the sol-gel scintillators produced to date are far from being optimized, the first results prove the feasibility of producing a fast, radiation hard scintillator using the sol-gel process.

3.3. Optical waveguides

Optical waveguides on a glass substrate represent the basis for passive components such as multiplexers, couplers, or wavelength filters used in integrated optical applications for optical communication and sensors .

Various techniques for fabricating glass waveguides have been reported in the literature and include: techniques such as sputtering, ion implantation, ion-exchange, and chemical vapor

deposition. Today, these last two techniques are the most successful. The ideal would be waveguides made in silica substrates, preferably without any dopant for tailoring the index profile, and maintaining the monolithic nature of the devices.

The sol-gel technology leading to the manufacture of porous gel-silica matrix offers a possible substrate for waveguides. Two approaches can be pursued. First, the selective doping of the substrate using controlled diffusion in the porous silica in order to change the refractive index of the material. Second, the local heating of some selected portion of the substrate to increase the density and index of refraction of the glass.[8] By CO_2 laser densification, optical waveguides have been made using laser writing of higher density tracks on porous gel-silica substrate.[9]

It was demonstrated that both of these techniques can induce the index of refractive changes of the right magnitude to fabricate single mode waveguides. The second technique presents the possibility to produce ideal pure silica waveguide. The major advantage of this type of waveguide is that it matches the index of refraction of silica fiber optics, which is not the case for ion-exchanged or diffusion based waveguides.

The technique of doping a pure gel-silica matrix with inorganic or organic compounds is not restricted to the applications described in this paper, but can be used for the preparation of a wide variety of optically active materials, such as optical filters [10], dye lasers, non linear optic components, optical data storage media, and many others.

4. Conclusion

This study showed that it is possible to produce stabilized sol-gel moncliths with a range of properties, and free of organic residues. The sintering of this type of gel silica occurs in roughly three stages, with the last resulting in pore closure and ultimate destruction of the sample above about 950℃. If heating is stopped prior to this a semi-stable, porous, gel-silica matrix can be produced. Demonstration of possible applications of such a matrix, such as microlens arrays, scintillating detectors, and waveguides have been reported.

Acknowledgments

The authors gratefully acknowledge financial support of Air Force Office of Scientific Research Contracts #F49620-86-C-0120 and F49620-88-C-0010 and the encouragement of D. R. Ulrich throughout this research. Also the technical assistance of Robert H. Krabill is greatly appreciated.

References

1. M. Grayson, Ed., Encyclopedia of Glass, Ceramics, and Cement, John Wiley & Sons, NY (1985) pp 823-826.
2. R. F. Bartholomew, B. L. Butler, H. L. Hoover, C. K. Wu, J. Amer. Ceram. Soc., 63 (9-10) (1980).
3. D. L. Wood, E. M. Rabinovich, D. W. Johnson, JR., J. B. MacChesney, E. M. Vogel, J. Amer. Ceram. Soc., 66 (10) (1983).
4. J. E. Shelby, J. Vitco Jr., R. E. Benner, Com. Amer. Ceram. Soc., 65 (4) (1982).
5. L. L. Hench, S. H. Wang, J. L. Noguès, SPIE Vol. 878 Multifunctional Materials, (1988) pp 81-85
6. M.M. Stallard, "Microoptical arrays", Presented at the US-UK Optical Glass and Macromolecular Materials Symposium, Pitlochry, Scotland (1988)
7. J. L. Noguès, S. Majewski, J. K. Walker, M. Bowen, R. Wojcik, W. V. Moreshead, J. Amer. Ceram. Soc., 71 (12) (1988).p 1159-63
8. R. V. Ramaswamy, T. Chia, R. Srivastava, A. Miliou, & J. West, SPIE Vol. 878 Multifunctional Materials, (1988) pp 86-93.
9. D.J. Shaw, A.J. Berry, T.A. King, "Laser Densification of Sol-Gel Matrices", Same as Ref. 6.
10. S. H. Wang and L. L. Hench, in Science of Ceramic Chemical Processing, Edited by L. L. Hench and D. R. Ulrich., John Wiley & Sons, NY (1986) pp. 201-207

Table Caption

1. Properties and characteristics of porous gel-silica monoliths vs densification temperature

Figure Captions

1. Thermomechanical analysis of a porous gel-silica monolith
2. Optical transmission of gel-silica monolith vs densification temperature
3. OH Radical Content ([OH]) and Sample Microhardness (SMH) vs Densification Temperature
4. Specific Surface Area (SSA) and Total Pore Volume (TPV) vs Densification Temperature

Temperature °C	SSA sq.m/g	TPV cc/g	APR Å	SBD g/cc	SMH Kg/sq.mm	[OH] a.u.
200	768	0.47	12.2	1.172	41	193
400	707	0.42	11.8	1.224	65	189
550	672	0.39	11.7	1.299	88	172
620	620	0.37	11.8	1.308	101	161
620	537	0.31	11.6	1.391	97	157
700	522	0.30	11.6	1.393	115	143
750	449	0.26	11.7	1.424	160	132
800	438	0.26	11.8	1.438	183	122
800	393	0.23	11.7	1.460	--	122
850	--	--	--	1.502	233	94
900	290	0.17	11.8	1.510	285	66
950	9	0.01	13.9	2.113	447	9
1000	4	0.00	15.6	2.109	--	--
1050	3	0.00	16.8	1.651	--	--

SSA: specific surface area; TPV: total pore volume; APR: average pore radius;
SBD: sample bulk density; SMH: sample microhardness; [OH]: OH radical content

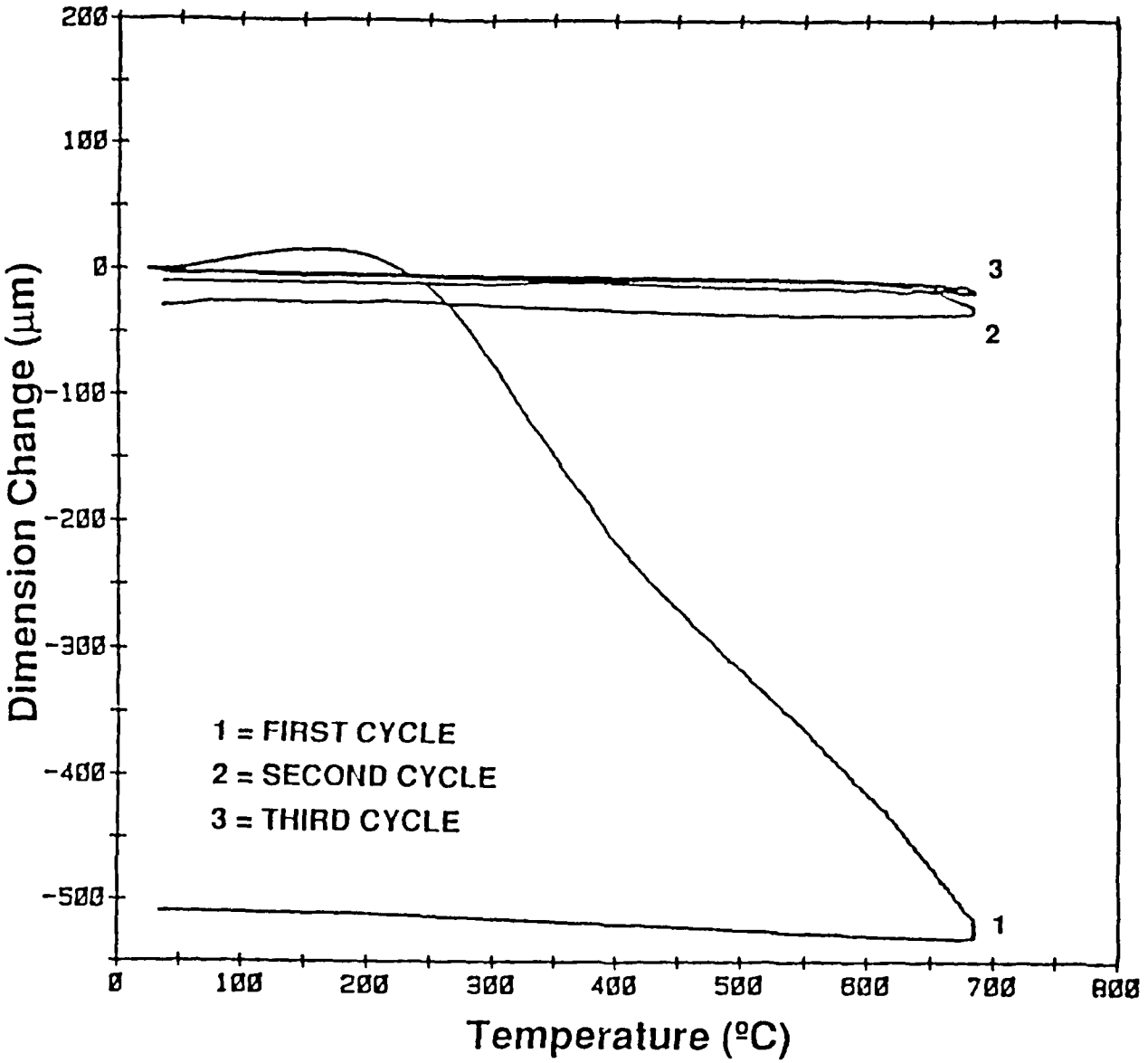
200
100
0
-100
-200
-300
-400
-500
Dimension Change (µm)
0
100
200
300
400
500
600
700
800
Temperature (ºC)
1 = FIRST CYCLE
2 = SECOND CYCLE
3 = THIRD CYCLE
1
2
3

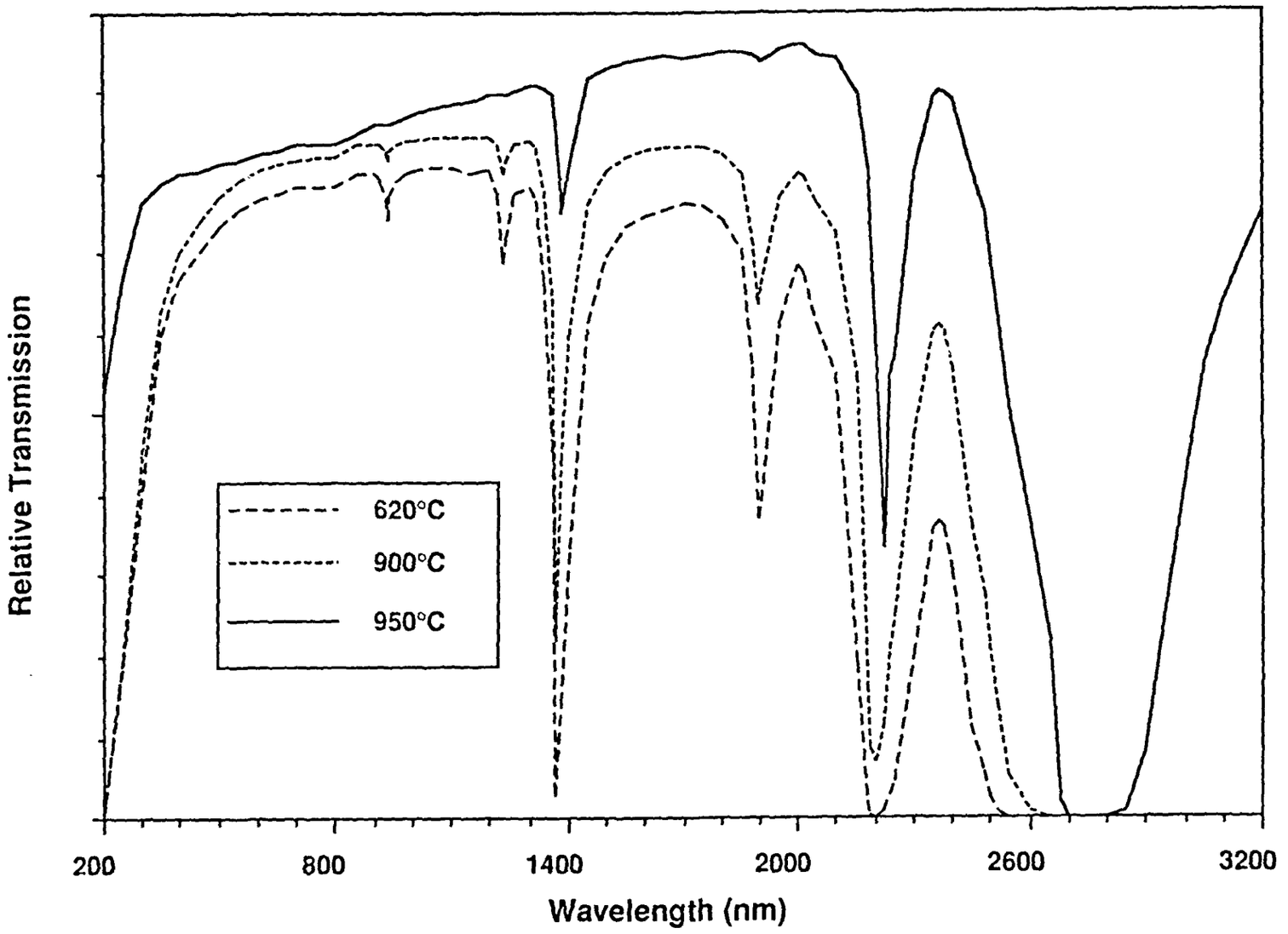
Relative Transmission
620°C
900°C
950°C
200
800
1400
2000
2600
3200
Wavelength (nm)

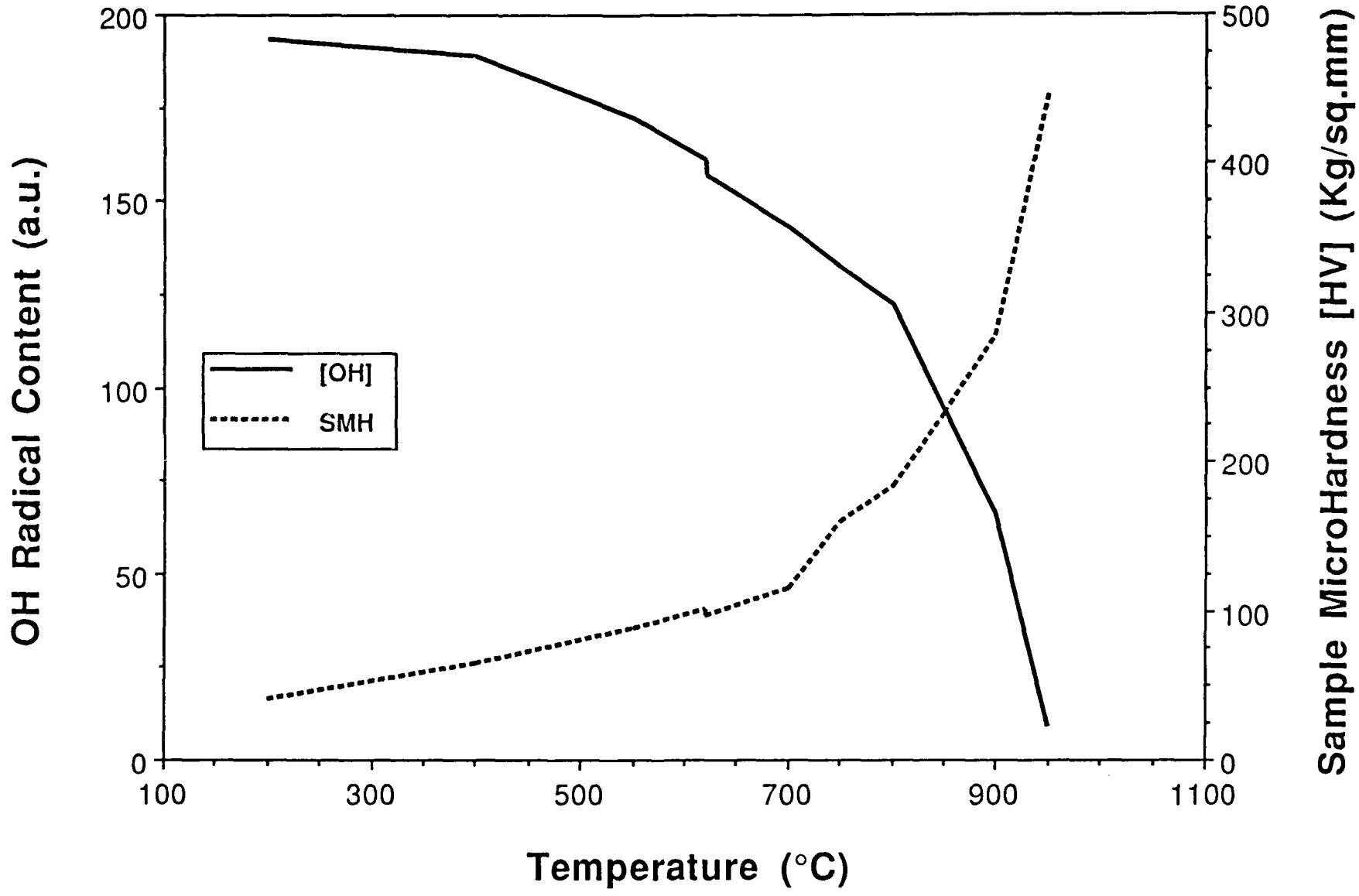
200
150
100
50
0
OH Radical Content (a.u.)
[OH]
SMH
500
400
300
200
100
0
Sample MicroHardness [HV] (Kg/sq.mm)
100
300
500
700
900
1100
Temperature (°C)

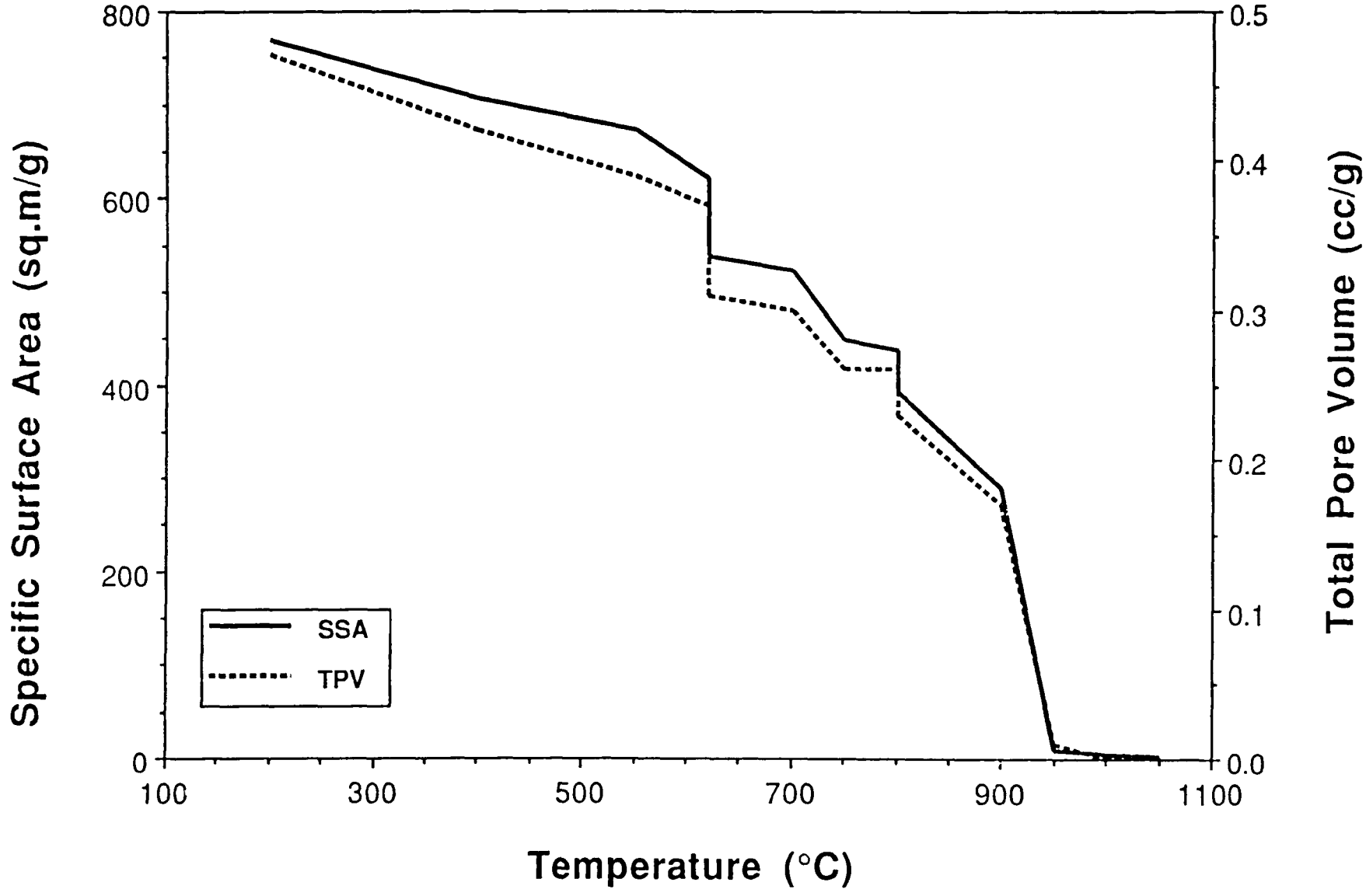
800
600
400
200
0
0.5
0.4
0.3
0.2
0.1
0.0
100
300
500
700
900
1100
Specific Surface Area (sq.m/g)
Total Pore Volume (cc/g)
Temperature (°C)
SSA
TPV

Silica Optics Manufacture Via Sol-Gel Technology

J.L. Noguès, C. Balaban, W.V. Moreshead, R.S. Sheu

GELTECH, Inc, One Progress Blvd., Box 18, Alachua, Fl 32615

Abstract

GELTECH, Inc. is a small company founded to develop and market products using sol-gel technology initiated at the University of Florida. The results of research and development efforts at GELTECH are briefly reviewed here with an emphasis on properties and potential applications of both porous and dense gel-silicas.

1. Introduction

In recent years sol-gel technology has received much attention from both universities and the private sector. For an overall background on sol-gel technology see references 1 to 3. Some of the advantages of sol-gel include the potential for greater chemical homogeneity, lower processing temperatures, and casting of shapes. GELTECH, Inc., was founded to develop and market products using sol-gel technology initiated at the University of Florida. In this paper a brief overview of the sol-gel process developed at GELTECH is given, and some of the potential products and their properties are highlighted. The primary effort at GELTECH to date has been in the area of pure silica with a focus on the optics and optoelectronics market.

2. Different Types of Silica

Silica optics are used in many optical systems because of their excellent transmission from ultraviolet (UV) to near infrared (NIR) wavelengths, their excellent homogeneity, their very good thermal and chemical stabilities, and their low coefficient of thermal expansion (CTE).

There are at the present time four major methods of producing pure silica optical glass, as summarized in table 1 (4). There are two main categories: Fused Quartz (Types I and II) produced by melting natural quartz crystals, and Fused Silica (Types III and IV) manufactured by vapor phase hydrolysis or oxidation of silicon tetrachloride.

The differences between these four types of silica lie in the level of cation impurity, the hydroxyl group content and other optical properties such as homogeneity, seeds, bubbles, inclusions and microcrystallites.

During the last few years the chemically derived process described in this paper has been developed and has lead to the manufacture of two new types of silica: Type V and Type VI (table 1). Type V silica offers the potential for improving many features of

commercially available silicas. Type VI represents a new kind of material, porous pure silica glass, which can potentially lead to new developments in optics and optoelectronics. The processing, properties and applications of these two new types of silica are described in the following part of this paper.

Table 1: Methods of Silica Optics Manufacture

Fused Quartz
Type I: Electric melting of natural quartz crystals SiO_2 (quartz) $\xrightarrow[\text{vacuum}]{\text{heat}}$ SiO_2 (glass) **Type II:** Flame fusion of natural quartz crystals SiO_2 (quartz) $\xrightarrow[\text{oxy-hydrogen}]{\text{heat}}$ SiO_2 (glass)
Fused Silica
Type III: Vapor-phase hydrolysis of pure silicon tetrachloride carried out in a flame $SiCl_4 + O_2 + 2\,H_2 \rightarrow SiO_2$ (glass) $+ 4\,HCl$ **Type IV:** Oxidation of pure silicon tetrachloride which is fused electrically or by means of a plasma $SiCl_4 + O_2 \rightarrow SiO_2$ (glass) $+ 2\,Cl_2$
Gel-Silica
Type V: Hydrolysis and condensation of organometallic precursor with fully densification (1150 to 1200°C) $Si(OR)_4 + 4\,H_2O \rightarrow Si(OH)_2 + 4\,(ROH)$ $Si(OH)_4 \rightarrow SiO_2$ (dense gel-silica) $+ 2\,(H_2O)$ **Type VI:** Hydrolysis and condensation of organometallic precursor with partial densification (600 to 950°C) $Si(OR)_4 + 4\,H_2O \rightarrow Si(OH)_4 + 4\,(ROH)$ $Si(OH)_4 \rightarrow SiO_2$ (porous gel-silica) $+ 2\,(H_2O)$

3. Overview of the Sol-Gel Process

In this process a silicon-containing precursor, such as tetramethyl or tetraethylorthosilicate, is hydrolyzed to form a sol. After complete homogenization, this sol is cast into molds where it sets into a very porous, wet gel having the shape of the mold. The gel is then dried to give a transparent, silica monolith. The resulting dry gel can be further heat-treated to strengthen it and at the same time reduce its porosity. Although this process removes much of the water, heating to temperatures necessary to fully densify the gel-silica normally results in bloating of the sample due to residual water being trapped in the porous structure. If a dehydration step is

carried out before the final densification, the bloating problem is avoided and fully dense glass can be obtained. For a summary of the overall process see figure 1. An approximate description of the time sequence of the process is given in figure 2.

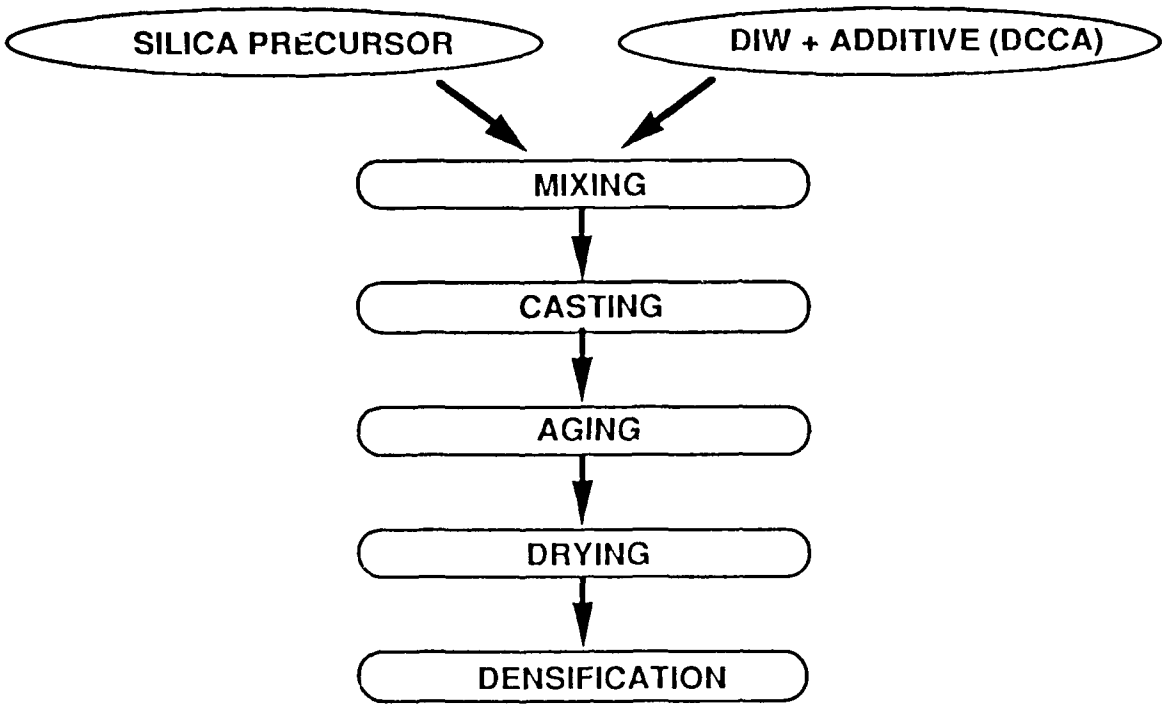

Figure 1: The Different Steps of the Sol-Gel Processing

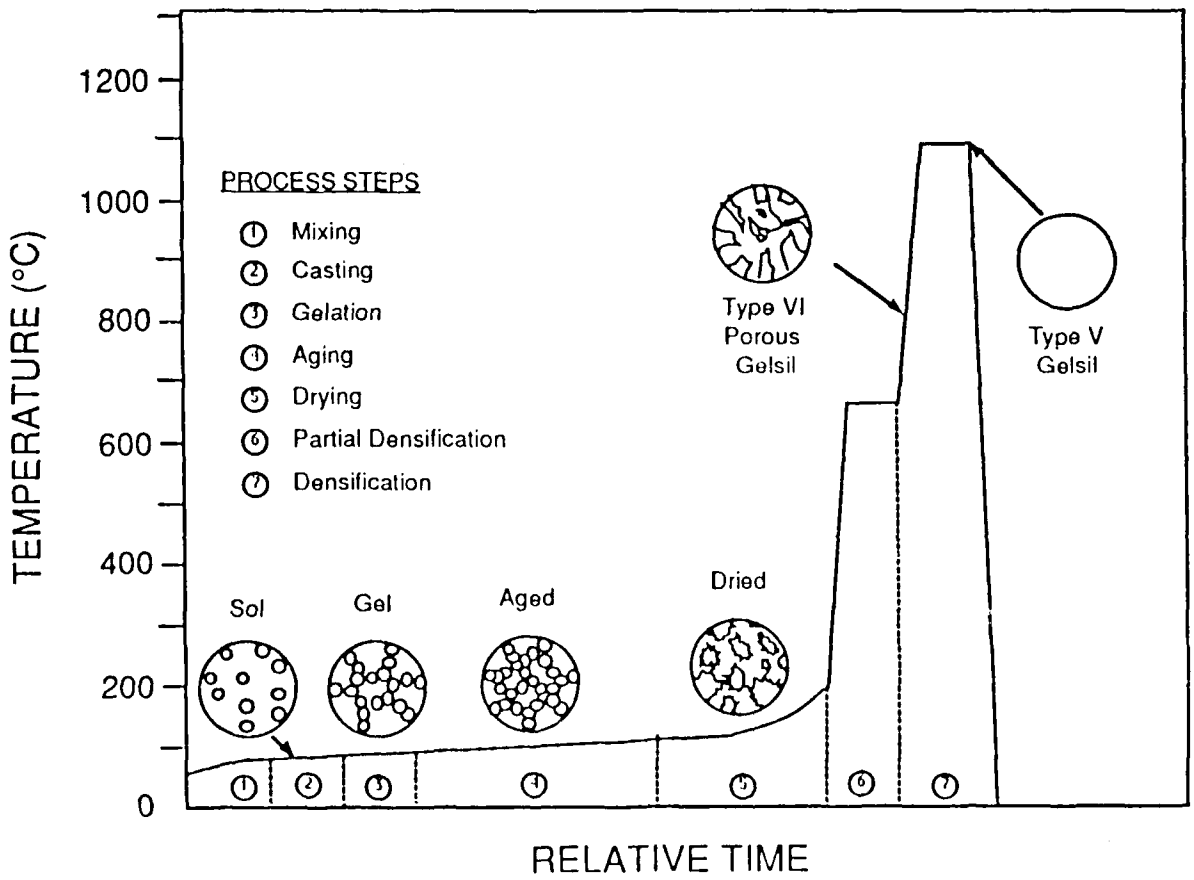

Figure 2: Gel-Silica Process Sequence

4. Porous Gel-Silica: Properties and Potential Applications

Once a gel is dried it is still very porous and weak, and contains some residual organic impurities. A heat treatment can be performed to burn out these organic residues and give the gel added strength. As the gel is heated it goes through essentially two stages before the pores close: (See figures 3 and 4)

1) Up to approximately 800°C to 850°C changes in the properties of the gel take place slowly. The surface area and total pore volume decrease, while the microhardness and bulk density increase.

2) Between 850°C and approximately 950°C these properties then change very rapidly until pores close. As mentioned previously, if pores close before water is removed the water is trapped and further heating causes the sample to bloat or foam due to expansion of the formed gas.

If the heat treatment is stopped before pore closure occurs a porous gel-silica monolith, designated Type VI silica, is obtained. This porous gel now has enough strength to withstand further treatments, such as impregnation with solutions of inorganic (5) or organic materials. A variety of materials have already been used for impregnation, such as fluors, wavelength shifters (6), non-linear optical compounds, liquid crystals and laser dyes. Table 2 lists several potential applications of this porous gel-silica material (7).

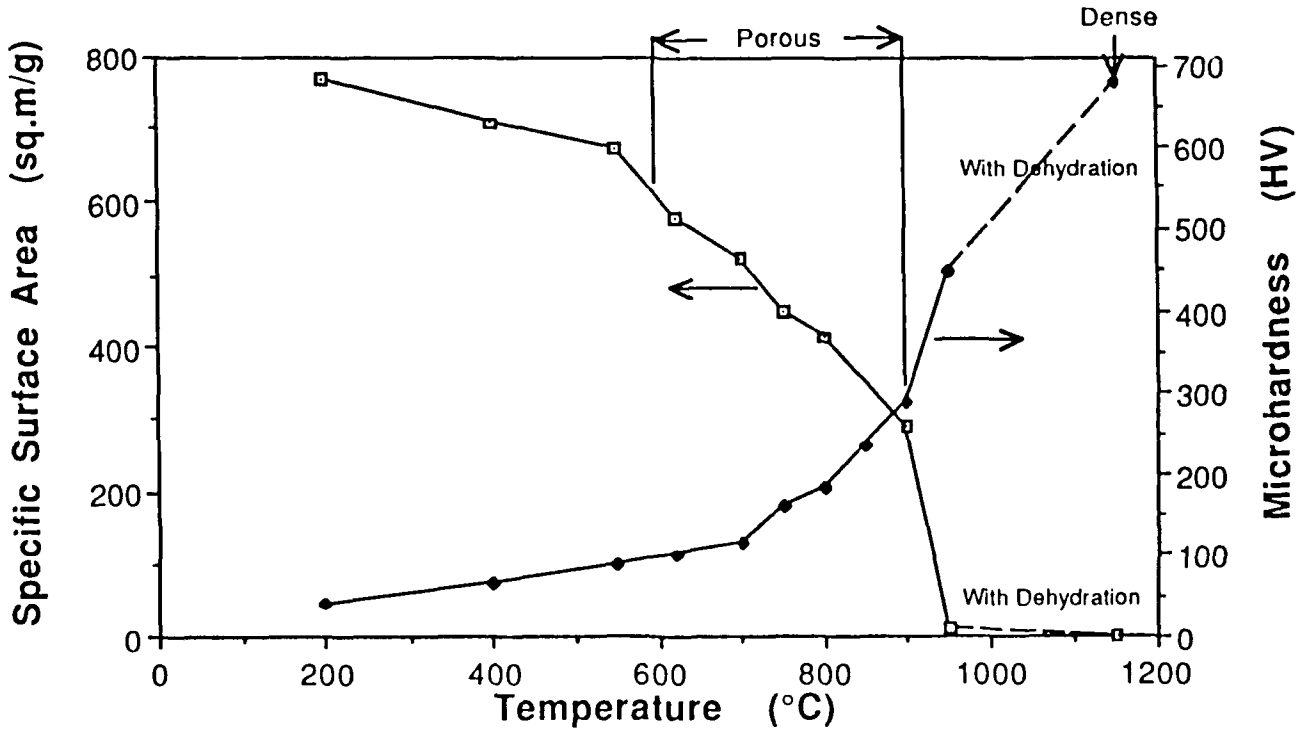

Figure 3: Specific Surface Area and Microhardness of Porous Gel-Silica (Type VI)

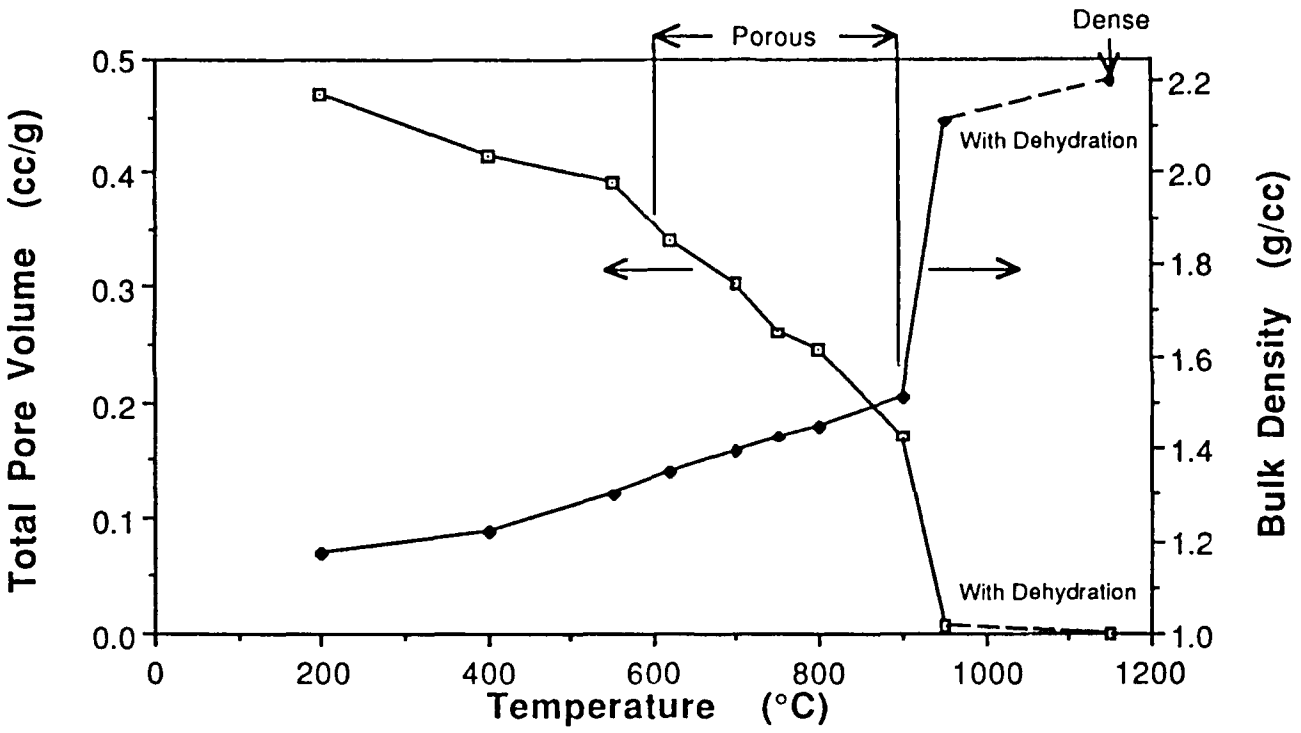

Figure 4: Total Pore Volume and Bulk Density of Porous Gel-Silica (Type VI)

Table 2: Potential Applications of Porous Gel-Silica (Type VI)

Lightweight optical components
Thermally cooled optics
Substrates for graded refractive index optics
Substrates for silica waveguides (8)
Matrices for fluors (6)
Matrices for non-linear optical compounds
Matrices for wavelength shifters (6)
Matrices for laser dyes
Matrices for liquid crystals
Matrices for micro-optical arrays

5. Dense Gel-Silica: Properties and Potential Applications

Gel silica monoliths are densified by removing tightly bound hydroxyl ions on the surface of pores prior to pore closure. Surface dehydroxylation occurs from 200°C to 1000°C. It is usually necessary to enhance the dehydroxylation process by flowing halogen-containing gases through the pore network before closure to produce water free pure silica. This is followed by the removal of any halogen left in the structure of the glass.

The densification process developed at GELTECH, Inc. allowed the production of plano/plano optics of 75 mm and plano/convex optics of 50 mm or larger diameters (9).

The physical properties of the alkoxide derived Type V silica are equal to or superior to Types I-IV optical silicas and include: Short UV cutoff, low optical absorption throughout the spectrum, high homogeneity, very few defects, low strain birefringence, and low coefficient of thermal expansion.

Figure 5 compares the optical transmission of a commercial optical silica (Type III) with a typical spectrum from an alkoxide derived gel-silica (Type V). The vacuum UV cutoff wavelength is substantially improved for the gel-silica material. Elimination of OH radicals from gel-silica optics also results in elimination of absorption bands in the near infrared as shown in this figure. Reliability of production of low OH radical content in Type V silicas (GelsilTM) has also been achieved.

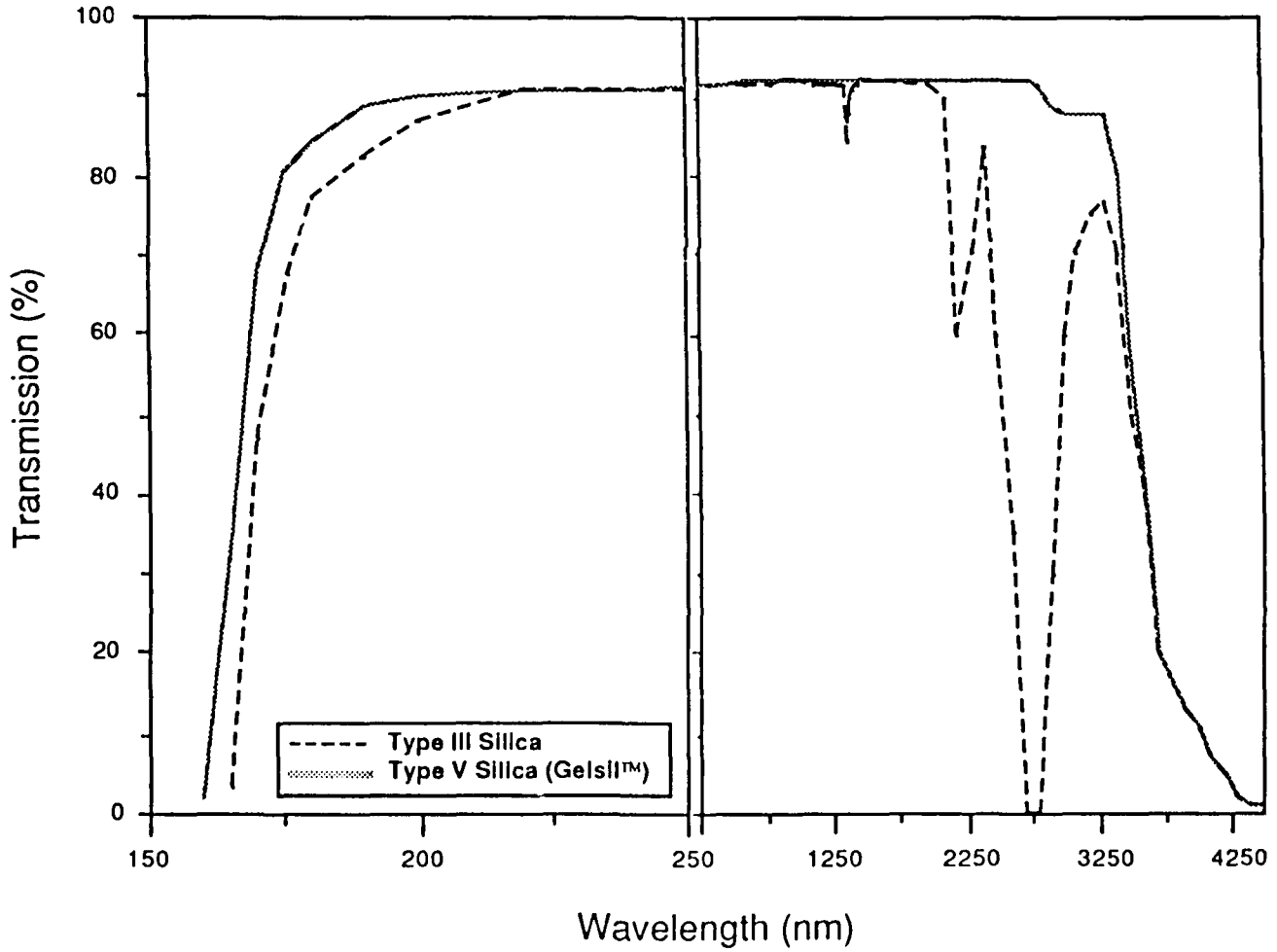

Figure 5: Optical Transmission of Dense Gel-Silica (Type V)

Results from optical property measurements show no evidence of bubbles, no striae, very low strain birefringence of 4 to 6 nm/cm and a superior index of refraction homogeneity of about 1 to 6×10^{-6} as shown in figure 6.

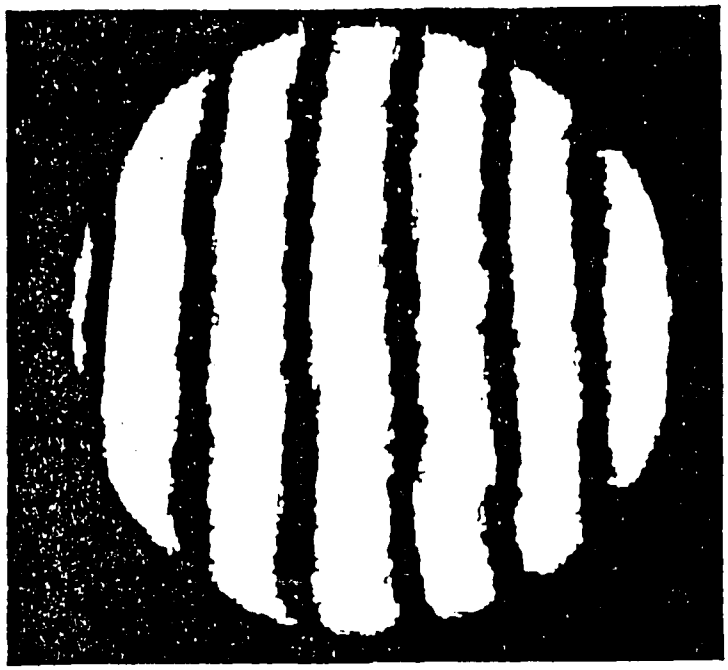

Figure 6: Interferometry Analysis of Dense Gel-Silica (Type V)

A very low coefficient of thermal expansion (CTE) is a very important physical characteristic of optical silica. Figure 7 compares the CTE values of a Type V silica (Gelsil™) optics with the National Institute of Standards and Technology (NIST) silica reference and Type III and IV commercial silicas over the temperature range of 25°C to 700°C. The sol-gel optical silica have lower values of CTE than the other types of silica. The typical CTE value for gel-silica (Gelsil™) is 0.54 ppm/°C @ 200°C.

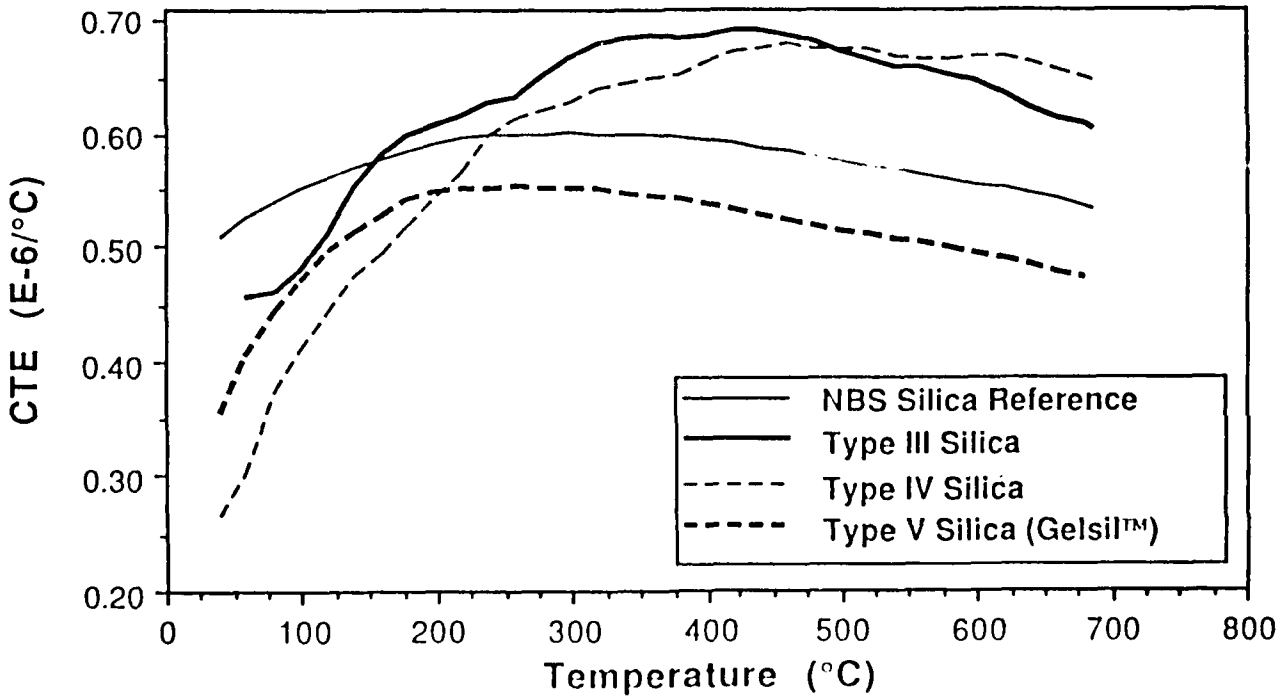

Figure 7: Coefficient of Thermal Expansion (CTE)

One of the advantages of sol-gel optics processing is to be able reproduce the shape of the mold used for casting. The parts produced with this method do not require extensive grinding and polishing. Figures 8 and 9 show intricately shaped as-cast monoliths and plano/convex as-cast gel-silica lenses respectively.

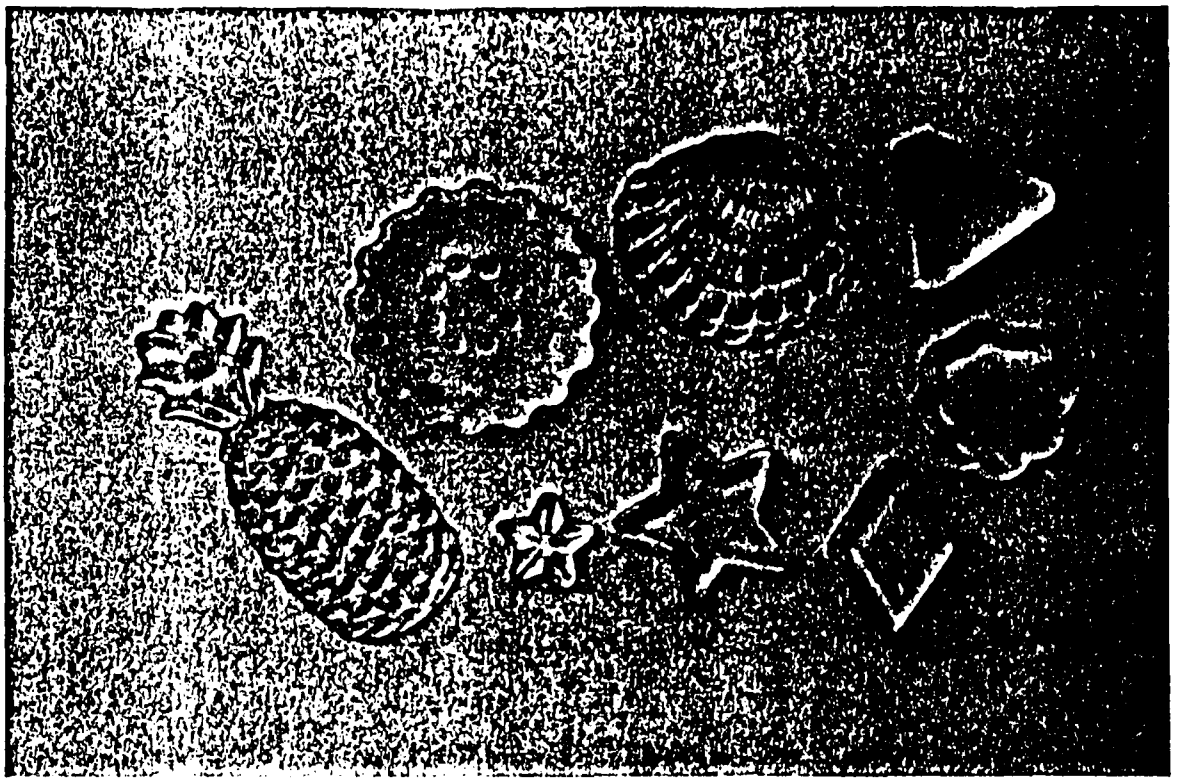

Figure 8: Intricately Shaped Dried Gel-Silica Monoliths

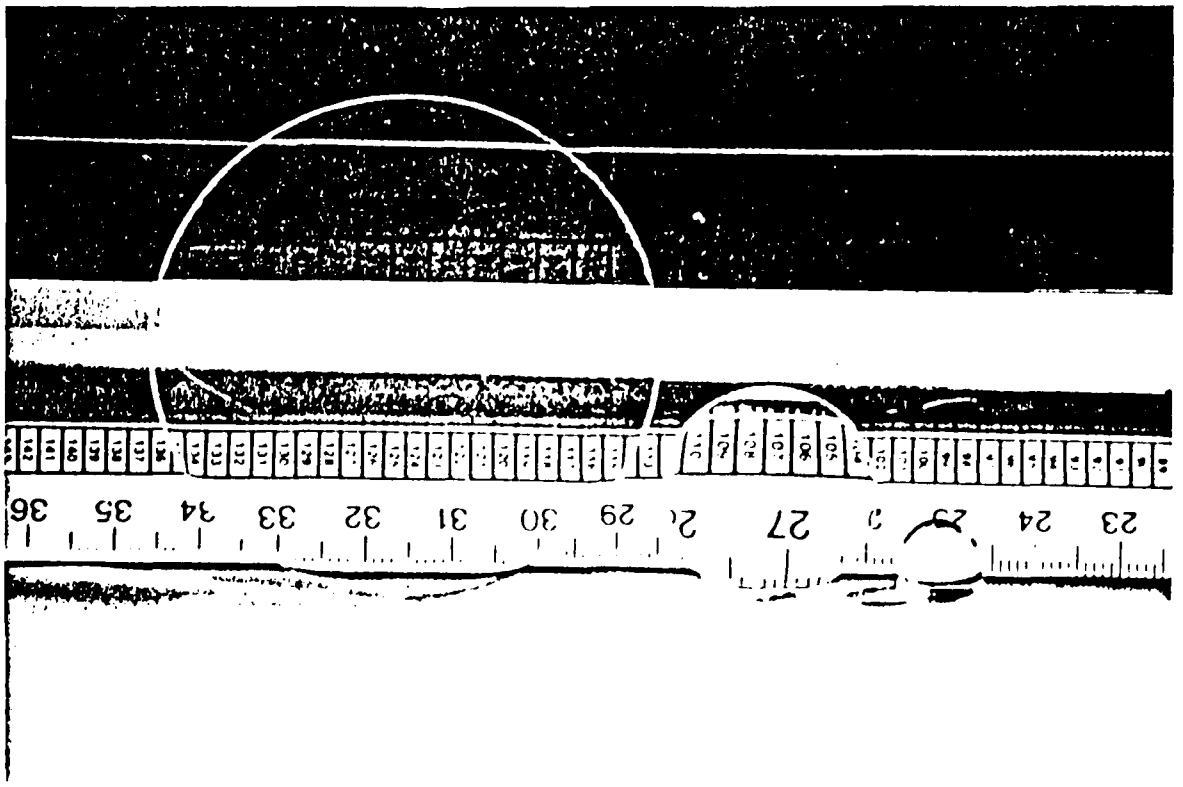

Figure 9: Plano/Convex Gel-Silica Lenses (Dried and Dense)

The sol-gel process can even replicate the most intricate surface details. Figure 10 shows a microscope photograph of a dry gel-silica Fresnel lens. The lens master was machined in a polymer and the sol-gel silica positive replica was made by direct casting against it. The precision of the master was maintained through densification to a Type V gel-silica. The advantages of the silica Fresnel lens over a polymer lens are its much lower thermal expansion coefficient and its greater thermal and radiation stability.

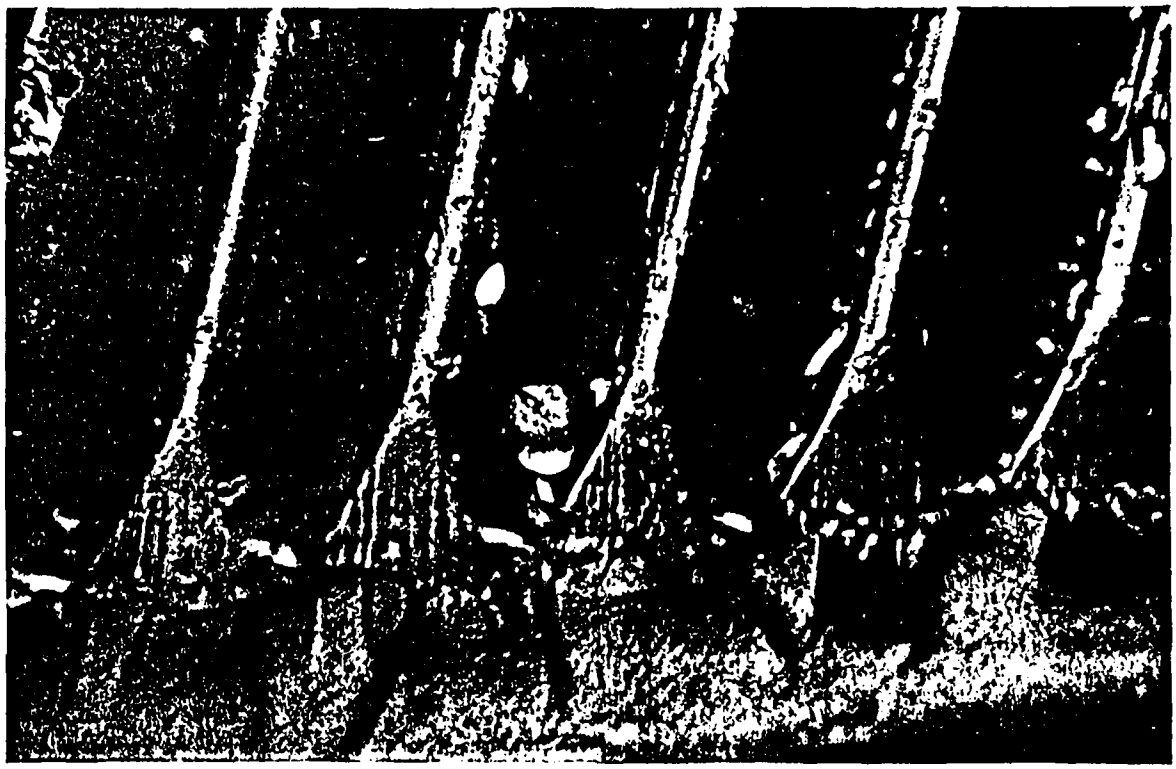

Figure 10: Microscope Photograph of a Dry Gel-Silica Fresnel Lens

6. Conclusion

The primary effort at GELTECH, Inc. to date has been in the area of silica manufacture using sol-gel technology initiated at the University of Florida. This technology has been further improved and refined to develop processes resulting in the production of porous gel-silica and dense gel-silica. Although GELTECH is mainly focusing on the optics and optoelectronics market,
the desirable optical and physical properties of these products are expected to make them useful in many other applications.

The process developed at GELTECH requires less energy compared to conventional glass manufacture and provides the advantage of casting shapes directly. Because the resulting glass requires minimal grinding and/or polishing the production costs of an optical component are less. The dense silica product has a low UV cutoff, low absorbtion throughout the spectrum, high optical homogeneity, very few defects, low strain birefringence, and low coefficient of thermal expansion.

Acknowledgements

The authors gratefully acknowledge financial support of Air Force Office of Scientific Research Contracts #F49620-86-C-0120 and F49620-88-C-0010 and the encouragement of D. R. Ulrich throughout this research.

References

1. L. L. Hench & D. R. Ulrich, eds., *Ultrastructure Processing of Ceramics, Glasses, and Composites*, John Wiley & Sons, NY, 1984, and *Science of Ceramic Chemical Processing*, John Wiley & Sons, NY, 1986. J. D. Mackenzie & D. R. Ulrich, eds., *Ultrastructure Processing of Advanced Ceramics*, John Wiley & Sons, NY, 1988.
2. C. J. Brinker, D. E. Clark, and D. R. Ulrich, eds., *Better Ceramics Through Chemistry*, Vol. 32, North-Holland, NY, 1984; *Better Ceramics Through Chemistry II*, Vol. 73, North-Holland, NY, 1986; and *Better Ceramics Through Chemistry III*, Vol. 121, North-Holland, NY, 1988.
3. V. Gottardi, ed., *Proceedings of the International Workshop on Glasses and Glass Ceramics from Gels*, J. Non-crystal. Solids, **48** [1], (1982); H. Scholze, ed., *Proceedings of the Second International Workshop on Glasses and Glass Ceramics from Gels*, J. Non-crystal. Solids, **63** [1&2], (1984); J. Zarzycki, ed., *Proceedings of the Third International Workshop on Glasses and Glass Ceramics from Gels*, J. Non-crystal. Solids, **82** [1-3], (1986); and S. Sakka, ed., *Proceedings of the Fourth International Workshop on Glasses and Glass Ceramics from Gels*, J. Non-crystal. Solids, **100** [1-3], (1988).
4. L. L. Hench, S. H. Wang, and J. L. Noguès, "Gel-Silica Optics", *Proceedings of the Society of Photo-optical Instrumentation Engineer's Symposium on Innovative Science & Technology*, Los Angeles, CA, (1988).
5. S. H. Wang and L. L. Hench, "Sol-Gel Derived Silica Optical Filters"; pp. 201-207 in *Science of Ceramic Chemical Processing*, Edited by L. L. Hench and D. R. Ulrich. John Wiley & Sons, NY, 1986.
6. J. L. Noguès, S. Majewski, J. K. Walker, M. Bowen, R. Wojcik, & W. V. Moreshead, "Fast, Radiation Hard Scintillating Detector, A Potential Application for Sol-Gel Glass", J. Am. Ceram. Soc., **71** [12] 1159-63 (1988).
7. J. L. Noguès and W. V. Moreshead, "Porous Gel Silica, a Matrix for Optically Active Components", poster to be presented at the *Fifth International Workshop on Glasses and Glass Ceramics from Gels*, Rio de Janeiro, August, 1989.
8. R. V. Ramaswamy, T. Chia, R. Srivastava, A. Miliou, & J. West, "Gel-Silica Waveguides", *Proceedings of the Society of Photo-optical Instrumentation Engineer's Symposium on Innovative Science & Technology*, Los Angeles, CA, (1988).
9. L. L. Hench, M. J. R. Wilson, C. Balaban, and J. L. Noguès, "Sol-Gel Processing of Large Silica Optics", Presented at the *Fourth International Conference on Ultrastructure Processing of Ceramics, Glasses, and Composites*, Tucson, AZ, February, 1989.

Note: † Gelsil™ is a trademark of GELTECH, Inc.

DILATOMETRIC MEASUREMENTS FOR LOW THERMAL EXPANSION GELS

by
B. F. Zhu, F. Wang and J. K. West
Advanced Materials Research Center
University of Florida
Alachua, Florida 32615

ABSTRACT

Differential dilatometry is a valuable technique for measuring both differential and absolute expansion of materials. This technique is also very useful for studying the sintering and densification kinetics of gels. The accuracy of high temperature expansion measurements is discussed in terms of the sources and magnitude of the measurement errors. Considerations for reducing the measurement errors are given.

INTRODUCTION

Differential dilatometry is a valuable technique for measuring both differential and absolute expansion of materials. This technique dictates the differential expansion between sample and reference specimens as a function of temperature and/or time. With the known thermal expansion data for the references and the measured differential expansion between the sample and reference specimens, the absolute values of sample expansion can be obtained. If the thermal expansion, thermal mass and thermal diffusivity of the sample and reference specimens are closely matched, (1) the measurement precision can be increased, (2) the errors due to the temperature and the linear variable differential transformer (LVDT) calibration can be reduced, and (3) the capacity of heating and cooling at high rates can be achieved[1]. Such a match is extremely important when one deals with materials with coefficients of

of thermal expansion in an order of $10^{-7}/°C$.

Differential dilatometry is also very useful for studying the sintering and densification kinetics of gels. The densification kinetics can be studied by analysis of the thermal expansion and relaxation as a function of porosity, densification temperature and processing.

Since gels shrink during the heat treatment, a smaller thermal expansion as compared to that of the fully densified material can dictate structural relaxation, densification and sintering of the tested material. The temperature(s) at which drastic shrinkage occurs can be taken as the beginning temperature of sintering. Also, by using a computer heating can be controlled to give the tested material a programed shrinkage at a predetermined rate to avoid cracking.

A dilatometer (Dilatronic II Research Dilatometer*) was installed in our laboratory to obtain high precision expansion measurements on gel-derived silica and silicate (SiO_2-TiO_2) monoliths.

The primary objective of this project was to evaluate the accuracy of high temperature thermal expansion measurements for silica and silica-titania gels at different stages of densification. The sources causing the measurement errors are discussed and considerations for reducing these errors are presented.

---

*Theta Industries, Inc., 26 Valley Road, Port Washington, NY.

INSTRUMENTATION

The coefficients of thermal expansion (CTEs) were measured using a Theta Industries' Dilatronic II Research Dilatometer. The temperature capability for the equipment is between -190° and 1600°C. In the present paper, only 200°-700°C data are used.

The dilatometer contains dual push rods to measure the differential expansion between the sample and reference specimens. The specimens were either 10 or 25 mm long and 5-8 mm in diam. Either a fused silica or alumina specimen holder was used, however, only the data obtained with the silica specimen holder are reported.

Both the heating and cooling rates were kept at 3°C/min. A water circulator was on line to keep the measuring head and the cold junctions of the thermocouples at constant temperature (∿37°C). The gauge block calibration was done before the measurements. This evolved putting a standard thickness of 0.25 mm between the micrometer and the ball point of the LVDT coil. The expansion factors were calculated based on the voltage produced due to the displacement of the coil when the gauge block was put in. An average voltage was obtained from six readings at a 15-sec interval.

The thermal expansion data of the NBS reference materials have been stored in the computer. When a reference material was used as the sample specimen, the measured thermal expansion data were compared with the known to get the correction factors. The correction factors obtained from three runs were averaged and stored for future use.

Figure 1 is a typical CTE curve for a silica-titania gel monolith densified at 900°C.

SOURCES AND MAGNITUDE OF ERRORS

Figure ~ shows the sources and magnitude of the possible errors in a typical conventional pushrod dilatometer with a temperature range of 1600°C and a total accuracy of 2%. There are three large portions corresponding to the thermocouple and the reference inaccuracy, sample temperature gradient and the correction factors.

1. Accuracy of Temperature Measurements

It is well known that not only the accuracy of the measurements of the length change but also that of the temperature measurements determine the accuracy of dilatometric measurements. Tables I and II show the accuracy of both the hot and cold junctions of thermocouples. It is important to choose the right type of thermocouples and to use a thermocouple reference compensator. In our laboratory, a constant temperature circulator is attached to the system to keep both the cold junctions of the thermocouples and the entire measuring head at constant temperature. The accuracy of the constant temperature circulator is $\pm$ 0.15°C.

2. Sample Temperature Gradient Inaccuracy

The resolution of a recent model of a transducer-digital recorder is 25×10^{-7} mm (1×10^{-7} inch). Therefore, a lengthy sample size is no longer essential for meaningful length change measurements. However, most materials which we deal with in our study have thermal expansions in the order of 10^{-7}/°C. Therefore, a 25 mm (1") long sample is recommended sometimes in order to insure the measurement accuracy. In this case, a sample temperature gradient may occur which imposes an inaccuracy in the dilatometer measurements.

In other cases, considerable shrinkage occurs when undensified gels are subjected to high temperatures. Thus, a slower increase or even a decrease in differential expansion may be observed. In such cases, a longer sample might be needed in view of the resolution of the transducer-digital recorder. In all cases, sample temperature gradient inaccuracy will be induced by using long samples.

3. Correction Factors

A set of correction factors must be established for each dilatometer system. These correction factors usually contain the thermal instability of the measuring head and the whole dilatometer system, as well as unexplainable phenomena. The set of correction factors will be valid only if the thermal expansion, thermal mass and thermal diffusivity are closely matched and the same test conditions are maintained.

Figure 3 is a plot showing the measuring head temperature as a function of the number of data points (time) for a silica-titania gel densified at 900°C for 4 hrs. The sample was held at 200°C for 4 hrs after cooling from high temperatures. Figure 4 is the corresponding differential expansion data for such a sample being held at 200°C. An increase in the differential expansion was observed as the measuring head temperature dropped. About 6 cycles are shown in these two figures. It is obvious that the fluctuation in the differential expansion is due to the cyclic changes in the measuring head temperature, although the change in the differential expansion was delayed by a phase of 90°. Both magnitudes of the measuring head temperature cycles and the differential expansion cycles did not change. For a decrease of every 0.12°C in the measuring head temperature, the differential expansion increased by 3.5×10^{-6}.

As the measuring head temperature increased during heating, a decrease in the differential expansion was observed. It appeared that with an 0.3°C increase in the measuring head temperature, the differential expansion decreased by 10×10^{-6}.

Assuming that the absolute value of the error due to the measuring head temperature change keeps constant (we found that this was true for a certain temperature profile), then

$$(\frac{\Delta L}{L})_m \times E = \text{constant.} \quad (1)$$

where $(\frac{\Delta L}{L})_m$ is the measured thermal expansion for the sample and E is the percentage of the error due to the measuring head temperature change.

Equation (1) indicates that for materials with different thermal expansions, the percentage of the error due to the measuring head temperature change is reversely proportional to their thermal expansions.

In order to increase the accuracy of the dilatometric measurements, the reference material should be chosen to have a close thermal expansion, thermal mass and thermal diffusivity as compared to those of the sample when the system is calibrated to obtain error data as the correction factors.

Figure 5 shows the influence of the measuring head temperature change on thermal expansion. The cyclic changes observed for every 120°C in the thermal expansion curve are due to the misuse of the correction factors obtained from a calibration using reference materials with large CTE values.

As shown in Figure 6, NBS silica appears to be the best reference material for measuring the thermal expansions of our gel monoliths. However, the thermal expansion at 700°C for silica is about 350×10^{-6}, while that of silica-titania gels is only 80-100 $\times 10^{-6}$. Therefore, considerable error will be introduced by using the correction factors calibrated using NBS silica. It

is an urgent task to develop new reference materials for measuring low thermal expansion gels with higher accuracy.

SUMMARY

Differential dilatometry is a valuable tool for measuring length changes of materials. This technique is also very useful for studying the sintering and densification kinetics of gels. Since the gels in our study exhibit low thermal expansion behavior (in the order of $10^{-7}/°C$), care must be taken in order to get meaningful measurements of the length change. It is extremely important to choose the right type of thermocouples, to keep both the cold junctions of the thermocouples and the entire measuring head at constant temperature by using a temperature compensator and to match closely the thermal expansion, thermal mass and thermal diffusivity between the reference and the unknown specimens. It is an urgent task to develop new reference materials for measuring low thermal expansion gels with high accuracy.

REFERENCES

1. G. R. Clusener, "Accuracy of High Temperature Thermal Expansion Measurements," presented at the 74th ACerS Annual Meeting, Washington, DC, May 1972.

2. W. A. Plummer, "Differential Dilatometry--A Powerful Tool," Corning Glass Works, Corning, NY 14830.

Table I

Thermocouple Accuracy[2]

	1000°C	1500°C
Pt, 10% Rh-Pt		
NBS Calibrated: estimated uncertainties	0.3°C	2.0°C
Commercial: Standard limits of error		
Grade A	2.7°C	3.6°C
Grade B	5.3°C	7.3°C

Base Metal	
NBS Calibrated (Table Curve)	±1° (0°C to 1100°C)
Specific Points	±0.2°C (above 300°C)

Table II

Accuracy of Thermocouple Reference Junctions[2]

Ice Bath (only when well maintained)	±0.01°C
Electrical Bridge Circuit in Lab Environment	±0.5°C
Constant Temperature Circulator (fully auto)	±0.15°C*

*Based on data in our laboratory.

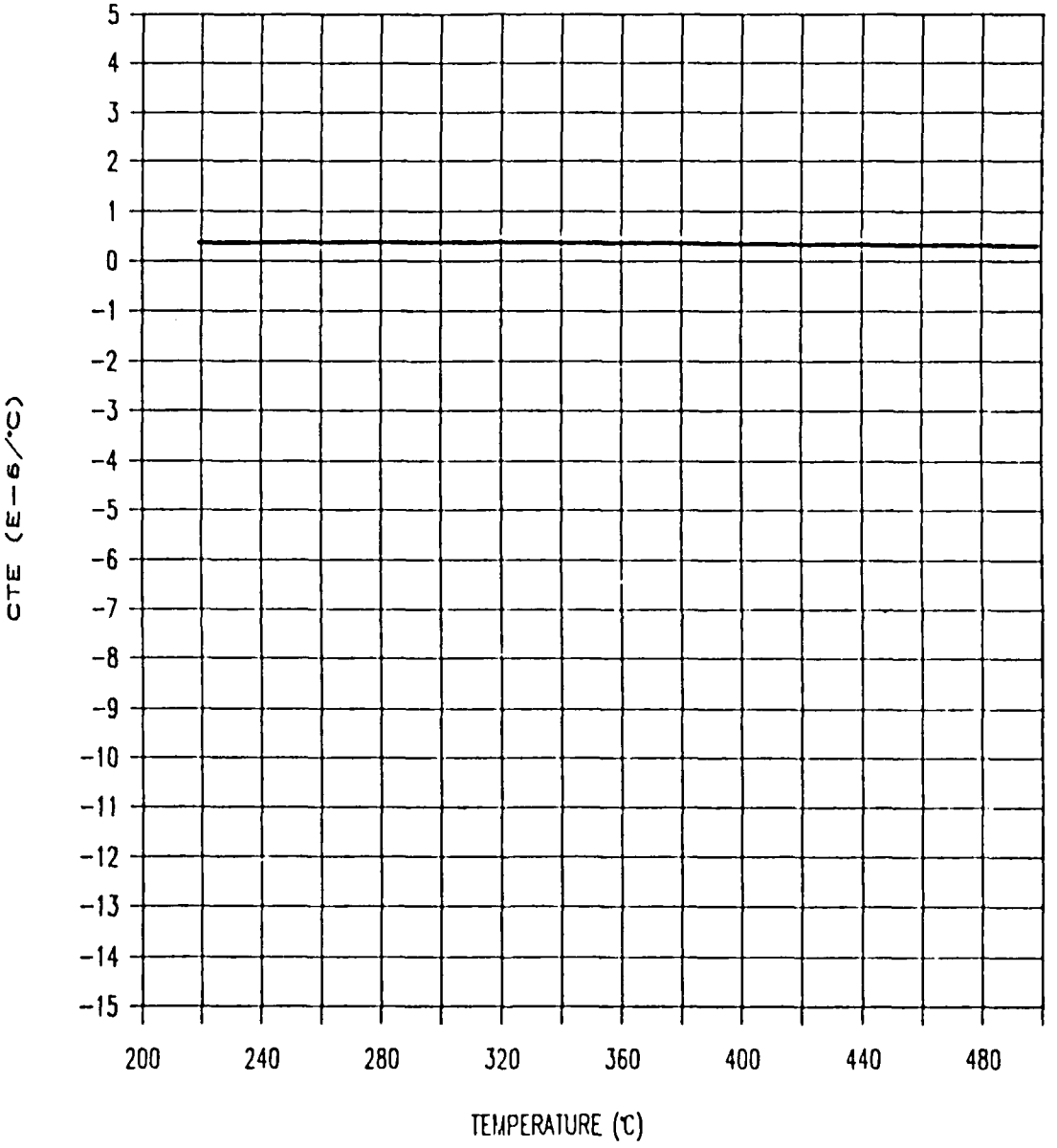

Figure 1. CTE curve for a silica-titania gel preheated up to 900°C.

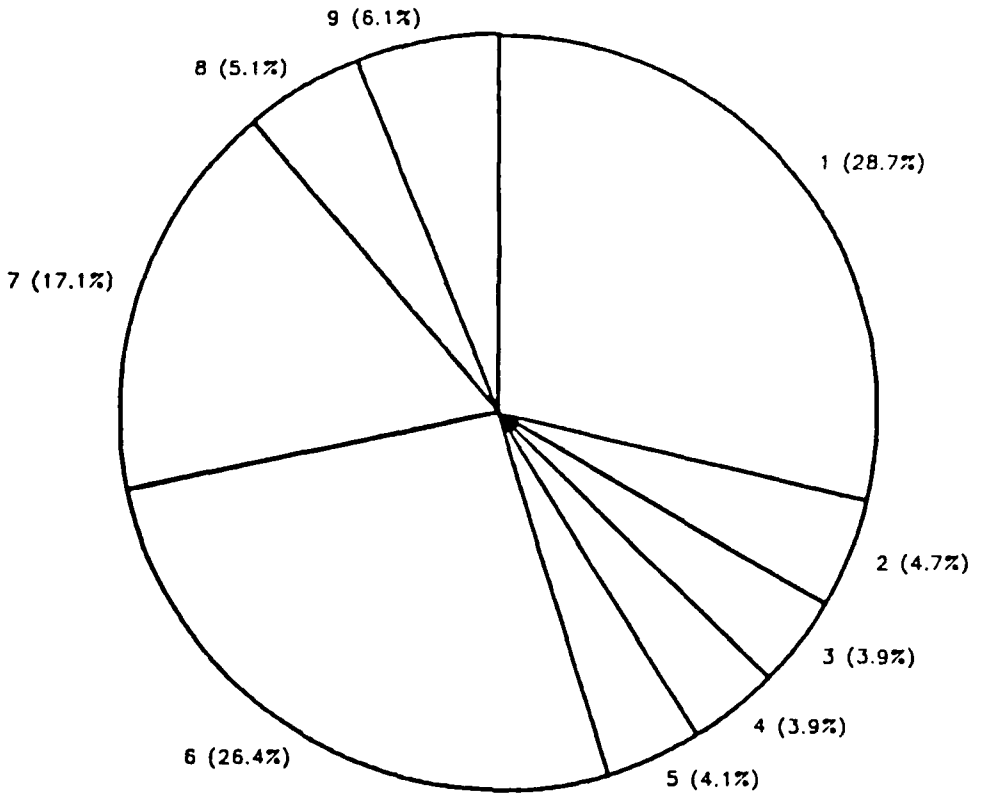

1. Thermocouple and thermocouple reference error
2. LVDT non-linearity
3. Gage block calibration
4. Pushrod friction and sample-measuring system interface
5. Error of thermal expansion reference material
6. Correction factors
7. Sample temperature gradient
8. Fluctuations in line voltage
9. Room temperature influence

Figure 2. Sources and magnitude of measurement errors in a typical conventional pushrod dilatometer.

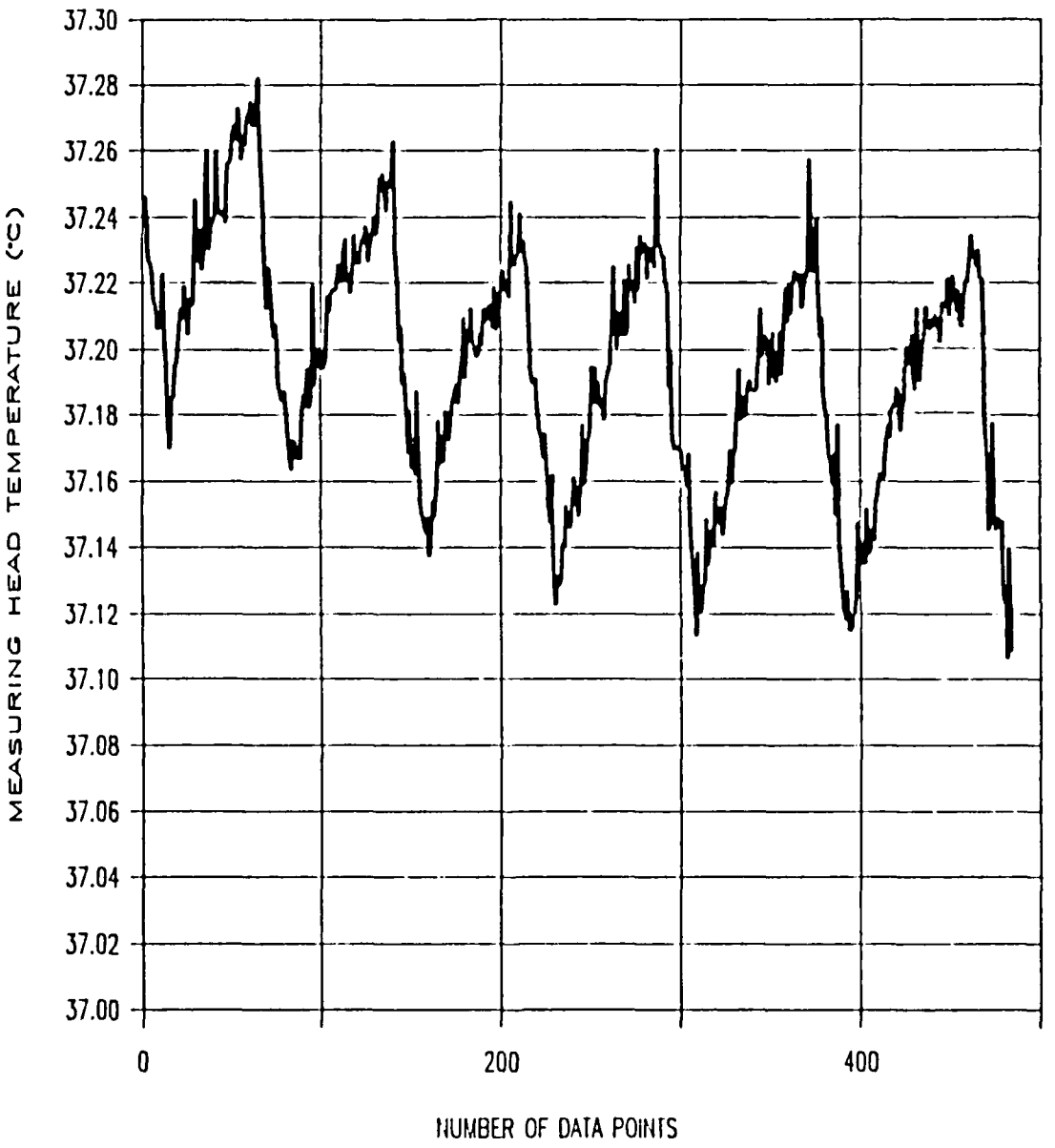

Figure 3 Plot showing the measuring head temperature as a function of the number of data points. The specimen was held at 200°C for 4 hrs after cooling from high temperatures.

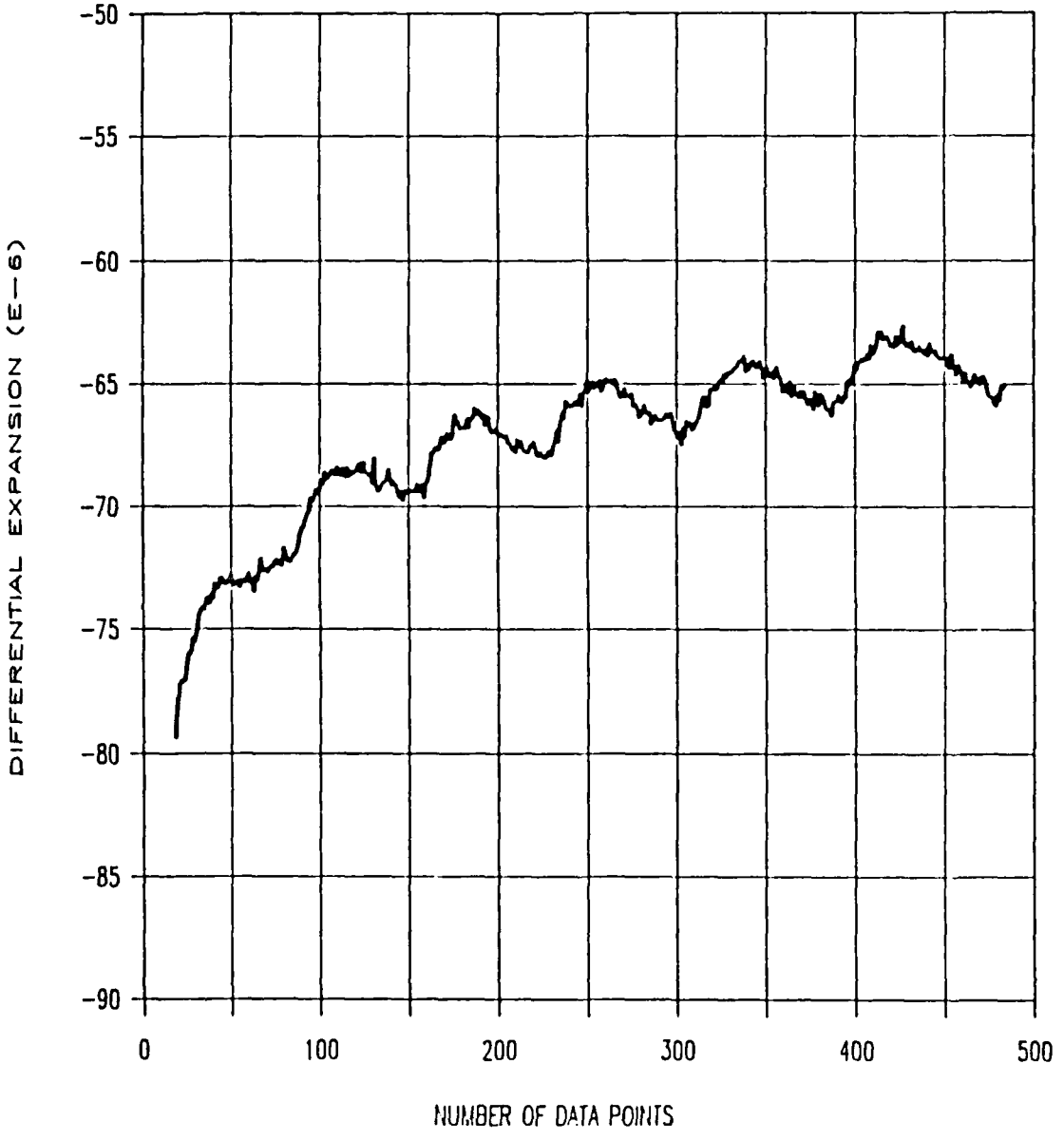

Figure 4. Differential expansion vs number of data points for a specimen held at 200°C for 4 hrs after cooling from high temperatures. The specimen was the same as in Figure 3.

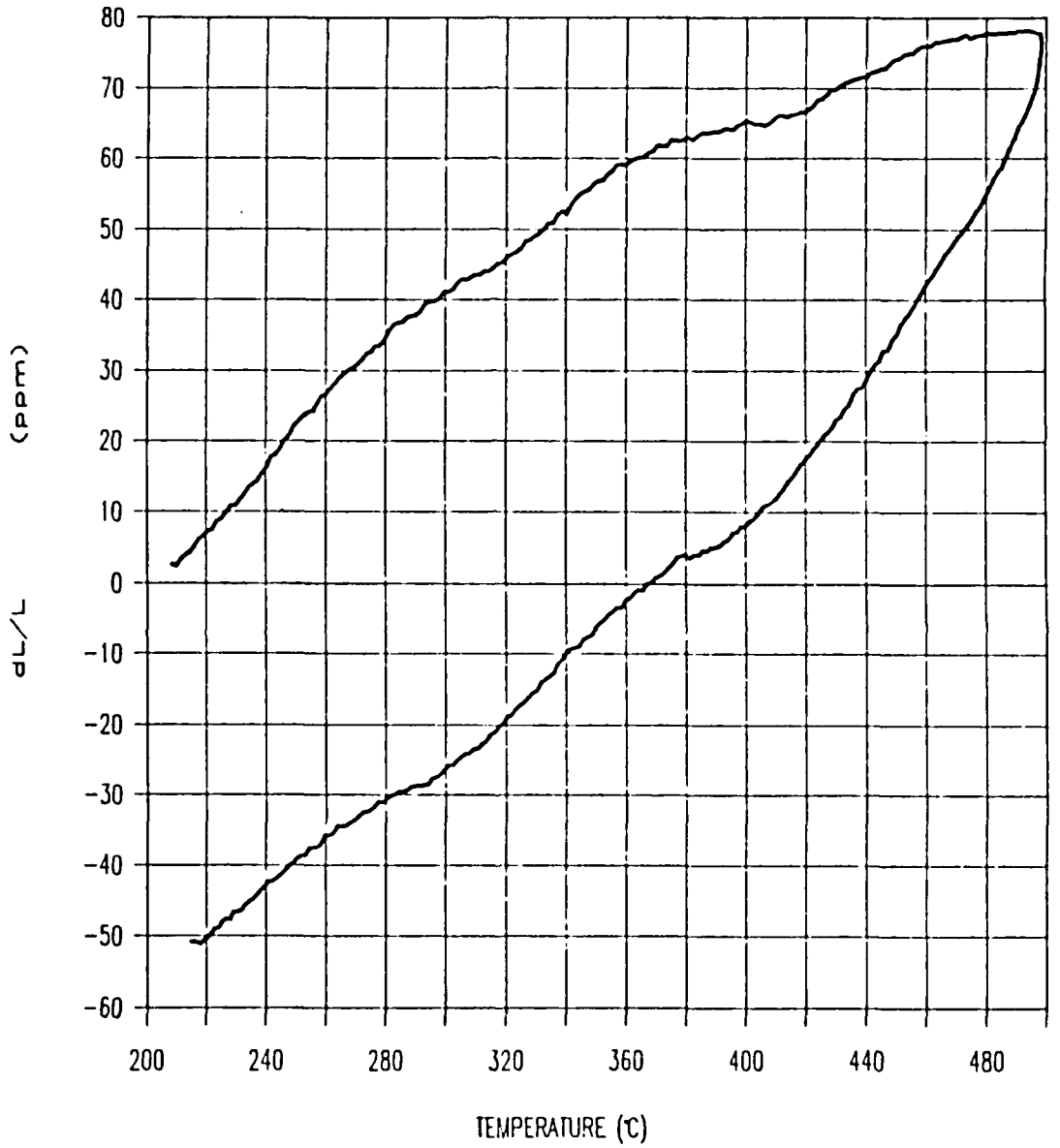

Figure 5. Thermal expansion data (corrected) vs temperature.

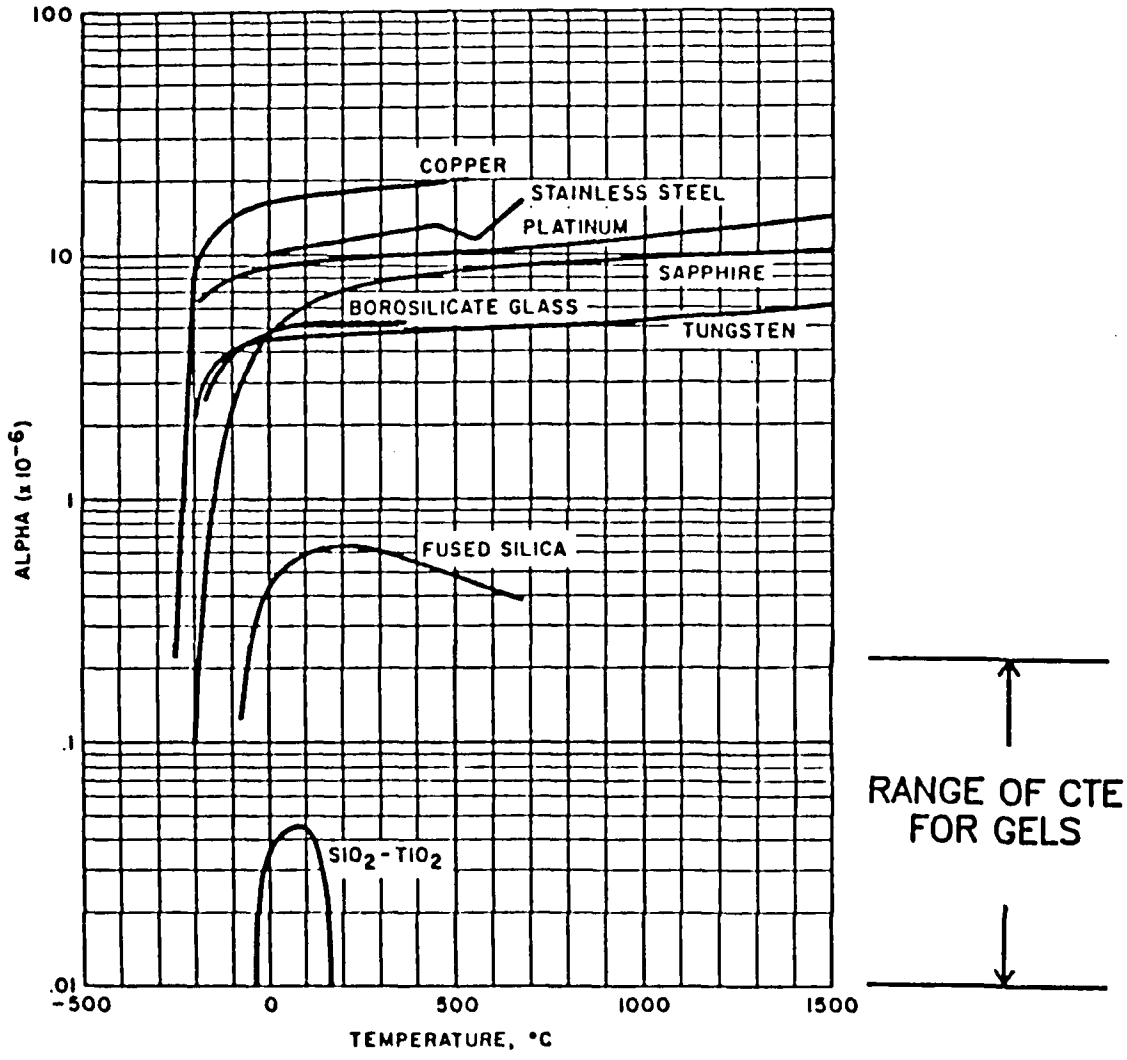

Figure 6. CTE's of the reference materials and the CTE range for our gels.